

**Towards development of a platform
process for novel Lantibiotic production**

By

Haroon Dawood Sadullah Khan

Engineering Doctorate Thesis

Submitted to

University College London

Declaration

I, Haroon Khan, confirm that the work presented in this thesis is my own. Where information has been derived from other sources, I confirm that this has been indicated in the thesis.

.....

Haroon Dawood Sadullah Khan

Acknowledgments

I would like to thank my supervisors from UCL, Gary Lye and Nicolas Szita for all their advice and support throughout this project. In addition, I would like to thank Sven Panke from ETH Zurich, who provided me with the *Staphylococcus gallinarum*Δ*gdmP::aphIII* cell strain. I would also like to thank Dr Mike Dawson from Novacta Ltd, who was initially involved in the establishment of this EngD project. Furthermore, I would like to thank the EPSRC and the ESF for funding my research.

I would like to dedicate this work to my dear grandfather, Lt.Col Mohammed Ashraf, who is no longer with us. His belief in my abilities was absolute, and I would never have made it far without him.

I would also like to thank my family, for their support, understanding and belief. They are the bedrock on which my life is built.

Finally, I would like to thank all my friends and colleagues at UCL for their morale boosting support and belief in me, especially Tim, Cyrus, Shaz, Eduardo, John, Akin, Jamie, Dougie, Iwan, Owen and Rummaz.

Abstract

The worldwide increase in antibiotic resistant bacteria has been identified as a major concern to the continued provision of healthcare. The lack of new antibiotic discoveries and the diminishing number effective against multi-drug resistant bacteria has increased efforts to identify new natural antimicrobials and to use synthetic biology to engineer artificial ones. Lantibiotics, a class of ribosomally synthesized antimicrobial peptides, with a broad spectrum of activity, have been identified as potential candidates to combat such bacteria. However no clinical lantibiotic products currently exist, owing to low product titres and lack of a suitable manufacturing process.

Initial studies on the lantibiotic gallidermin have managed to increase product titre by modifying the producer strain, *Stapylococcus gallinarum* Tü3928, to synthesize the biologically inactive precursor, pregallidermin. This helps overcome product auto-toxicity and may be a generic route to enhancing the production of novel engineered lantibiotics.

This thesis investigates the scalability of a pregallidermin production process to determine whether it could serve as a production platform for novel lantibiotics. Initially, fed-batch cultures were performed in 7.5 L stirred tank bioreactors to characterise the parameters necessary for achieving high cell density. These identified aeration, agitation and nutrient feed rates as important parameters to optimal product formation. The fed-batch culture was repeated at pilot scale (30 L) under the same process conditions, yielding 0.7 g.L^{-1} of pregallidermin.

A scalable downstream process was also developed and evaluated. The overall process flowsheet comprised of pregallidermin capture on the hydrophobic resin Amberlite XAD-7, followed by cation exchange chromatography to purify the pregallidermin. This was then trypsinised to release the required gallidermin. The final purity of gallidermin was 70 % (w/w) with an overall process yield of 13.5 %. Using this downstream process sequence 1.9 g (0.09 g.L^{-1}) of pregallidermin was isolated from the 30 L fermentation. Confirmation of the identity of the purified pregallidermin and gallidermin was obtained by HPLC and mass spectrometry.

Microscale methods were developed to optimise the downstream process and determine product physico-chemical properties with a view to informing process design. These determined that higher purity gallidermin recovery was possible with the optimisation of the XAD-7 adsorption/desorption. Optimal conditions for pregallidermin adsorption, resin wash and pregallidermin elution from resin were determined using the microscale methods. A redesign of the downstream process based on optimised pregallidermin capture increased overall recovery of mature gallidermin 3-fold to 0.3 g.L^{-1} .

In summary, this work has demonstrated a novel process for lantibiotic production and purification at pilot scale. The process is sufficiently generic that it could serve as a manufacturing platform for production of next generation engineered lantibiotics. It has also demonstrated the utility of microscale methods in optimising the production process.

Table of Contents

| | |
|--|----|
| Declaration..... | 2 |
| Acknowledgments..... | 3 |
| Abstract..... | 4 |
| Table of Contents..... | 6 |
| Table of Figures..... | 10 |
| List of Tables..... | 14 |
| Nomenclature..... | 15 |
| 1. Introduction..... | 17 |
| 1.1.1 Need for new antibiotics..... | 17 |
| 1.1.2 Synthetic Biology based solutions..... | 18 |
| 1.2 Synthetic Biology for novel antibiotic development..... | 20 |
| 1.2.1 Principles of Synthetic Biology..... | 20 |
| 1.2.2 <i>Stapylococcus gallinarum</i> Tü3928 and the modified <i>Stapylococcus gallinarum</i> ΔgdmP::aphIII..... | 24 |
| 1.2.3 Creation of ‘chassis’ organisms..... | 25 |
| 1.2.4 Advantages and limitations of developing novel organisms..... | 26 |
| 1.2.5 Application of Synthetic Biology to Natural Product Synthesis..... | 27 |
| 1.3 Lantibiotics..... | 29 |
| 1.3.1 Basic Structure..... | 29 |
| 1.3.2 Properties of Lantibiotics..... | 30 |
| 1.3.3 Structural grouping of Lantibiotics..... | 32 |
| 1.3.4 Type A Lantibiotics..... | 32 |
| 1.3.5 Gallidermin..... | 33 |
| 1.3.6 Type B Lantibiotics..... | 36 |
| 1.3.7 Mode of Action..... | 38 |
| 1.3.8 Regulation of Biosynthesis: Quorum Sensing..... | 39 |
| 1.3.9 Lantibiotic auto-toxicity..... | 40 |
| 1.3.10 Therapeutic potential..... | 42 |
| 1.4 Lantibiotic Synthesis..... | 43 |
| 1.4.1 Biosynthesis of Lantibiotics..... | 43 |
| 1.4.2 Precursor Production..... | 46 |
| 1.5 Production of Lantibiotics..... | 47 |
| 1.5.1 Upstream Processes..... | 47 |
| 1.5.2 Downstream Process Sequences..... | 49 |
| 1.5.3 Isolation and purification..... | 52 |

| | | |
|-------|--|----|
| 1.5.4 | Identification & Analytics | 54 |
| 1.5.5 | The impact of lantibiotic physical properties on Downstream Processing | 55 |
| 1.5.6 | Challenges imposed by synthetic biology on Downstream Processing | 56 |
| 1.6 | Microscale Approaches to Downstream Process design | 58 |
| 1.6.1 | Microscale Methods | 58 |
| 1.6.2 | Rapid characterization, identification and analysis | 60 |
| 1.6.3 | Economic Benefits..... | 61 |
| 1.7 | Current status of the Bioprocessing aspects..... | 61 |
| 1.8 | Novelty of the work performed | 63 |
| 1.9 | Aims and Objectives | 65 |
| 2. | Materials and Methods | 67 |
| 2.1 | Materials | 67 |
| 2.1.1 | Organism..... | 67 |
| 2.1.2 | Preparation of glycerol stocks | 68 |
| 2.1.3 | Fermentation media and feed for fed-batch fermentations..... | 69 |
| 2.2 | Fermentation of <i>S. gallinarum</i> Δp | 70 |
| 2.2.1 | Shake flask fermentation of <i>S.gallinarum</i> Δp | 70 |
| 2.2.2 | 7.5L fermentation of <i>S.gallinarum</i> Δp : batch mode | 71 |
| 2.2.3 | 7.5L fermentation of <i>S.gallinarum</i> Δp : fed-batch mode | 73 |
| 2.2.4 | 30L Fed-Batch fermentation of <i>S.gallinarum</i> Δp | 76 |
| 2.2.5 | Fermentation substrate feed strategies | 77 |
| 2.2.6 | Anti-foaming agent utilised | 80 |
| 2.2.7 | Measurement and calculation of off-gas data..... | 80 |
| 2.3 | Purification of Pregallidermin | 81 |
| 2.3.1 | Small Scale centrifugation..... | 81 |
| 2.3.2 | Large Scale Centrifugation..... | 82 |
| 2.3.3 | Adsorption using XAD-7 | 82 |
| 2.3.4 | Desorption..... | 83 |
| 2.3.5 | Ion Exchange Chromatography..... | 83 |
| 2.3.6 | Adsorption/Desorption..... | 84 |
| 2.3.7 | Lyophilization | 85 |
| 2.4 | Trypsinization of PGDM..... | 85 |
| 2.5 | Analytical Techniques..... | 86 |
| 2.5.1 | UV-VIS spectroscopy | 86 |
| 2.5.2 | Biomass quantification | 86 |
| 2.5.3 | Quantification of antibiotic concentration and purity | 87 |
| 2.5.4 | Mass Spectrometry for product identification | 88 |

| | | |
|--------|---|-----|
| 2.6 | Microscale Methods for product analysis | 89 |
| 2.6.1 | Temperature stability studies | 89 |
| 2.6.2 | pH stability studies | 89 |
| 2.6.3 | Stability at varying ionic strength | 90 |
| 2.7 | Microscale methods for optimisation of product capture | 90 |
| 2.7.1 | Optimisation of product capture on XAD-7 | 91 |
| 2.7.2 | Optimisation of product elution from XAD-7 | 91 |
| 2.7.3 | Optimisation of impurity removal from XAD-7 | 92 |
| 3. | Optimisation of Pregallidermin production by Fed-batch fermentation of <i>S.gallinarum</i> Δp | 94 |
| 3.1 | Introduction and Aims | 94 |
| 3.2 | Overview of fermentation development strategy | 96 |
| 3.3 | Shake Flask culture | 98 |
| 3.4 | 7.5 L STR Fermentation: <i>S.gallinarum</i> Δp growth in batch mode | 101 |
| 3.5 | 7.5 L STR Fermentation: <i>S.gallinarum</i> Δp growth in fed-batch mode | 106 |
| 3.5.1 | Fed-batch – Maltose feed..... | 107 |
| 3.5.2 | Fed Batch- Maltose and yeast extract feed | 113 |
| 3.6 | 30 L STR Fermentation: Scale up of pregallidermin production..... | 121 |
| 3.7 | Factors influencing the oxidative production of PGDM by <i>S.gallinarum</i> Δp | 127 |
| 3.7.1 | Aeration..... | 127 |
| 3.7.2 | Feed..... | 129 |
| 3.7.3 | Agitation | 131 |
| 3.7.4 | OUR, CER and RQ | 133 |
| 4. | Downstream Process Design for recovery and optimisation of pregallidermin | 138 |
| 4.1 | Introduction | 138 |
| 4.1.1 | Aim | 140 |
| 4.2 | Overview of Downstream Process Sequence | 142 |
| 4.3 | Solid-Liquid separation by centrifugation | 142 |
| 4.4 | Hydrophobic Interaction: Batch Adsorption..... | 143 |
| 4.5.1 | Hydrophobic Interaction: Wash | 145 |
| 4.5.2 | Hydrophobic Interaction: Desorption | 147 |
| 4.6 | Ion Exchange Chromatography | 149 |
| 4.7 | Salt removal from eluted product stream..... | 153 |
| 4.8 | Trypsinisation of pregallidermin to produce mature gallidermin | 154 |
| 4.9 | Identification of pregallidermin and gallidermin | 154 |
| 4.10 | Assessment of overall downstream process performance | 160 |
| 4.10.1 | Solid-Liquid separation by centrifugation | 162 |

| | | |
|--------|---|-----|
| 4.10.2 | Hydrophobic Interaction | 163 |
| 4.10.3 | Ion Exchange Chromatography | 164 |
| 4.11 | Discussion and Summary | 166 |
| 5. | Microscale Methods for Rapid Analysis | 170 |
| 5.1 | Introduction | 170 |
| 5.1.1 | Aims | 171 |
| 5.2 | Overview of the microscale methods | 172 |
| 5.3 | Impact of pH on impurity removal | 173 |
| 5.4 | Stability of PGDM and Gallidermin | 176 |
| 5.4.1 | pH..... | 176 |
| 5.4.2 | Ionic Strength | 177 |
| 5.4.3 | Temperature..... | 179 |
| 5.5 | Impact of Methanol and co-solvent ionic strength on elution | 183 |
| 5.6 | Impact of Methanol and ionic strength on wash impurity removal..... | 186 |
| 5.7 | Selection of optimised downstream process conditions..... | 189 |
| 5.7.1 | Impact of pH on antibiotic recovery and processing..... | 189 |
| 5.7.2 | Impact of increasing methanol content and buffer ionic strength on resin wash and product elution efficiency..... | 191 |
| 5.7.3 | Potential as a platform for informing process design..... | 193 |
| 5.8 | Summary | 196 |
| 6. | Conclusions and future work..... | 199 |
| 6.1 | Conclusion and novel findings | 199 |
| 6.2 | Future Work..... | 203 |
| 7. | Outlook and Practical Applications† | 206 |
| 7.1 | Outlook | 206 |
| 7.2 | Practical Implementation..... | 207 |
| | Appendix..... | 210 |
| | Appendix 1: Full list of Chemicals used | 210 |
| | Appendix 2: Calibration Curves | 211 |
| | Appendix 3: 30 L STR fermentation: automated dual feed fed-batch | 212 |
| | Appendix 4: Contour Plot Data | 213 |
| | References..... | 214 |

Table of Figures

| | |
|--|-----|
| Figure 0.1.1 The various component disciplines of Synthetic Biology an interdisciplinary field, adapted from (www.esf.org) | 24 |
| Figure 1.2 Structure of (A) Lanthionine and (B) Methyllanthionine residues | 29 |
| Figure 1.3 The structure of (A) Nisin (amino acid residues and thioether rings), (B) Lacticin 481 and (C) Gallidermin, adapted from (Willey and Donk, 2007) ... | 35 |
| Figure 1.4 The structure of type B lantibiotics (A) Mersacidin and (B) Actagardine (amino acids and thioether ring structures), adapted from (Willey and Donk, 2007). | 37 |
| Figure 1.5 The modes of action of Type A and Type B lantibiotics with A) a type A lantibiotic (Nisin depicted by the black peptide chain) forming wedge like pores in the cell phospholipid layer at micromolar concentrations, B) a type A lantibiotic (depicted by Nisin) using lipid II as a docking molecule to form target mediated pores at nanomolar concentrations and C) a type B lantibiotic (Mersacidin) blocking cell wall synthesis by halting the incorporation of lipid II into peptidoglycan (Type A lantibiotics also possess this attribute). Adapted from (Hechard <i>et al.</i> , 2002) | 41 |
| Figure 1.6 The mechanism of lanthionine (Lan) and methyllanthionine (MeLan) formation in lantibiotics with A) the enzymatic dehydration of Ser and Thr, to Dha and Dhb, followed by B) nucleophilic attack from the thiol group on the Cys residue to form the thioether bridge, adapted from (Valesia, 2008). | 45 |
| Figure 1.7 Downstream processing sequences with A) common production process for lantibiotics in literature and B) production using the pregallidermin precursor molecule. Adapted from (Medaglia, 2009) | 51 |
| Figure 2.1 The Dimensions of the BioFlo 110 7.5 L bioreactor, with A) showing the vertical cross-section and B) showing the horizontal cross-section. X= the impeller shaft; Y= impeller blade; Z= baffle. All measurements are displayed in millimetres (mm). | 75 |
| Figure 2.2 The two substrate feed profiles used for the fermentation studies, with A) depicting an exponential feed regime in which an attempt is made to map the feed rate onto the microbial growth curve and B) showing a 'step-up' feed profile, with step changes in the feed rate to ensure the substrate is maintained in excess and does not become growth limiting. | 79 |
| Figure 3.1 Overview of the types of fermentation performed as outlined in Section 2.2. | 97 |
| Figure 3.2 Representative shake flask batch growth kinetic profile of <i>Staphylococcus gallinarum</i> Δp . The error bars represent one standard deviation about the mean. (n=3, average of 3 fermentations) Experiments performed as described in Section 2.2.1. | 100 |

- Figure 3.3 Logarithmic growth curve for *Staphylococcus gallinarum* Δp . The error bars represent one standard deviation around the mean. (n=3)..... 100
- Figure 3.4 Batch growth kinetics of *Staphylococcus gallinarum* Δp at 7.5 L scale. (A) Biomass increase with DOT maintained at 40% (B) the corresponding OUR, CER and Agitation profiles. Error bars represent one standard deviation around the mean (n=3, average of 3 fermentations). Fermentations performed as described in Section 2.2.2. A summary of fermentation performance is provided in Table 3.2. 104
- Figure 3.5 RQ profile for the 7.5L scale batch fermentation of *Staphylococcus gallinarum* Δp 105
- Figure 3.6 Fed-batch growth kinetics of *Staphylococcus gallinarum* Δp at 7.5L scale using a maltose feed.(A) showing cell growth, the maltose feed and PGDM production. (B) DOT and the aeration rate. (C) Agitation, CER and OUR (Off-gas analysis) as fermentation progresses. The error bars represent one standard deviation about the mean (n= 3, average of 3 fermentations).Fermentations performed as described in Section 2.2.3. A summary of fermentation performance is provided in Table 3.1. 111
- Figure 3.7 Fed-batch growth of *Staphylococcus gallinarum* Δp on 21B medium and 500g.L⁻¹ maltose feed at 7.5L scale with A) showing the maltose feed rate and feed profile applied to the culture and B) showing the RQ. 112
- Figure 3.8 Fed-batch growth kinetics of *Staphylococcus gallinarum* Δp at 7.5L scale using dual Maltose and yeast extract feed.(A) Biomass and pregallidermin production. (B) Cumulative maltose (500g.L⁻¹) and yeast extract (300g.L⁻¹) feed addition. (C) Aeration and DOT (set-point minimum 30%). Error bars represent one standard deviation around the mean. (n=2).Fermentations performed as described in Section 2.2.3. A summary of fermentation performance is provided in Table 3.2. 119
- Figure 3.9 Fed-batch growth of *Staphylococcus gallinarum* Δp at 7.5L scale using dual maltose and yeast extract feed with A) showing the feed rates of the 500g.L⁻¹ maltose feed and 300g.L⁻¹ yeast-extract feed B) the agitation rate and CER and C) the RQ. Error bars represent one standard deviation around the mean. (n=2). Fermentations performed as described in Section 2.2.3. 120
- Figure 3.10 Fed-batch growth kinetics of *Staphylococcus gallinarum* Δp at 30L scale using dual feed of maltose and yeast extract.(A) Biomass and pregallidermin production. (B) Cumulative total maltose (600g.L⁻¹) and yeast extract (200g.L⁻¹) feed added to culture and (C) showing the feed rates. Fermentation performed as described in Section 2.2.4. A summary of fermentation kinetics is provided in Table 3.2 125
- Figure 3.11 Fed-batch growth of *Staphylococcus gallinarum* Δp at 30L scale using dual feed of maltose and yeast extract with A) showing aeration and DOT (set-point 30%) and B)showing Agitation and CER (Determined by the BIOStat C-Plus as a percentage of total exit gas). Fermentation performed as described in Section 2.2.4. A summary of fermentation kinetics is provided in Table 3.2. 126

Figure 4.1 Downstream processing options for the purification of pure gallidermin from the PGDM. (A) trypsinization in-situ after cell removal. (B) trypsinization of crude PGDM directly after initial capture from solution. (C) showing the DSP sequence for trypsinization after purification of PGDM. 141

Figure 4.2 The adsorption profile of PGDM from clarified culture broth on Amberlite XAD-7. Adsorption performed as described in Section 2.3.3. A summary of the DSP sequence and the performance for each component process is provided in Table 4.2. 144

Figure 4.3 Washing and desorption of PGDM from Amberlite XAD-7 resin with A) representing the yeast extract impurities removed by each successive wash and B) the PGDM captured in solution when eluted with 100% methanol and 60% methanol. Wash and desorption performed as described in Section 2.3.4. A summary of the DSP sequence and the performance for each component process is provided in Table 4.2. 148

Figure 4.4 Chromatograms for ion exchange of pregallidermin product. A) elution profiles of the PGDM solution at 20 dilutions, 10 dilutions and no dilution. B) load profiles of the PGDM solution at 20 dilutions, 10 dilutions and no dilution (raw solution injection). Ion exchange chromatography performed as described in Section 2.3.5. A summary of the DSP sequence and the performance for each component process is provided in Table 4.2. 152

Figure 4.5 Identification of PGDM. A) HPLC chromatogram of the PGDM product solution obtained from Ion Exchange chromatography show the retention times 8.4 min and 8.9 min for variants PGDM 1 and PGDM 2 respectively. B) Mass-spectrum of the same product solution using MALDI-MS, the spectrum shows the relative abundance of ions (%) relative to the mass of ions (m/z). The molecular masses obtained correspond to values obtained by Valsesia *et al.*, (2007). 157

Figure 4.6 The trypsinization of PGDM to produce gallidermin. A) HPLC chromatogram of the PGDM product solution 6 min after the introduction of Porcine Trypsin, the presence of Gallidermin with a retention time of 9.1 minutes is notable, indicating the conversion of PGDM to active Gallidermin. B) Mass Spectrum of the same sample, confirming the presence of Gallidermin (mass: 2166) along with PGDM variant 1. The Maldi-MS spectrum shows the abundance of the ions (%) relative to the mass of ions (m/z). 158

Figure 4.7 MALDI-TOF mass spectrum of Gallidermin) Gallidermin (2168.1) obtained from the near-total trypsinization of PGDM product solution, note the presence of small traces of PGDM variant 1 (3411.2). B) commercially produced gallidermin, from Enzo Life Sciences. The Maldi-MS spectrum shows the abundance of the ions (%) relative to the mass of ions (m/z). 159

Figure 4.8 Summary of the final overall process used for the production of PGDM, including the finalised DSP sequence that was used to achieve the PGDM yields and purity outlined in Table 4.2 169

Figure 5.1 Contour plots of microscale XAD-7 adsorption/desorption data at different broth pH values for adsorption and wash pH values for elution: (A) the

amount of impurity removal, the colour bands represent the sum of all impurity peak areas in mAU on an HPLC chromatogram; (B) the concentration of eluted PGDM with colour bands representing the eluted PGDM in mg.L^{-1} and (C) the purity of the eluted PGDM with the colour bands displaying the percentage purity (%) of the PGDM. Microscale method performed as described in Section 2.7.3..... 175

Figure 5.2 The Stability of PGDM and GDM under varying pH. (A) PGDM and (B) GDM in microwells buffered at pH 6, 7 and 8 over a 24 hour time span, maintained at 25°C and shaken at 1200 rpm. Microscale studies performed as described in Section 2.6.2. Error bars represent standard error. 178

Figure 5.3 The Stability of PGDM and GDM under changing temperature. (A) PGDM and (B) pure GDM in microwells at 25 °C and 37 °C, buffered at pH 7 over a 24 hour time span and shaken at 1200 rpm. Microscale studies performed as described in Section 2.6.2. Error bars represent standard error. 182

Figure 5.4: Contour plots of microscale XAD7 product elution data at different values for elution buffer methanol content and ionic strength of H_2SO_4 in the acidified water fraction. (A) Showing the impact on PGDM product purity. The coloured bands represent the percentage purity (%) of the recovered PGDM product in comparison to the all eluted components. (B) Illustrates the impact on product recovery with the coloured bands representing the concentration of recovered PGDM in g.L^{-1} . Microscale method performed as described in Section 2.7.2..... 185

Figure 5.5 Contour plots of microscale XAD-7 adsorption/desorption data on the impact of increasing the ionic strength of the wash buffer and including methanol. A) impurity removal from the XAD-7 resin beads, with the coloured bands representing the sum of impurities removed in mAU as determined by HPLC, B) the purity of PGDM product eluted after the Methanol/high ionic strength buffer wash, the coloured bands represent percentage purity (%). C) the PGDM product yield upon elution after resin wash with the Methanol/high ionic strength buffer, the coloured bands represent PGDM concentration in g.L^{-1} . Microscale method performed as described in 2.7.1 188

Figure 7.1: Flowsheet representing the platform lantibiotic production process with integrated microscale methods for process optimization and rapid product analysis..... 209

Figure 7.2: How the rapid manufacturing and analysis platform (from figure 7.1) can become part of a complete antibiotic design and manufacturing process, with the microscale methods generating process and product data that can optimize manufacture by providing feedback to both process and antibiotic development. 209

List of Tables

| | |
|---|-----|
| Table 1.1 Relationship of physical properties to downstream processing | 56 |
| Table 2.1 Composition of media and feed solutions used in the various fermentations | 70 |
| Table 3.1 Summary of Fermentation Strategy | 136 |
| Table 3.2 Summary of Average Fermentation Kinetics | 137 |
| Table 4.1 Summary of wash variation data | 149 |
| Table 4.2 Purification table summarising PGDM step yield and purity for the whole downstream process sequence | 161 |
| Table 5.1 Purification table summarizing the PGDM step yield and purity for the whole downstream process sequence | 195 |
| Table 5.2 Purification table summarizing the step yield and purity for the redesigned downstream process sequence | 195 |

Nomenclature

| Abbreviation | Description |
|--------------------------------|--|
| °C | Degrees Centigrade |
| Å | Angstrom (1×10^{-10} m) |
| CER | Carbon dioxide evolution rate |
| Cys | Cysteine |
| Da | Daltons |
| DAD | Diode Array Detector |
| DCW | Dry Cell Weight |
| Dha | 2, 3 Didehydroalanine |
| Dhb | (Z)-2,3-didehydrobutyrine |
| DNA | Deoxyribonucleic Acid |
| DOT | Dissolved Oxygen Tension |
| DSP | Downstream Process |
| FDA | Food and Drug Administration |
| g.g ⁻¹ | Grams per Gram |
| g.L ⁻¹ | Grams per Litre |
| GC-MS | Gas Chromatography followed by Mass spectrometry |
| GDM | Gallidermin |
| GDP | Gross Domestic Product |
| GRAS | Generally recognised as safe |
| h | Hour |
| H ₃ PO ₄ | Phosphoric Acid |
| HI | Hydrophobic Interaction |
| HPLC | High Performance Liquid Chromatography |
| IEX | Ion Exchange |
| IU | International Units |
| kDa | Kilo-daltons |
| K _L a | Volumetric Oxygen Mass Transfer Coefficient |
| L | Litre |
| Lan | Lanthionine |
| m | Metre |
| M | Molar (moles per Litre) |
| m/z | Relative mass of ions |
| MALDI | Matrix-assisted laser desorption/ionization |
| MALDI-TOF | Matrix-assisted laser desorption/ionization-Time of Flight |
| mAU | milli-Absorbance Units |
| MeLan | (2S, 3S, 6R)-3-methylanthione |
| MeOH | Methanol |
| mg | Milligram |
| mL | Millilitre |

| | |
|------------------|--|
| mmol | Millimolar |
| MS | Mass Spectrometry |
| NaCL | Sodium Chloride |
| nm | Nanometer |
| NMR | Nuclear Magnetic resonance |
| O ₂ | Oxygen |
| OD | Absorbance Units |
| OTR | Oxygen Transfer Rate |
| OFAT | One factor at a time |
| OUR | Oxygen uptake rate |
| PGDM | Pregallidermin |
| PPG | Polypropylene Glycol |
| Q _{air} | Volumetric flow rate of air |
| R & D | Research and Development |
| RO | Reverse Osmosis |
| rpm | Revolutions per minute |
| Ser | Serine |
| STR | Stirred tank reactor |
| Thr | Threonine |
| USD | Ultra Scale-Down |
| UV-VIS | Ultraviolet-Visible Light |
| v/v | Concentration volume divided by volume |
| vvm | Gas volume flow per unit of liquid volume per minute |
| w/v | Concentration weight divided by volume |
| w/w | Concentration weight divided by weight |
| µm | Micrometer |

1. Introduction

1.1.1 Need for new antibiotics

The emergence of antimicrobial resistance over the past few decades has been declared a global crisis. A report commissioned by the UK government predicts that over the intervening years until 2050, antibiotic resistance will have caused 300 million premature deaths and caused \$100 trillion in losses to the global economy (O'Neill, 2014). The overuse of antibiotics within global health systems has resulted in the emergence of these antibiotic resistant microorganisms (Wenzel *et al.*, 2012; Okeke *et al.*, 1999; Yoneyama & Katsumata, 2006). These cover a wide range of illnesses, from mutated strains of tuberculosis to a deadly version of *Staphylococcus aureus* (methicillin resistant *S.aureus* or commonly abbreviated as MRSA) that has been responsible for many deaths in western hospitals. However, it has been noted that the use of antibiotics is not being scaled back; rather with the economic emergence of much of the developing world, consumption is expected to increase (Reardon, 2014). This would lead to an increase in bacterial mutations which would in turn leave more of the present selection of antibiotics ineffective. The resultant impact on human health could be devastating, thus it becomes imperative that modern medicines keep pace with the changing bacteria.

There are also other very compelling reasons for the pursuit of new antibiotic treatments, chief among which is the economic impact of not being able to tackle infectious diseases. A well publicised example is MRSA, which has \$8 billion in annual treatment costs in the US alone (Smith & Hillman, 2008) and is

responsible for nearly 20,000 deaths every year (Joo & Otto, 2015). If a single infection can have such a massive economic impact, the cost of a whole range of untreatable infections for the global economy would be dire. Research shows that large scale infection not only has enormous treatment cost, but also causes a negative impact on GDP growth rates (O'Neil, 2014; Gallup & Sachs, 2001). The added burden on global healthcare systems would be enormous.

Thus the search for alternative antibiotics becomes crucial in the fight against infectious disease and for the advancement of human socio-economic development. This is where the new field of synthetic biology offers a golden opportunity, as it allows for the generation of artificial antibiotics. The ability to selectively modify biological molecules and give them desirable properties has the potential to provide solutions to infectious disease (Field *et al.*, 2015). The added benefit of being able to grow these artificial antibiotics within biological host organisms, specifically designed for purpose, potentially offers a cheap manufacturing pathway, that makes synthetic biology a vital tool in the battle against drug resistant infection (Heinmann & Panke, 2006).

1.1.2 Synthetic Biology based solutions

Synthetic biology promises to deliver a large variety of new products and find many applications in both existing and future technologies (Zhang *et al.*, 2016; Ferber, 2004). The most high-profile application is within healthcare and biopharmaceuticals, with synthetic biology promising custom drugs that are capable of treating an ever increasing plethora of diseases. These include applications such as smart-drugs, capable of tracking down certain types of disease vectors and cancers based on chemical signal recognition 'built-in' to

the biological products (Andrianantoandro *et al.*, 2006). They also find numerous potential applications as diagnostic devices, with researchers already having developed cells capable of changing colour and glowing.

Another very high profile application is found in the production of Biofuels (Patel *et al.*, 2017). Synthetic biology techniques would allow the 'fabrication' of host organisms developed specifically to feed on certain material and produce fuel for industry and transport (Keasling & Chou, 2008). Similarly there is huge potential for using synthetic biology to replace existing chemical production methods, specifically the production of optically pure enantiomers which remain a challenge for the purely chemical techniques (Lye *et al.*, 2002). Most industrial applications for synthetic biology utilize the concept of biological organisms as a factory (Ferber, 2004) and will rely on the ability of researchers to have complete control of the biological systems applied to any process.

There are numerous other possible applications, such as in food production and use in agriculture. Researchers have also looked at creating biological computers by utilizing whole sets of biological systems in smart feedback loops (Benner & Sismour, 2005; Ferber, 2004). Biological toxin detection systems for the environment have also been suggested.

The list of potential synthetic biology applications is seemingly endless; however it is dependent on a complete understanding of biological systems. The possible rewards are great, as has been demonstrated by the use of synthetic biological techniques in some existing systems (Andrianantoandro *et al.*, 2006). However, there must be adequate resources made available for

rigorous testing and research if effective and completely safe applications are to be found. Furthermore, the development of the tools for synthetic biology remain in the initial stages (Kuthning *et al.*, 2016), with greater effort required to obtain a comprehensive understanding of biological processes before their modification to the necessary degree becomes cost effective and less challenging (Benner and Sismour, 2005).

1.2 Synthetic Biology for novel antibiotic development

1.2.1 Principles of Synthetic Biology

Synthetic biology is the name given to a multidisciplinary field that combines current knowledge in the fields of the biological sciences with techniques and methodologies developed for engineering (Garcia-Ojalvo *et al.*, 2016; Andrianantoandro *et al.*, 2006; Heinemann & Panke, 2006). It can be difficult to use a standard definition for synthetic biology, with the definition varying based on the expertise of the individuals involved. To the molecular biologist, the field deals with the modification (in some cases artificial fabrication) of cellular microorganisms. The chemist would say synthetic biology involves designing synthetic systems that replicate the behaviour of biological systems. The computer scientist calls it the use of artificial intelligence and simulations to better understand biological systems, while to the engineer it involves utilizing biological components to build new 'devices' in order to achieve desirable outcomes (Benner & Sismour, 2005).

Regardless of how it is defined, the overarching aim of synthetic biology is the ability to utilize living microorganisms as 'factories' for the production of novel products or compounds that are too difficult to manufacture by chemical synthesis (Garcia *et al.*, 2016; Ferber, 2004). In many cases, chemical synthesis of compounds, such as proteins or antibiotic molecules requires a large number of expensive manufacturing stages, making them prohibitively expensive (Lye *et al.*, 2003). Living cells on the other hand can utilize their complex cellular machinery in order to perform the synthesis within themselves, greatly reducing the overall stages required within the production process and effectively reducing the chemical synthesis stages to a limited number of steps (Khosla & Keasling, 2003). Thus there is great hope that the use of synthetic biology will allow the production of a large number of valuable compounds cheaply and in a much more environment-friendly manner.

The economic and environmental benefits of synthetic biology make it advantageous in comparison to certain chemical processes. However it is not currently possible to replace these production methods with biological ones. This is due to the limited understanding of the all complexities associated with the living cell (Smanski *et al.*, 2016). Engineering non-biological systems is made considerably easier based on a full understanding of all the component parts, mainly because the system components are man-made. In comparison biological systems are far more complex, with many cellular interactions yet to be deciphered (Benner & Sismour, 2005).

Living cells will usually never be found individually, acting instead in concert with a mass of other cells, in either tissues or organs to respond to various

stimuli. This gives rise to great difficulty when attempting to utilize the wild-type of the cells for specific purposes; they usually will not grow very well under such circumstances (Andrianantoandro *et al.*, 2006). This is where the biological knowledge gathered from fields such as genetic engineering, metabolic engineering and molecular biology can be utilized to modify and adapt the wild-type cells to a synthetic environment. Process engineering techniques can then be utilized to scale-up the processes to full scale production facilities

The development of novel organisms by genetic manipulation and metabolic engineering procedures is work conducted at the microlitre or millilitre scales. In order to produce commercially useful quantities of product, it becomes vital that the same organisms can be cultured at large scale. This translation from the lab-bench to pilot scale to commercial scale culture remains a significant challenge (Chubukov *et al.*, 2016).

The development of viable scale up strategies involves detailed process characterisation in order to identify the key stress factors and process parameters influencing cell growth and product yield. However, it is notable that there is no common generally applicable scale-up strategy, with the most commonly prescribed scale-up techniques suggesting that engineering characteristics such as impeller tip speed, superficial gas velocity, mixing time, volumetric mass transfer coefficient or power per unit volume should remain constant (Junker, 2004).

It has been suggested that using the power to volume ratio and the oxygen mass transfer coefficient, k_La , is the dominant scale up strategy in the industry

(Nuebauer & Junne, 2016). Studies conducted at UCL by Islam *et al.*, (2007) and Gill *et al.*, (2008) demonstrated that cultures grown at different scales under conditions of matched k_{La} values had a greater degree of reproducibility than those grown under a matched power to volume ratio (P/V_g). Thus, it is suggested that for highly aerobic fermentations, maintaining the k_{La} may be an effective strategy for bench-scale to pilot scale translation.

Recent work by Voulgaris *et al.*, (2016) utilized a scale-up strategy where the fermentation of a modified *Escheria coli* was translated from 1 L scale to 20 L scale by maintaining the dissolved oxygen levels (DOT). This strategy coupled with the maintenance of the substrate feed rate at the various scales may be relevant to the current research involving *Staphylococcus gallinarum* Δ *gdmP::aphIII*.

It is hoped that with greater understanding of the various component processes in biological systems, it will eventually become possible to develop totally new organisms from scratch, using an existing cell as a chassis for the efficient large scale production of novel, economically important compounds or creating completely new 'artificial' living organisms that have been designed to do the same job (Smanski *et al.*, 2016; Garcia-Ojalvo *et al.*, 2016; Heinemann & Panke 2006).

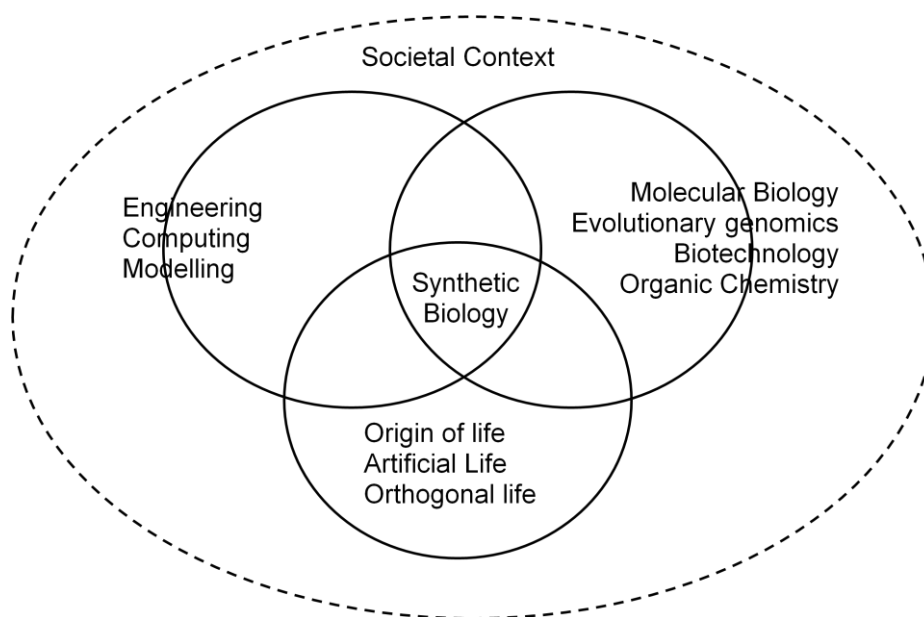


Figure 0.1.1 The various component disciplines of Synthetic Biology an interdisciplinary field, adapted from (www.esf.org)

1.2.2 *Stapylococcus gallinarum* Tü3928 and the modified *Stapylococcus gallinarum*Δ*gdmP::aphIII*

Staphylococcus gallinarum Tü3928 was first identified in the early 1980s (Devriese *et al.*, 1983) with Gallidermin, the lantibiotic it produces, first described by Günther Jung's group at the University of Tübingen in 1988 (Kellner *et al.*, 1988). In nature the organism can be found living on chicken crests. The species displays novobiocin resistance and a wide range of positive carbohydrate reactions.

Early research with the organism to understand the lantibiotic product machinery involved site-directed mutagenesis on the lantibiotic structural genes allowing the creation of modified variants of Gallidermin, identifying the organism as a good candidate for target oriented peptide engineering (Ottenwälder *et al.*, 1995). It was determined that the mode of action of lantibiotic compounds resulted in auto-toxicity to the producer strains (Sahl *et*

al., 1998), meaning that lantibiotic yield from fermentations involving *S.gallinarum* Tü3928 are low (Fiedler *et al.*, 1999; Hille *et al.*, 2001).

In order to overcome this limit on lantibiotic yield, Valsesia *et al.*, (2007) created a mutant strain of *S.gallinarum* Tü3928 called *Staphylococcus gallinarum*Δ*gdmP::aphIII* (*Staphylococcus gallinarum* Δ*p*), that lacked an extracellular protease (referred to as GdmP) responsible for activating the inactive lantibiotic precursor peptide into the active lantibiotic. The mutant was an insertional-deletion, with genes for Kanamycin resistance inserted in place of the deleted GdmP expressing genes. Later work by Medaglia (2009) with *S.gallinarum* Δ*p* showed that the inactive gallidermin precursor, pregallidermin (PGDM) produced was almost 30 times less toxic to *S.gallinarum* Tü3928 than activated gallidermin (GDM).

The well characterised genetic machinery of *S.gallinarum* Tü3928 and the relative ease with which it could be modified in order to produce novel GDM and PGDM variants was the reason behind its choosing as the test bed organism in this research. Additionally, it enabled the testing of lantibiotic precursor peptide production at scale.

1.2.3 Creation of ‘chassis’ organisms

The ability to use synthetic biology for the modification of organisms in order to achieve desired compounds is of huge potential benefit to the biotech industry. However, it may not be efficient to utilise large amounts of resource on engineering countless different organisms, an approach which may also be

limited by the complexity of existing biological systems (Heinemann & Panke, 2006).

A solution to this problem may be to use synthetic biology approaches to express the targeted genes in selected 'chassis' organisms that have been well studied and characterised, in order to improve production of the desired compound and obtain higher yields (Patel *et al.*, 2017). In the case of PGDM production, Valsesia (2009) demonstrated this to be possible by transferring the pregallidermin gene cluster to a *Staphylococcus aureus* mutant, resulting in a 1.3 fold higher yield of PGDM than in *S.gallinarum* Δp under equivalent conditions.

Chassis organisms could be created by removing portions of their genome in order to reduce their complexity (Andrianantoandro *et al.*, 2006). Recently, the first such organism was constructed using this methodology that has a genome smaller than that of the smallest known natural bacterium (Hutchinson *et al.*, 2016).

1.2.4 Advantages and limitations of developing novel organisms

The creation of novel organisms specifically to serve as factories for biological compounds could provide several advantages over native producer strains. Firstly, the novel organisms could be created from existing strains that are very well researched and have been used in industry for a long time, allowing production to be optimised efficiently by using rational or semi-rational host

engineering strategies. Secondly, organisms could be engineered to be more genetically stable, consistently producing the desired compounds to the required standards. Finally, the creation of novel chassis organisms could allow the production of products from organisms that are currently not possible or difficult to culture e.g. rare terrestrial or marine organisms (Zhang *et al.*, 2016).

However, it is unlikely that an organism can be created which is able to express metabolites from all available biosynthetic pathways, especially considering that one of the key strategies to create such organisms is to minimise its genome (Juhas, 2016). In comparison to native producer strains, synthetic organisms are unlikely to possess all the cellular factors necessary for production of the desired compound, meaning they will have to be introduced, which could result in incompatible regulatory systems. Additionally, the creation of organisms by minimizing their genome may not yield organisms that operate with precision and reliability (Andrianantoandro *et al.*, 2006). Neither is it necessary that an organism with a minimum genome would allow production to be optimised efficiently.

1.2.5 Application of Synthetic Biology to Natural Product Synthesis

Products produced by living organisms tend to be more environmentally friendly or 'natural' (Zhang *et al.*, 2016). This is mainly due to the removal of large numbers of processing steps required in chemical synthesis of the same product (Ross *et al.*, 2010), often using corrosive and hazardous chemical substances. The complex mining and refining processes providing raw

materials for chemical synthesis serve to increase the cost and environmental footprint of many substances that are vital to the global economy. In essence this makes them more artificial and less 'natural' than those produced by biological systems.

The scope of synthetic biology to produce large numbers of natural products is vast (Smanski *et al.*, 2016; Baker *et al.*, 2006). It is hoped that a short to medium-term application can be the replacement of complex chemical manufacturing processes by highly optimized biological ones that are less resource intensive. The potential exists for highly modified living cells to produce numerous substances for all manner of applications such as pharmaceuticals, fuel, diagnostics and purification technologies (Ferber, 2004).

An added advantage of synthetic biology is the fact that the production systems are living cells, part of biological systems; hence the products should be safer for use in living organisms than comparable products based on chemical synthesis, indeed a few microbial strains of interest are commensal organisms (Joo & Otto, 2015). However, this adds another layer of complexity to developing biological technologies as keeping the modified organisms healthy and in 'production mode' requires stringent monitoring of the cellular environments (Andrianantoandro *et al.*, 2006). Development of more robust variants of the host organisms, capable of surviving harsher environmental conditions will aid in the process of bringing more synthetic biological processes to market (Baker *et al.*, 2006).

It is of note that although much of the research described will find future applications, synthetic biology is already in use to produce many valuable compounds. Much of global penicillin production is based on engineered organisms, as is most of the biosynthetic 'human' insulin. These technologies made the specific substances much cheaper and production more easily scalable than conventional production methods; as an example, prior to producing human insulin biosynthetically, it was taken from pigs, a method ill suited to provide sustained long term global supplies.

1.3 Lantibiotics

1.3.1 Basic Structure

Lantibiotics are a class of antibiotic peptides named after the lanthionine residues that they contain. The lanthionine residues in these compounds, which are formed very rarely in nature, form ring structures through thioether bonding (Van Heel *et al.*, 2013). Lantibiotics usually also contain a methyl-substituted lanthionine derivative, (2S, 3S, 6R)-3-methylanthione (figure.1.2) and typically (though not always) will contain the unsaturated amino acids 2, 3 Didehydroalanine (Dha) and (Z)-2,3-didehydrobutyrine (Dhb) (Chatterjee *et al.*, 2005; Jung & Sahl, 1991; Kuipers *et al.*, 1996).

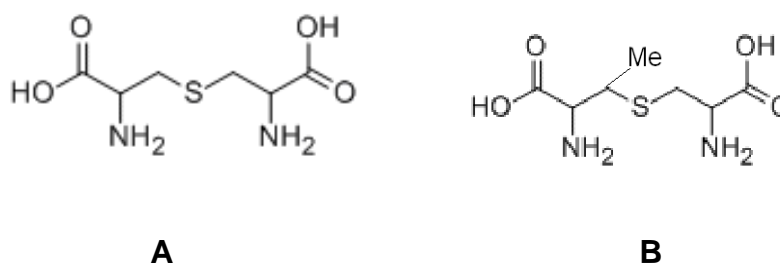


Figure 1.2 Structure of (A) Lanthionine and (B) Methylanthionine residues

The molecules will also contain other structures that are introduced due to post-translational modification (Montalbán-López *et al.*, 2015); D-alanine, 2-oxybutyrate, lactate and pyruvate are just a few of those found (Kuipers *et al.*, 1996). It is of note that almost one-third of all amino acid residues present within the original peptide molecules undergo post-translational modifications during biosynthesis to form the final lantibiotic.

Lantibiotic peptides are very small (<5 kDa) (de Freire Bastos *et al.*, 2014) and about 5 nm long (Kuipers *et al.*, 1996). The thioether rings in lantibiotics are believed to be responsible for their antimicrobial properties. It is also believed that the same thioether rings allow for recognition of the peptides during biosynthesis, allowing for appropriate immune responses and the prevention of proteolytic degradation (Bellancini, 2015; Chatterjee *et al.*, 2005).

1.3.2 Properties of Lantibiotics

There are a number of basic properties that are common to Lantibiotics. These properties are responsible for the antimicrobial and antibiotic function of the peptides. Indeed alteration in them will often result in the loss of activity (Zhou *et al.*, 2015; Cotter *et al.*, 2005; Rollema *et al.*, 1995).

Thiol Bridge Formation: All lantibiotic molecules will form thiol and thioether ring structures due to the presence of lanthionine and methyllanthionine residues (Tabor, 2011). The ring structures represent the unifying motif within all lantibiotic molecules and are important for microbial activity as well as structural stability (Nagao *et al.*, 2006).

Presence of Dha/Dhb residues: Most lantibiotics possess either of the unsaturated and dehydrated amino acid residues Dha or Dhb (Tabor, 2011; Cotter *et al.*, 2005). In the molecules that do possess these residues, it has been found that they are essential for activity e.g. in the Type A (I) lantibiotic Nisin, it has been found that the modification of the Dha residue at position 5 leads to a loss of antimicrobial activity (Chan *et al.*, 1996).

Presence of a Hinge region: All lantibiotic molecules contain a hinge region; any region flexible or rigid that connects the thioether ring domain to the other domains of the lantibiotic (Chatterjee *et al.*, 2005). It has been shown that changes to the hinge region can have negative effects for the antimicrobial activity of the peptides (Zhou *et al.*, 2015).

Presence of a Charge: All type-A lantibiotics are cationic (Nagao *et al.*, 2006). Type-B lantibiotics have not been found to possess any charge. In type-A lantibiotics the charge influences solubility of the peptides and is believed to contribute to their pore forming abilities and bactericidal activity (Van Staden, 2015; Cotter *et al.*, 2005).

Binding to Lipid II in microbes: Most lantibiotics have been found to bind to lipid II in the microbial cell wall (Islam *et al.*, 2012; Cotter *et al.*, 2005). Lipid II is an essential intermediate in cell wall biosynthesis, the lantibiotic Nisin uses Lipid II as a docking molecule and subsequently forms pores in the cellular membrane (Nagao *et al.*, 2006).

1.3.3 Structural grouping of Lantibiotics

Over 100 different Lantibiotics are known, all with varying structures, size and mode of action (Ongey & Neubauer, 2016). Originally these were classified as either Type A or Type B dependant on the topology of their ring structures and biological activities (Jung & Sahl, 1991), though new classification schemes have been proposed based on an analysis of their biosynthetic pathways, the original scheme is still in general use (Suárez *et al.*, 2013;Tabor, 2011). The classification of the different types is described in the following sections.

1.3.4 Type A Lantibiotics

Type-A lantibiotics form elongated screw shaped structures and are amphipathic when in solution (Al-Mahrous & Upton, 2011). They range in length from 20 to 34 amino acid residues and have a net positive charge. Their bacterial action was initially thought to be based on pore formation to cause permeabilization of the cell membranes; however recent advances have shown that a number of lantibiotics interfere with peptidoglycan biosynthesis by binding to Lipid II, this behaviour is not limited to Type-A only (Kuipers *et al.*,1996).

Type-A Lantibiotics can be further divided into Type A (I) and Type A (II) based on the number of post-translational enzymes involved in the creation of their Lanthionine residues, and a third type, two-component lantibiotics in which two structurally different peptides act synergistically to kill the target organism (Islam *et al.*, 2012). Type A (I) lantibiotics have their lanthionine residues formed by the action of two distinct enzymes, named LanB and LanC. Type A (II) lantibiotics have theirs formed by a single enzyme, LanM (Gomes *et al.*, 2017).

Type A lantibiotics are generally flexible molecules with a hinge region between their C and N-terminal rings, however there are some molecules within Type A (I) that show some inflexibility in water (Pep5) (Kuipers *et al.*, 1996). The prototype lantibiotic for Type A (I) is Nisin (Figure 1.3A), one of the most extensively studied Lantibiotics, due to its use in food preservation. The prototype lantibiotic within Type A (II) is Lacticin 481 (fig 1.3B).

1.3.5 Gallidermin

Gallidermin is a natural variant of Epidermin, produced by *Staphylococcus gallinarum* Tü3928. The only difference between the peptides is the interchange of a Leucine residue in Gallidermin for an Isoleucine residue in Epidermin (Kellner *et al.*, 1988).

Gallidermin has characteristic lanthionine rings between residues 3 and 7, plus a hinge region from residues 12 to 15. The average length of the peptide is 30 Å and the average diameter ranges between 8 to 10 Å, giving the peptide a screw shape. It is an amphiphilic, screw shaped peptide with a lipophilic C-terminus and a hydrophilic N-terminus (Kuipers *et al.*, 1996).

Gallidermin possesses the same putative lipid II binding motif as nisin; however, it is considerably shorter (22 amino acids in gallidermin, compared to 34 in nisin). It has been demonstrated that pore formation in the bacterial cell membrane by gallidermin depends on membrane thickness, and that it is the interaction with lipids I and II rather than pore formation that contributes to its

bactericidal activity. The superior activity of gallidermin over nisin in a cell wall biosynthesis assay may explain its high killing potency (Bonelli *et al.*, 2006).

It has been demonstrated that nisin and gallidermin not only bind to lipid II but also to the lipid intermediates lipid III (undecaprenol-pyrophosphate-N-acetylglucosamine) and lipid IV (undecaprenol-pyrophosphate-N-acetylglucosamine-N-acetyl-mannosamine) of the wall teichoic acid (WTA) biosynthesis pathway. The specific interaction with the WTA precursors promoted pore formation in artificial lipid bilayers (Saising *et al.*, 2012).

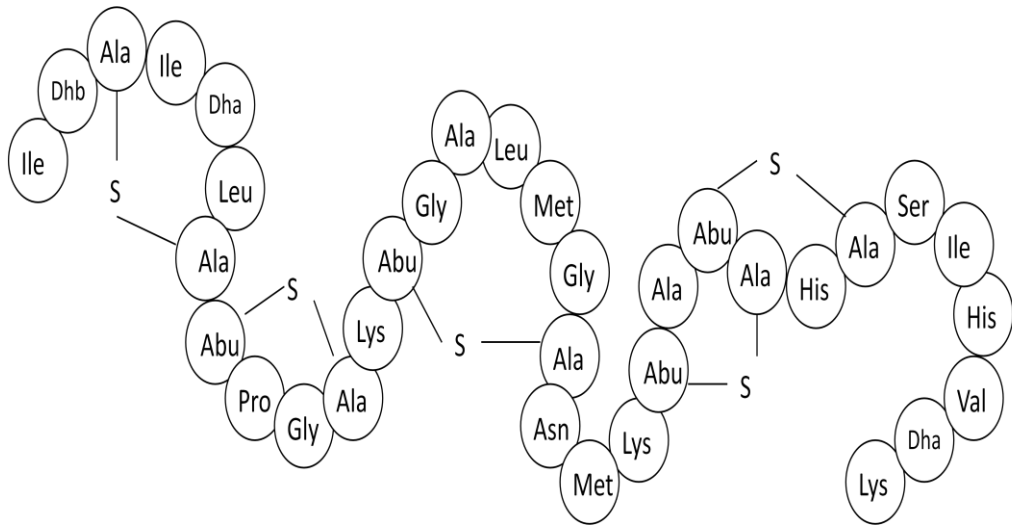
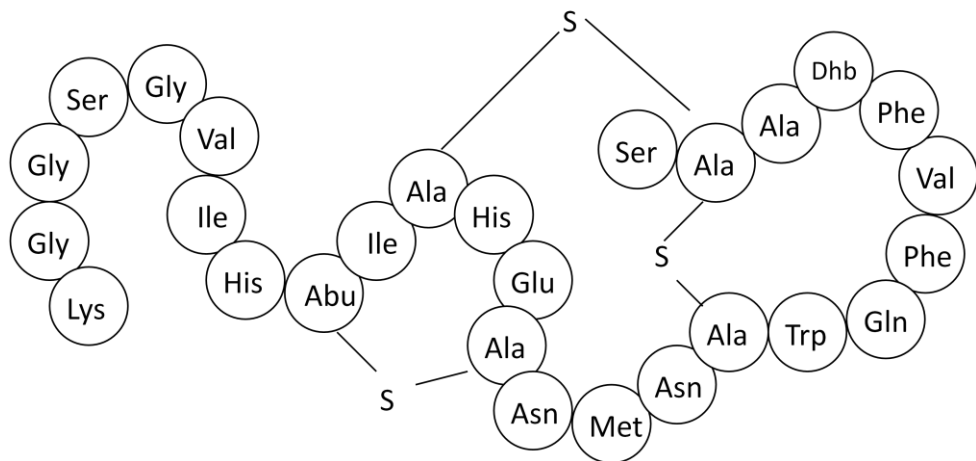
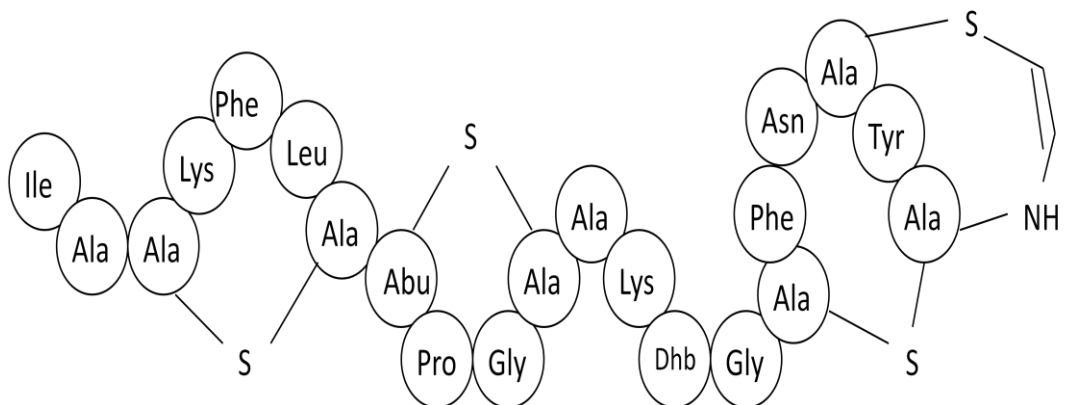
A**B****C**

Figure 1.3 The structure of (A) Nisin (amino acid residues and thioether rings), (B) Lactacin 481 and (C) Gallidermin, adapted from (Willey and Donk, 2007)

1.3.6 Type B Lantibiotics

Type B lantibiotics are globular in shape and from 19-20 amino acid residues long. They possess no net charge or a negative charge (Islam *et al.*, 2012), unlike Type A, but they are flexible molecules with a hinge region. Originally, their mode of activity was thought to be the inhibition of specific enzymes involved in cell wall biosynthesis however, they were later shown to also interact with lipid II (Brötz *et al.*, 1998). The representative lantibiotic for Type B is Mersacidin, illustrated in figure 1.4 A.

Actagardine is a Type B lantibiotic with a rigid and compact globular shape. The molecule has no net charge and contains three short β -sheets at the C-terminal end which provide stability (Zimmermann & Jung, 1997). The N-terminal ring is between residues 1-6 and the intertwined C-terminal rings are located between residues 7-12, 9-17 and 14-19.

However, Actagardine (figure 1.4B) has a single negative charge in solution at neutral pH. It is also notable for containing an oxidized C-terminal melan residue (Kuipers *et al.*, 1996).

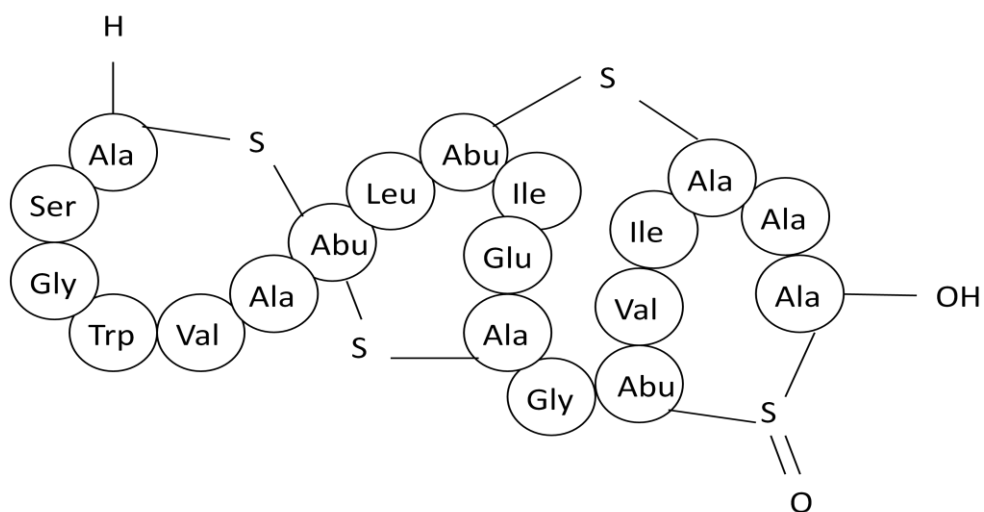
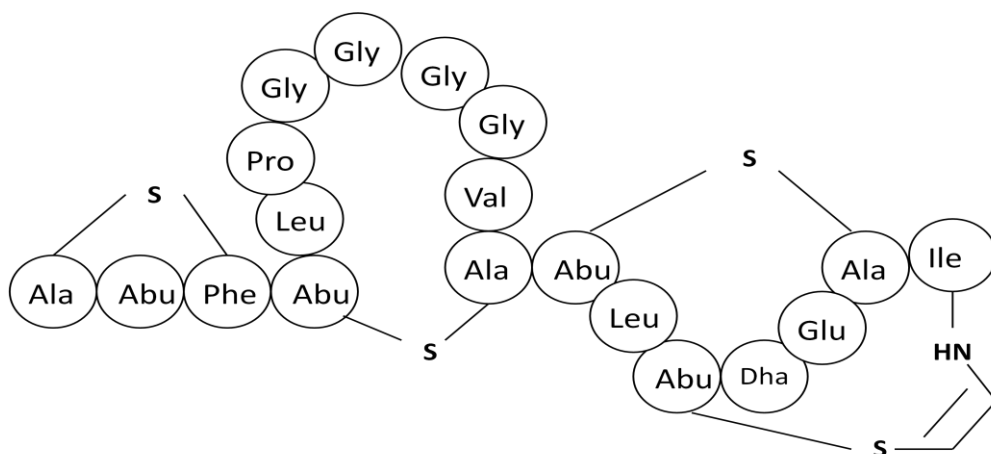
A**B**

Figure 1.4 The structure of type B lantibiotics (A) Mersacidin and (B) Actagardine (amino acids and thioether ring structures), adapted from (Willey and Donk, 2007).

1.3.7 Mode of Action

Lantibiotics have been shown to display a broad spectrum of antimicrobial activity owing to the structural diversity of the different types (Willey & Donk, 2007). Type A lantibiotics, which are positively charged, flexible elongated structures, have been shown to possess a dual mode of antibacterial action. They are capable of disrupting the bacterial cytoplasmic membranes by forming non-targeted pores (Zhou *et al.*, 2015) at micromolar concentrations; additionally when available in nanomolar concentrations they are also capable of blocking bacterial cell wall synthesis by binding to lipid II in the cell wall, preventing its incorporation into the peptidoglycan layer (Figure 1.5B) (Hechard *et al.*, 2002). The specific targeting of lipid II is promising from the perspective of developing a clinical product, as lipid II is only involved in bacterial cell synthesis, meaning lantibiotic compounds would show low cytotoxicity to animal cells. Additionally the bacterial cell walls usually possess a small amount of lipid II, which has a high turnover rate during peptidoglycan biosynthesis. Consequently lipid II represents an ideal target for antibiotic action (Breukink & Kruijff, 2006).

It is notable that when the lantibiotic nisin bound to lipid II in the bacterial cell cytoplasmic membrane, the pores formed had larger diameters and increased stability in comparison to pores formed when lipid II was absent (Wiedemann *et al.*, 2004). However the lantibiotic gallidermin, a Type A lantibiotic that also possesses the dual antibacterial mode of action, is considerably shorter than Nisin and thus the non-targeted pore formation depends on the membrane composition (Wenzel *et al.*, 2012; Bonelli *et al.*, 2006). However, gallidermin was still found to be very effective at killing bacterial cells based on the halt to

bacterial cell wall biosynthesis (Brotz *et al.*, 1998 b). The type B lantibiotics kill bacterial cells through their interaction with lipid II, which inhibits bacterial cell wall synthesis, however unlike type A, type B lantibiotics do not form pores in the cytoplasmic membrane (Brotz *et al.*, 1998). Thus, type A lantibiotics kill bacterial cells quicker than type B (Guder *et al.*, 2000).

1.3.8 Regulation of Biosynthesis: Quorum Sensing

All bacterial strains that produce lantibiotics have regulatory mechanisms for their production. Most of these mechanisms are based on quorum-sensing systems, which enable the bacteria to act in a coordinated manner (Ali *et al.*, 2017; Kleerbezem, 2004). The quorum-sensing mechanisms involve the production of peptide pheromones that accumulate during bacterial growth. Once a specific threshold concentration of peptides is reached, they trigger a signal transduction pathway that leads to target gene expression. The signal transduction pathway is based on two-component regulatory systems (Willey & van der Donk, 2007), which are mediated by the interaction of the peptide pheromone with its cognate receptor, a membrane-bound histidine kinase sensor protein (LanK for lantibiotics), which results in the phosphorylation of an aspartic acid residue of a response regulator (LanR in lantibiotics). This activates the transcription of target genes (Valesia, 2008).

An autoregulation mechanism was demonstrated for nisin production by *L. lactis*, in which the lantibiotic has been shown to act as a peptide pheromone (Kuipers *et al.*, 1995).

1.3.9 Lantibiotic auto-toxicity

Lantibiotics are a class of peptide antibiotics synthesized by a number of gram-positive bacteria, which show a broad spectrum of bactericidal activity against other gram-positive bacteria (Götz *et al.*, 2014; Willey & van der Donk, 2007). As such, any bacterial strain that produces antimicrobial compounds that are active against closely related strains must also protect itself against its product compounds (Chatterjee *et al.*, 2005).

In the case of lantibiotics, this immunity can be conferred by a specific immunity protein (LanI) and by specialized ATP binding cassette (ABC) transporter proteins, which are encoded by the LanFEG genes e.g. for the lantibiotic Pep5; a single Pepl peptide appears to bind at the membrane-cell wall interface, thereby masking the Pep5 target molecule. In comparison NisI, which is anchored to the outer face of the membrane by a lipoprotein signal sequence, intercepts the nisin to reduce its concentration in the immediate local environment. Although in many cases, LanI cannot confer full resistance and it functions cooperatively with the ABC transporters (Willey & van der Donk, 2007; Chatterjee *et al.*, 2005).

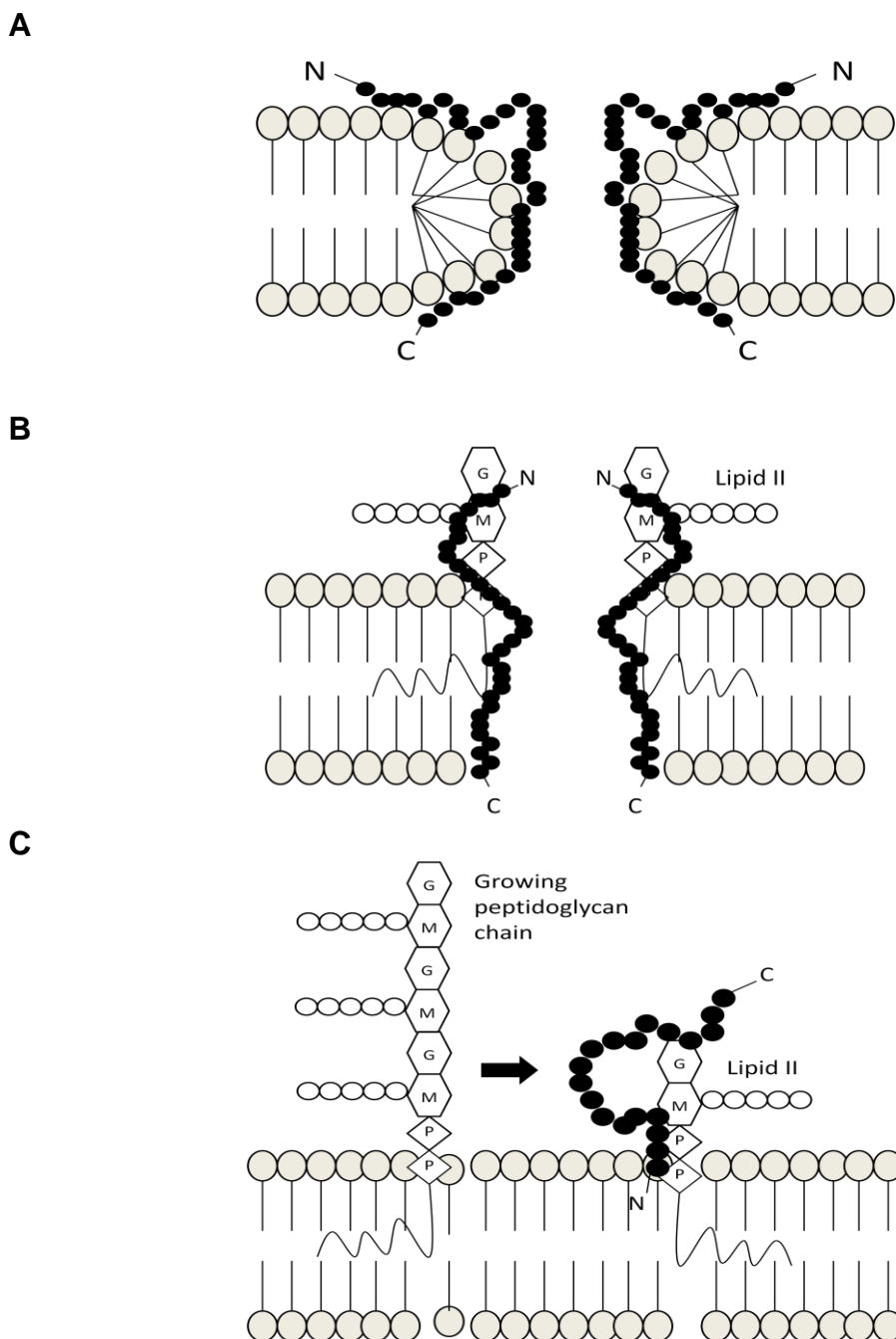


Figure 1.5 The modes of action of Type A and Type B lantibiotics with A) a type A lantibiotic (Nisin depicted by the black peptide chain) forming wedge like pores in the cell phospholipid layer at micromolar concentrations, B) a type A lantibiotic (depicted by Nisin) using lipid II as a docking molecule to form target mediated pores at nanomolar concentrations and C) a type B lantibiotic (Mersacidin) blocking cell wall synthesis by halting the incorporation of lipid II into peptidoglycan (Type A lantibiotics also possess this attribute). Adapted from (Hechard *et al.*, 2002)

1.3.10 Therapeutic potential

The only lantibiotic that currently has wide commercial application is Nisin, with its application in the food industry to prevent spoilage (Cotter and Ross, 2005) although it has not been used therapeutically (Field *et al.*, 2015). However, lantibiotics have been identified as having the potential to treat variety infections caused by *Clostridium difficile*, *Staphylococci*, *Enterococci*, and *Streptococci*. (van Heel *et al.*, 2011; Hancock & Sahl, 2006).

At the present time though, the most important application for lantibiotics would be there potential in the treatment of antibiotic resistant bacteria e.g. the type B lantibiotic Mersacidin has shown promise in the treatment of MRSA nasal colonization (Kruszewska *et al.*, 2004). Nisin was found to be active against vancomycin resistant *enterococci*, multidrug resistant strains of *Staphylococcus aureus* and *Streptococcus pneumoniae* (Severina *et al.*, 1998). Additionally nisin has shown potential in the treatment of *C.difficile*, by preventing the germination of clostridial spores, displaying killing kinetics similar to vancomycin when tested *in vitro* (Kerr *et al.*, 1997). Other potential therapeutic uses for lantibiotics could be in the treatment of cancer, in combating viruses, treatment of inflammation and pain relief (Gomes *et al.*, 2017).

There has also been some research focused on the topical application of lantibiotics to treat skin infections. Gallidermin has been proposed as a candidate for the treatment of eczema, cellulitis, impetigo and acne (Valsesia, 2008); with Lacticin 3147 showing similar scope (Allgaier *et al.*, 1991).

Lantibiotics, specifically Nisin, are also being considered for the potential treatment of *H.pylori* (Al-Mahrous & Upton, 2011; Jerris, 1995), due to their stability under acidic conditions (Rollema *et al.*, 1995; Delves-Broughton *et al.*, 1996). Mutacin 1140 has been investigated for the treatment of dental caries caused by *Streptococcus mutans* (Hillman, 2002); with duramycin in trials to potentially clear mucus secretion associated with cystic fibrosis and other airway diseases (Willey *et al.*, 2007).

The large number of structurally diverse lantibiotics indicates a wide spectrum of antibacterial activity; however with the continued advances in synthetic biology, it has become possible to alter existing lantibiotics to produce artificial variants by combining components of different peptides to produce novel hybrid antibiotics (van Heel *et al.*, 2013), some of which display higher activity against targeted bacteria than the original peptides (Arnusch *et al.*, 2008).

1.4 Lantibiotic Synthesis

1.4.1 Biosynthesis of Lantibiotics

The lantibiotics are a class of ribosomally synthesised peptides that are produced by a complex process that includes formation of a precursor, post-translational modification followed by N-terminal leader sequence cleavage and secretion (Gomes *et al.*, 2017; van Kraaij *et al.*, 1999).

The highly modified nature of the lantibiotics means that the percentage of residues undergoing modification ranges from 24% to 58% (Valsesia, 2008).

These post-translational modifications are enzymatically initiated; with the majority involving Serine (Ser) and Threonine (Thr), the hydroxyl amino acids, and Cysteine (Cys), the sulfhydryl.

Initially, the Ser and Thr residues are dehydrated to form Dha and Dhb, which are then subjected to a nucleophilic attack by the thiol group of a Cys residue to form the characteristic thioether lanthionine (Lan) and 3-methylanthionine (MeLan) bridges as shown in figure 1.6 (Valseesia, 2008). However it is notable that there are usually more dehydrated amino acids than Cys residues, which results in lantibiotics usually containing unmodified dehydrated amino acid residues.

The lantibiotics gallidermin and epidermin have been shown to undergo an additional modification, with enzymatic cyclization occurring at the C-terminus, the terminal C residue is first oxidized and then decarboxylated before the nucleophilic assault on the dehydrated residues, forming 2-aminovinyl-D-cysteine (Kupke *et al.*, 1995).

These post-translationally modified residues give rise to certain structural properties of lantibiotics, such as enhanced temperature stability (Hurst, 1991), stability under oxidizing conditions (Sahl *et al.*, 1995), increased acid tolerance and resistance to proteolytic degradation.

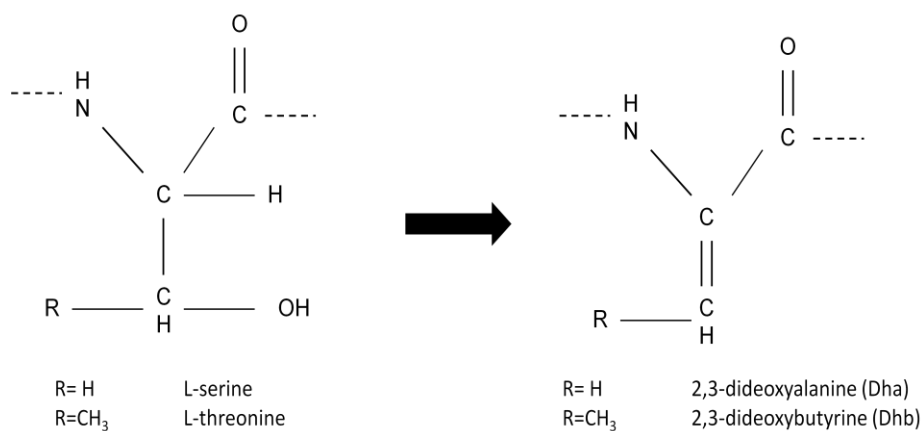
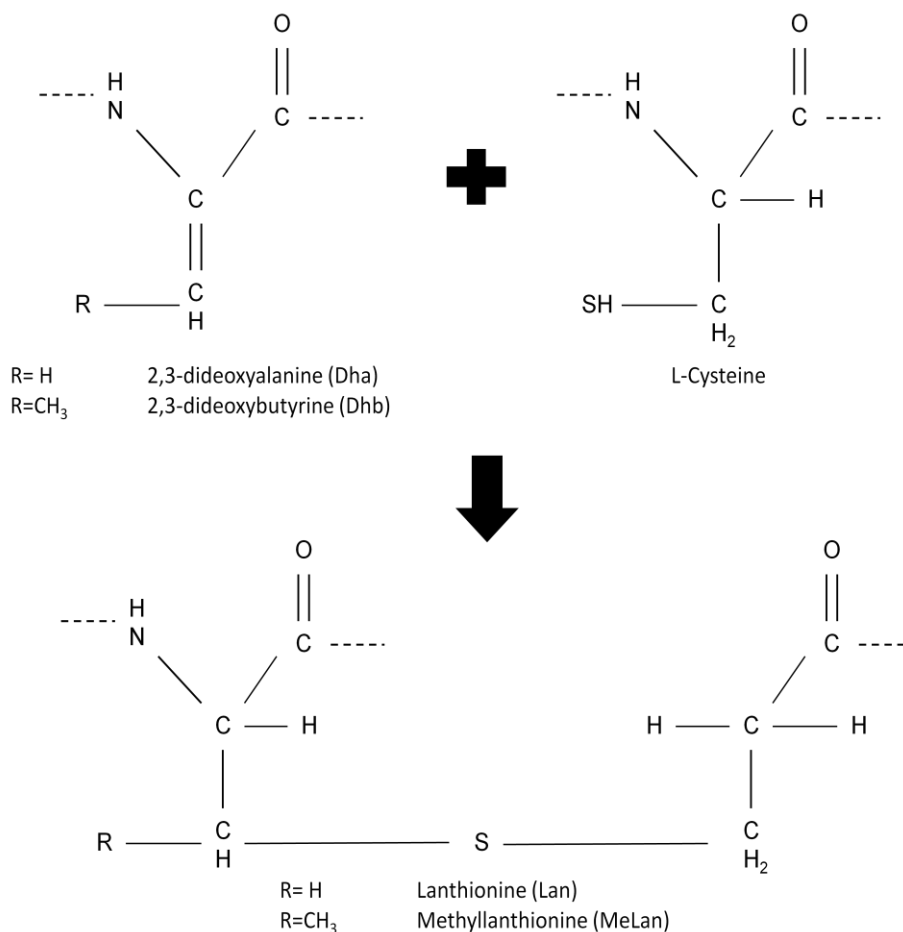
A**B**

Figure 1.6 The mechanism of lanthionine (Lan) and methyllanthionine (MeLan) formation in lantibiotics with A) the enzymatic dehydration of Ser and Thr, to Dha and Dhb, followed by B) nucleophilic attack from the thiol group on the Cys residue to form the thioether bridge, adapted from (Valesia, 2008).

1.4.2 Precursor Production

Prior to achieving the final active form, lantibiotics are produced as biologically inactive precursor peptides (Gomes *et al.*, 2017; van der Meer *et al.*, 1993). These carry a 'leader peptide' an N-terminal extension, and a C-terminal propeptide moiety that undergoes post-translation modifications (Weil *et al.*, 1990). The C-terminal moiety is activated after the post-translational modifications by removal of the leader peptide via proteolytic cleavage.

The leader peptide is thought to stabilise the precursor peptide during translation, ensures it stays biologically inactive, preserves its specific conformation during processing and assists with the precursor translocation by specific transport systems (Ongey & Neubauer, 2016; van Heel *et al.*, 2013; de Vuyst & Vandamme, 1994).

The biological inactivity of the precursor lantibiotics, as opposed to the auto-toxicity and self-regulation of the activated lantibiotics, has been identified as a potential solution to achieving high product titres in fermentation. Indeed, work by (Valesia *et al.*, 2007) utilises synthetic biology to remove the gene encoding for the extracellular protease that activates the lantibiotic gallidermin by proteolytic cleavage of the leader peptide. The result was a fully post-translationally modified lantibiotic precursor.

1.5 Production of Lantibiotics

1.5.1 Upstream Processes

Nisin was the first and so far continues to be the sole lantibiotic used commercially, mainly used in the food industry to prevent spoilage, it has been known since the early 20th century (Field *et al.*, 2015; Jack *et al.*, 1995). Nisin, accorded GRAS (generally recognised as safe) status by the American FDA (Food and Drug Administration), has been produced industrially since 1953 (Parente & Ricciardi, 1999). However, there are no lantibiotics produced commercially for therapeutic use in humans (Ongey & Neubauer, 2016).

The current industrial production method for nisin involves treating pasteurized milk, which has an added yeast extract, with a protease. This is then used as a substrate in batch fermentations at a controlled temperature and pH. The broth is then subjected to concentration step and a spray drying step to obtain the nisin. The resulting powder is standardized with common salt (NaCl) to 1×10^6 IU g^{-1} . Any further purification is expensive and hence not commercially viable for the food industry (Parente & Ricciardi, 1999).

There are no comparable large scale commercial production processes for other lantibiotics. However, due to their potential for treatment of human ailments, since 1988 many lab scale studies have been conducted in order to develop high yielding processes for these molecules (Chatterjee *et al.*, 2005; Kempf *et al.*, 1999). In the case of gallidermin, a lantibiotic of interest to this project, most bench scale studies have been conducted using a batch or fed-batch fermentation (Valsesia *et al.*, 2007; Medaglia, 2009; Valsesia, 2008), with a large number of studies focussing on the effect of the feeding regime .

In the case of Gallidermin, early literature points towards the optimal medium containing yeast extract with an added calcium source, the role of the calcium however remains unclear (Kempf *et al.*, 1999). However, later in later work by Medaglia (2009), maltose appears to be the most favourable carbon source, it is also the feed material used within most fed-batch productions for Gallidermin.

In studies for the production of other lantibiotics, simple batch fermentations and some continuous culture experimentation has been utilized (Arias *et al.*, 2013; Kempf *et al.*, 1999), however self-regulation by the host cells (Kleerebezem, 2004) means that the yield of the desired lantibiotic is usually limited to a few hundred milligram per litre of fermentation culture. In effect product-host regulation presents the greatest difficulty in increasing yields from all production processes (Valsesia *et al.*, 2007).

In order to get around the problem of cellular self-regulation, (Medaglia, 2009), researched modification of a host organism, *S.gallinarum* Tü3928, for the production of the inactive precursor, rather than the activated Gallidermin. The modified host, renamed *S.gallinarum* ΔP , was found to produce inactivated pregallidermin (PGDM) with yields of greater than 1 g.L⁻¹ in optimised media. The conditions utilized for the fermentations were similar to previous fed-batch cultures by Kempf *et al.*, (1999) that were pulsed with a maltose feed; however an additional step in order to obtain the active gallidermin from the precursor becomes necessary. A trypsinization step is sufficient for separation of the precursor leader peptide from the active molecule.

It appears logical to use the two step approach in order to circumvent the difficulties associated with product inhibition in the wild type organisms. It is plausible that with further work on cellular product expression and the eventual development of a defined medium (Medaglia, 2009), highly optimized production processes would become possible, resulting in the greater product titres required to make large scale manufacture economically viable. There is thus great scope for research into the various engineering parameters in pursuit of producing optimal process conditions.

1.5.2 Downstream Process Sequences

One of the main reasons for the lack of commercially produced lantibiotics, with the exception of Nisin, is the difficulty in obtaining sufficient quantities of active product (Medaglia, 2009). The primary problem has been low product titres, which when scaled up, would result in volumetrically large processes, increasing plant capital and operating costs. There remains a lack of high yield and well characterised processes for the production of lantibiotics (Ongey & Neubauer, 2016).

Laboratory scale research on lantibiotics shows preference for downstream purification processes involving multiple chromatography steps, in some cases preceded by a precipitation step as a primary extraction method. (Section 1.5.3)

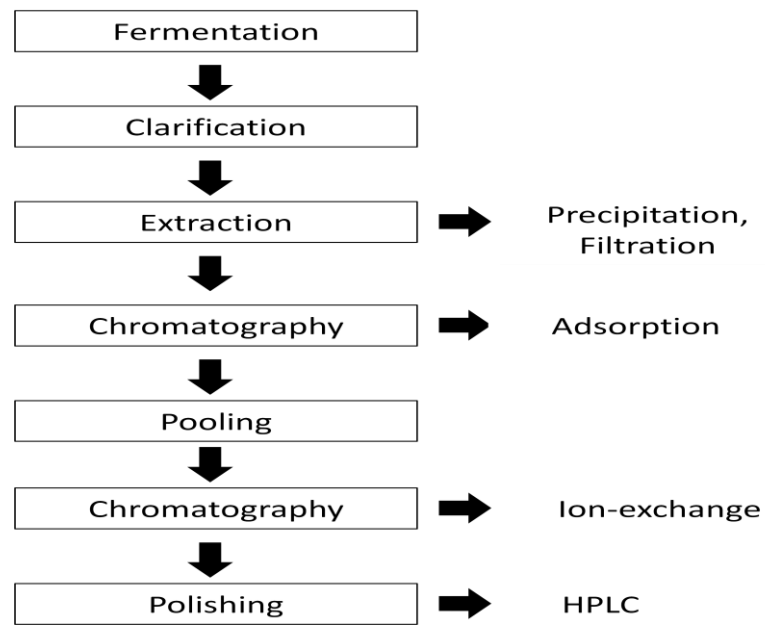
The downstream process sequence shown in figure 1.7 A represents the most common scheme found in literature, although there has been research into modifications to the process such as a single step immuno-affinity separation procedure, pH dependant host absorption or a sequence involving butanol

extraction. These methodologies nonetheless suffer from the same problems of scale as mentioned previously due to the limited productivity achievable of the lantibiotic molecule in its active form (Field *et al.*, 2015).

However, part of this project will attempt the development of an optimized downstream process, for the inactive gallidermin precursor pregallidermin, due to its' ability to obtain much higher lantibiotic titres in culture (Valesia *et al.*, 2007). The ability to achieve high titres from an optimized pregallidermin production process should allow for a significant reduction in plant investment based on smaller process volumes. Fed-batch methods having been established as the preferred choice for organism growth (Medaglia, 2009; Valesia, 2008; Valesia *et al.*, 2007; Kempf *et al.*, 1999; Kempf *et al.*, 1999b). High titre strains potentially allow for higher productivity per litre and allow for smaller equipment sizing, regardless of the downstream processing path chosen.

The possible downstream processing sequences for Gallidermin production using pregallidermin are illustrated in figure 1.7 B (Medaglia, 2009). The choice is heavily dependent on the economics of each process sequence. The optimal sequence would be the least cost intensive, yet allow for high productivity, purification and product yield. Thus the choice becomes dependant on the reaction of the downstream process to the physical properties of the product.

A



B

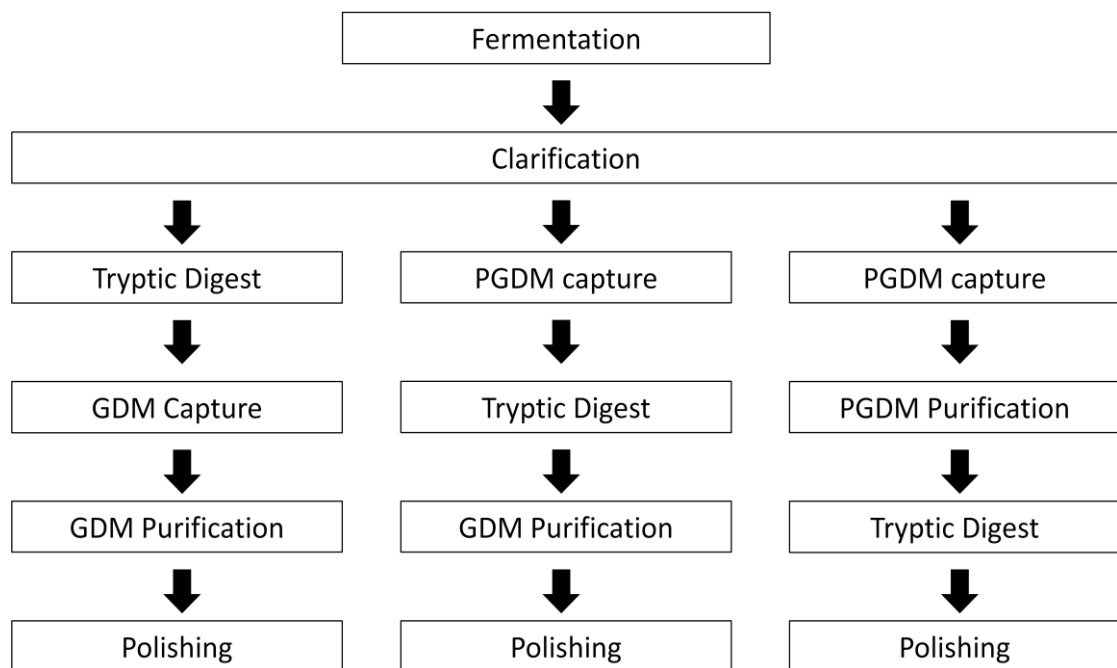


Figure 1.7 Downstream processing sequences with A) common production process for lantibiotics in literature and B) production using the pregallidermin precursor molecule. Adapted from (Medaglia, 2009)

1.5.3 Isolation and purification

The most common method utilized in order to isolate Lantibiotic molecules in recent literature is resin based absorption chromatography, usually with Amberlite resins (Arias *et al.*, 2013; Valsesia *et al.*, 2007; Fiedler *et al.*, 1988). Further downstream purification to achieve the final product is then performed using ion-exchange chromatography, utilizing the cationic properties of Type A1 lantibiotics (Barbour *et al.*, 2013; Furmanek *et al.*, 1999; Kellner *et al.*, 1988).

Alternatively, the isolation of Lantibiotics and bacteriocins (protein products of bacteria) has also been performed previously using ammonium sulphate precipitation from solution (Parente & Ricciardi, 1999). The method appears to have been popular as a generic purification strategy for bacteriocins and is not specific to lantibiotics; however it has also been used for the isolation of Nisin and Staphylococcin T (a natural variant of Gallidermin) (Furmanek *et al.*, 1999). However, further downstream purification after using the precipitation method still relies on two chromatographic separation stages; hence logically the preferred method would rely on fewer purification stages and therefore reduce the expense of the overall process.

There are also reports in literature of a primary separation process utilizing butanol extraction (liquid-liquid extraction) (Piva & Headon, 1994); however as non-polar solvents seem to denature and inactivate the product, there is a greater loss of activity. It is worth noting that there is further scope for research into the use of liquid-liquid extraction as an economically viable purification technique by utilising developments such as micelles (Lye, 1994).

Lantibiotics have also been shown to adsorb to the host cells at high pH, opening the possibility of utilizing host adsorption as a means of primary separation (Yang *et al.*, 1992). Thus a pH dependant extraction is a possible exploration avenue; however the method has been tested with wild-type lantibiotics and none of the synthetic strains, hence further research is required into the behaviour of the precursor molecules.

Another development in lantibiotic separation technology is the use of immuno-affinity chromatography as a single stage purification process to produce the purified final product direct from the fermentation broth. The method reportedly achieves greater yields in comparison to multi-stage extraction and purification processes (Suárez *et al.*, 1997). However, as research has so far focussed on the wild type, 'active' molecule, it is intuitive that overall process yield is still low due to product toxicity. The method also requires research time and resource allocation to determining suitable antibodies for the chromatography. While it remains an expensive method to perform small scale purification attributable to the cost of antibodies, it is possible that large scale production facilities based on single-step extraction and purification may become viable.

The most common final purification technique is an ion-exchange chromatography (AlKhatib *et al.*, 2014; Kellner *et al.*, 1988; Ottenwälder *et al.*, 1995), based on the cationic nature of type A1 lantibiotics, however reverse-phase HPLC at preparative scale has also been utilized; primarily using silica based C-18 columns. The reverse-phase HPLC has been shown to achieve purities of greater than 95% (Parente & Ricciardi, 1999).

It is interesting to note that although there are numerous methods in use in lab and research scale, they may not necessarily be economically viable at production scale. A need exists for much more research into the downstream processing methodologies best suited and optimized for any synthetic biology product, enabling Lantibiotic availability at quantities necessary for clinical use.

1.5.4 Identification & Analytics

There is a general consensus use of reversed-phase HPLC as the preferred method of peptide purification in the literature (Ross *et al.*, 2010; van Kraaij *et al.*, 1999; Kuipers *et al.*, 1996). It provides good resolution of the sample without needing large amounts of it. The analytical HPLC methods also utilize silica based columns, most notably C18; however other columns have also been utilized (Valesia *et al.*, 2007; Wescombe & Tagg, 2003). The method is almost exclusively a gradient elution, utilizing a weak buffer, usually TFA based, and Acetonitrile (or an Acetonitrile based solution) as the mobile phase.

A whole host of techniques have been utilized for peptide sequencing of lantibiotics with the primary method of choice being Edman degradation (Kellner *et al.*, 1988; Kuipers *et al.*, 1996; Zimmermann & Jung, 1997). It is noticeable that because of the difficulty posed to the method by the thioether bridges and dehydrated residues, chemical and enzymatic fragmentation needs to be performed first in order to form detectable residues (Ottenwalder *et al.*, 1995).

The other analytical methods utilized include GC-MS analysis, MALDI-TOF and various NMR based analyses (Barbour *et al.*, 2013; Kuipers *et al.*, 1996). These are used mainly for identification of the peptides and confirming their presence.

1.5.5 The impact of lantibiotic physical properties on Downstream Processing

The physical and chemical properties of the product determine the preferred strategy for purification, processing, and practical applications (Rollema *et al.*, 1995). It is thus important to understand the interactions the intended product will have with the production media, the purification setup and the extraction techniques. Some of the potential relationships are shown in Table 1.1.

It would be illogical to perform a tryptic digest initially if it is found that the product has low stability in its final form. Similarly if the product is determined to show varying solubility in different solvents, it would be much more logical to utilize a liquid-liquid extraction process compared to expensive chromatography procedures. A detailed understanding of all physical and chemical properties of the intended product is thus a necessary prerequisite for the translation of any new research work to large-scale production (Chubukov *et al.*, 2016).

It therefore becomes critical to establish a robust and reliable analysis method to determine the physical-chemical properties of lantibiotics to aid in downstream process development and selection, on an optimized cost-benefit basis.

Table 1.1 Relationship of physical properties to downstream processing

| Physical properties | Impact on DSP |
|----------------------------|--|
| Solubility | Choice of extraction and purification method |
| pH stability | Choice of reagents and buffer solutions |
| Temperature stability | Heating/Cooling needs |
| Reactivity | Downtimes, scheduling and reagent choices |
| Viscosity | Choice of equipment based on shear |
| Size | Impacts filtration and purification |
| Biological Activity | Choice of assays and strains |

1.5.6 Challenges imposed by synthetic biology on Downstream Processing

It is suggested that synthetic biology has the potential to enhance the antibiotic pipeline by providing new drugs for treating infection (Chubokov *et al.*, 2016; Elander, 2003). It also enables medicine and pharmaceuticals to keep pace with rapidly evolving microorganisms that have acquired resistance to a large number of existing drugs (Yoneyama & Katsumata, 2006).

However there are major challenges imposed by synthetic biology, in terms of finding the ideal candidate drugs and treatments that fulfil all requirements of efficacy, safety, scalability, affordability and ease of processing (Zhang *et al.*, 2016). Even though synthetic biology provides the necessary tools that allow for modification and customization, the complexity of living organisms and DNA means that inducing an organism into making a particular molecular product remains extremely resource intensive and difficult (Benner & Sismour, 2005; Heinemann & Panke, 2006). It is expected that with further research, greater understanding will result in enhanced abilities to develop 'scratch built'

organisms, however that aim requires the cataloguing of the vast number of possible combinations that result in the production of useful compounds and determine certain product behaviour.

In the present circumstances, until global biological expertise and knowledge reaches the aforementioned level, the production of biological products that display desirable modification and characteristics will continue to require the 'sieving' of a vast number of mutant variants. This process itself creates challenges for the biotech industry in the requirement of high throughput-screening and analysis techniques, with novel high throughput screening methods under development (Walser *et al.*, 2009). Unless faster methodologies and analysis techniques are utilized, they could potentially become a bottleneck in the application and utilization of synthetic biology (Ongey & Neubauer 2016).

Thus the advance of synthetic biology means that the ability to rapidly characterize and define the physical and chemical properties of novel compounds becomes crucial. The success of any product both commercial and medical depends on how rapidly it can come to market and how many of the desired characteristics it possesses. Inability to do so would potentially make the synthetic drug discovery process both extremely time consuming and costly.

1.6 Microscale Approaches to Downstream

Process design

1.6.1 Microscale Methods

The global biotechnology industry has been promoting the use of microscale methodologies and technology as part of ultra scale down (USD) studies. This includes both the use of microwells and microfluidics in the pursuit of process development (Rayat *et al.*, 2016). Microscale technologies allow testing and experimentation to be performed without the need for much material, a critical advantage in allowing for high throughput screening of new molecules (Lye *et al.*, 2003; Titchener-Hooker *et al.*, 2008).

In the search for new and better drugs and treatments, it is expected that with the aid of synthetic biology, vast libraries of compounds will be produced, each variant possessing some of the characteristics needed for the purpose. Determining which candidate would be the optimal choice requires the rapid screening of the candidate in order to determine the assimilation of the modifications. This has become more easily achievable with the spread of microscale technology. The ability to sort through vast libraries of cells within greatly reduced timeframes offer the potential benefit of bringing drugs to market much faster or identifying potential failures before having to expend any more resources (Titchener-Hooker *et al.*, 2008). Thus it is unsurprising that the potential benefits have encouraged its uptake in the drug discovery process.

In the same way as microscale technologies have aided drug discovery, they have the potential to aid early process development. Much work has been done

at UCL on mimicking process unit operations at microscale, with the focus on fermentation and bioreactors (Titchener-Hooker *et al.*, 2008). The ability to conduct process development studies at microscale has recently been referred to as micro biochemical engineering and the reproduction of a unit operation at microscale has been referred to as an ultra scale down (USD) study. The challenge with conducting USD studies has been the complexity faced when comparing large-scale with microscale environments, with the cellular behaviour changing dramatically. Research has been conducted into the best ways to ensure that key coefficients can be maintained, such as K_{LA} and the oxygen transfer rate (OTR) (Lye *et al.*, 2003; Micheletti *et al.*, 2006). Ensuring this allows comparisons to be made based on normalized data.

In comparison to fermentation, there remains lots of scope for the application of microscale technology to downstream processing. There are investigations in the literature about the availability of microscale methods for downstream processes such as chromatography, centrifugation and filtration (Voulgaris *et al.*, 2016; Titchener-Hooker *et al.*, 2008). However, much work still needs to be done in order to fully compare the performance of microscale downstream processing with its full-scale equivalents.

The ability to use microscale methods would greatly aid process development of new drug candidates. It could potentially allow process development to take place immediately after drug discovery, allowing for reduced risk and greater focus when setting up actual pilot scale production for clinical trials (Micheletti & Lye, 2006).

1.6.2 Rapid characterization, identification and analysis

Microscale techniques allow for rapid identification and analysis of drug candidates by using minimal quantities and high throughput methods in order to screen vast libraries of compounds (Micheletti & Lye, 2006). They could also allow the rapid analysis of their physical and chemical properties in order to aid process development immediately after drug discovery, substantially reducing the time taken for experimentation and providing scale data that could be incorporated into models for simulating pilot scale facilities. This would allow more focus on key unit operations, while reducing risk. The use of microfluidic devices enables parallel microscale studies to be conducted, increasing throughput substantially (Davies *et al.*, 2014).

An advantage of microscale techniques is that with the use of standardized microplates and microwells, automation of the liquid handling and plate movement would allow for extremely high throughput systems (Nealon *et al.*, 2005). These when programmed to carry out tasks, could be left to conduct the analysis without the requirement for supervision allowing for minimum manpower requirements. The TECAN® automated platform is an example of such a technology that can be integrated with microwell methods (Lye *et al.*, 2003; Micheletti *et al.*, 2006).

1.6.3 Economic Benefits

The economic benefits are incurred by a combination of reduced times to market and reduction of risk in the drug development process. The reduced resource requirements for initial testing and reducing the number of pilot-scale production to those drug candidates with the highest chances of success also provide great savings in resources (Lye *et al.*, 2002; Micheletti & Lye, 2006; Titchener-Hooker *et al.*, 2008).

The ability to screen vast libraries in a cost effective manner also implies more resources can be diverted to new research. Another advantage of microscale technology is that by making initial research cheaper, the cost of failure is considerably reduced, as a more directed effort would allow the optimum allocation of resources, eliminating the waste associated with trial and error strategies during pilot scale development.

1.7 Current status of the Bioprocessing aspects

Despite recognising the potential of lantibiotic compounds in treating disease (Smith & Hillman, 2008; Valsesia, 2008); it is notable that there is currently no lantibiotic in human clinical use.

One of the contributing factors for these antibiotics having not been translated into commercial products is the lack of a well defined large scale manufacturing process (Ongey & Neubauer, 2016). The development of manufacturing routes for lantibiotics and modified lantibiotics is still in the early stages. As described in Section 1.3.10 most published work focuses on characterizing lantibiotics with useful antimicrobial properties and creating novel variants rather than

attempting their production at anything beyond laboratory scale. While attempts have been made to modify organisms to increase lantibiotic yield during fermentation (Kuipers *et al.*, 1996; Valsesia *et al.*, 2007), there currently exists no fermentation process with well defined operational parameters that provides a platform for reproducible antibiotic production in bioreactors. Neither is there any published work on the reproducible production at pilot or manufacturing scale, of antibiotics that have been modified using synthetic biology.

Likewise, while there are numerous publications on the isolation and purification of selected lantibiotics for analytical purposes, no published work currently exists on the preparative or manufacturing scale downstream processing of this class of molecules. A variety of methods such as ion exchange chromatography, immuno-affinity chromatography, hydrophobic interaction resins, product precipitation and adsorption onto the producer organisms by pH variation have been proposed as described in Section 1.5.3. However none of these methods have been tested beyond laboratory scale and have tended to be studied as isolated steps rather than within a whole downstream processing sequence. The one strong indication from the available literature is a general preference for the use of hydrophobic interaction resins, with adsorption/desorption used as a primary capture step (Valsesia *et al.*, 2007; Fiedler *et al.*, 1988; Arias *et al.*, 2013; Medaglia, 2009).

The work by Giovanni Medaglia (2009) in the Bioprocess laboratory, at the department for Biosystems Science and Engineering, ETH Zurich using *S.gallinarum* Δp is the closest attempt at designing a complete process for lantibiotic production that could be attempted at pilot scale. The research is

based on prior work by Valsesia *et al.* (2007) and Fiedler *et al.* (1999) on the *S.gallinarum* Tü3928 cell strain and seeks to optimise the production of lantibiotic by performing high cell density cultures and identifying possible DSP strategies for the capture and purification of PGDM. A search of the literature did not reveal any similar attempts at developing a complete bioprocess for lantibiotic production at scale since then.

Additionally, while the properties of a number of lantibiotics have been characterized, there is a lack of basic knowledge about the physico-chemical properties of lantibiotics that would influence their behaviour in downstream process environments (Table 1.1). Investigations have been reported on the stability and solubility of Nisin (Rollema *et al.*, 1995) which are factors which would influence process design. Similar data on other lantibiotics is lacking and methods to rapidly acquire this data for libraries of engineered novel lantibiotics would greatly enhance downstream process synthesis and design.

1.8 Novelty of the work performed

The past two decades have seen a lot of research focused on the development of novel lantibiotics by studying the producer organisms and understanding the molecular mechanisms of production (Sandiford, 2014). This has allowed a wealth of knowledge to be gained on the genetic sequences and enzymes involved in the synthesis of these antimicrobial peptides, which has led to development of tools that allow them to be modified on the genetic level, creating libraries of novel compounds.

However, over the same time period, very few studies have attempted to characterise a production process that would allow large amounts of these compounds to be obtained for clinical use. Work on individual bioprocess unit operations (Suarez *et al.*, 1997; Kempf *et al.*, 1999; Fiedler *et al.*, 1988) has been performed but so far only Medaglia (2009) has attempted to identify a complete process by which clinically significant amounts could be produced.

This work has built heavily on the work of Medaglia (2009) as a foundation to identify a complete process that could potentially provide a platform for research into the large scale production of novel lantibiotics. However, unlike the previous work, it attempts to characterise the microenvironment of the *S.gallinarum* Δp fermentation and demonstrate reproducibility between batches. It is also the first work to perform a 30 L scale fermentation using *S.gallinarum* Δp to produce the gallidermin precursor peptide, pregallidermin.

Fiedler *et al.* (1988) and Medaglia (2009) identified and outlined potential DSP sequences that could be utilized for the isolation and purification of gallidermin and pregallidermin respectively. However, those studies were conducted at bench scale. This is the first work to utilise pilot scale DSP operations to attempt the purification of a lantibiotic precursor. This is also the first work that attempts to combine the pilot scale fermentation, DSP operations and microscale optimisation studies into a complete pilot scale platform process. This platform process can be used to obtain information that can aid the biotechnologist in process design for lantibiotic producing organisms.

1.9 Aims and Objectives

The absence of a well defined manufacturing process to allow production of modified lantibiotics at scale and generic rules for their downstream process remains a barrier to their further development. The **aim** of this thesis is to systematically analyse options for lantibiotic production at pilot/manufacturing scale and to develop microscale methods for acquiring the physic-chemical property data that will aid downstream process synthesis. The approach will be illustrated using the *S. gallinarum* Δp cell line; a modification of the *S.gallinarum* *tü 3928* cell line, that produces pregallidermin, the inactive precursor to the lantibiotic gallidermin (Valsesia, 2008). Production of the pre-lantibiotics is a novel approach that overcomes the auto-toxicity of the lantibiotic to the producing organism but requires an additional downstream processing step, trypsination, for removal of the leader-peptide on the actual lantibiotic molecule (Chapter 1.4.2). The specific **objectives** of this research are:

- To systematically characterise the fermentation parameters that allow reproducible fermentations and maximisation of antibiotic production. These parameters will be used to identify the conditions needed to achieve optimal antibiotic production and the reproduction of these results at pilot scale. This study is reported in Chapter 3.
- To systematically develop a whole downstream process sequence for the removal of cell mass, followed by the capture and purification of PGDM that is applicable at pilot and manufacturing at scale. This study will aim to identify generic rules for the design of lantibiotic purification processes

and the necessary physico-chemical property data required to inform downstream process design. This work is described in Chapter 4.

- To develop microscale methods that can be used to rapidly acquire physico-chemical property data on lantibiotic molecules that will help inform early stage downstream process design. Additionally, the microscale data will be used to optimise a process identified in Chapter 4. Stability studies will also demonstrate the potential of these methods to allow informed choices on DSP design, with the process redesigned in light of the data from the microscale analysis. This work is described in Chapter 5.

Chapter 2, which follows immediately after this section, details the experimental materials and methods used throughout this thesis along with the relevant analytical techniques.

Chapter 6 will summarise the novel insights gained from this research and attempt to derive a set of conclusions based on the results, additionally it will outline avenues of future work.

Finally, Chapter 7 will consider practical applications for the knowledge obtained. The chapter is included as part of the requirements for award of the UCL EngD. It will provide a concise argument for the platform process developed to be used in the design and future production of libraries of novel lantibiotic compounds.

2. Materials and Methods

2.1 Materials

All consumables and reagents were procured from Sigma-Aldrich (Dorset, United Kingdom), unless otherwise stated, and were of the highest purity available. A list of all chemicals used is given in Appendix 1. All solutions were made up with RO water or higher purity Milli-Q water (Merck Millipore, Darmstadt, Germany).

All materials and lab-ware were sterilised by autoclaving at 121°C for 20 minutes where possible. All transfer of cells, plating and preparation of glycerol stock was performed under sterile conditions in a Class II biological safety cabinet to prevent any contamination of stocks and samples. Where it was not possible to sterilise by autoclaving i.e. in the case of antibiotic preparation, materials were filter sterilised using 0.2 µm Sartorius (Göttingen, Germany) syringe filters.

2.1.1 Organism

The modified bacterial strain *Staphylococcus gallinarum*Δ*gdmP*::*aphIII* (*S.gallinarum* Δ*p*) was a kind gift provided for use in this research by Professor Sven Panke's group at the Bioprocess Laboratory of ETH Zurich in Basle, Switzerland.

S.gallinarum Δp is a modification of the wild-type *S.gallinarum* *tü* 3928 producing the lantibiotic precursor pregallidermin (PGDM), rather than the wild-type active gallidermin. The strains were received from ETH Zurich plated onto agar slopes.

The organism was created by Valseia *et al.* (2007) in order to increase the yield of lantibiotics from culture by negating the effect of auto-toxicity towards the host strain displayed by gallidermin (Sahl *et al.*, 1998). The wild-type *S.gallinarum* *tü* 3928 was modified by developing a new plasmid vector that knocked-out the genetic sequence for the extracellular protease GdmP (responsible from cleaving the leader peptide for the lantibiotic precursor molecule) and replaced it with the sequence for resistance to the antibiotic Kanamycin. The wild-type *S.gallinarum* *tü* 3928 is not naturally resistant to Kanamycin, allowing the antibiotic to be used to ensure selectivity for the mutant strain in culture.

2.1.2 Preparation of glycerol stocks

Glycerol stocks were prepared by initially plating the strains on process media with the addition of 2 % (w/v) agar. The antibiotics Kanamycin, 20 $\mu\text{g.mL}^{-1}$, and Tetracycline, 10 $\mu\text{g.mL}^{-1}$, were added to the agar solution before it had solidified and subsequently poured into Petri dishes. The antibiotics were separately filter sterilised through a 0.2 μm syringe filter before use. The plates were then sealed using Para-film (Bemis, Wisconsin, United States) and incubated overnight at 37 °C.

50 mL Falcon tubes were filled with 10 mL of fresh media and the antibiotics were added. From the agar plates, single colonies of the bacterial strains were inoculated into the Falcon tubes, which were then placed into Kühner orbital shakers (Basel, Switzerland) at 37 °C and 250 rpm overnight. 0.5 mL of the bacterial culture was then pipetted aseptically into 1.5 mL Eppendorf tubes along with 0.5 mL of glycerol, which were then vortexed and stored at -80°C.

2.1.3 Fermentation media and feed for fed-batch fermentations

All fermentations performed in the course of this research utilised the same yeast extract based complex media for bacterial growth. The media, referred to as Medium 21B by Medaglia (2009) in the initial process development studies conducted at ETH Zurich, was a solution of 50 g.L⁻¹ yeast extract and 20 g.L⁻¹ sodium chloride per litre dissolved in RO water (the original recipe did not specifically require the use of RO water due to the complex nature of the ingredients, however as the original plan had called for the research to be conducted across multiple labs in various locations, RO water was utilized to maintain consistency between all media and feed solutions).

The two feed solutions were simply made by dissolving either maltose or yeast extract in water and then sterilising by autoclaving for 20 minutes at 120°C.

Table 2.1 Composition of media and feed solutions used in the various fermentations

| Operation | Fermentation media components | | Feed composition | | |
|---------------|-------------------------------|---------------------|----------------------|----------------------|-------|
| | Yeast Extract | Sodium Chloride | Maltose Feed | Yeast-Extract Feed | Scale |
| Shake Flask | 50 gL ⁻¹ | 20 gL ⁻¹ | None | None | 0.5L |
| STR Batch | 50 gL ⁻¹ | 20 gL ⁻¹ | None | None | 7.5L |
| STR Fed-Batch | 50 gL ⁻¹ | 20 gL ⁻¹ | 500 gL ⁻¹ | None | 7.5L |
| STR Fed-Batch | 50 gL ⁻¹ | 20 gL ⁻¹ | 500 gL ⁻¹ | 300 gL ⁻¹ | 7.5L |
| STR Fed-Batch | 50 gL ⁻¹ | 20 gL ⁻¹ | 500 gL ⁻¹ | 300 gL ⁻¹ | 30.0L |
| STR Fed-Batch | 50 gL ⁻¹ | 20 gL ⁻¹ | 600 gL ⁻¹ | 200 gL ⁻¹ | 30.0L |

2.2 Fermentation of *S. gallinarum* Δp

2.2.1 Shake flask fermentation of *S.gallinarum* Δp

Fermentation media for cell culture of *S. gallinarum* Δp was prepared by dissolving 50 g of yeast extract and 20 g of sodium chloride per litre of RO (reverse osmosis) water as described in Section 2.1.3. The media was sterilised by autoclaving at 121 °C for 20 minutes, and then allowed to cool before use.

A pre-culture was prepared by pipetting 10 mL of media into 50 mL falcon tubes. Antibiotics used to ensure selectivity of the strain were 20 $\mu\text{g.mL}^{-1}$ Kanamycin and 10 $\mu\text{g.mL}^{-1}$ Tetracycline. The pre-culture was inoculated with 100 μL of *S.gallinarum* Δp frozen glycerol stock and left overnight in a Kühner (basel, Switzerland) orbital shaker at 37 °C and 250 rpm.

Sterile 500 mL conical flasks were filled with 90 mL of fermentation media and fresh Kanamycin and Tetracycline was pipetted into them. The conical flasks were inoculated with 10 mL of *S. gallinarum* Δp pre-culture, the tops were sealed with cotton wool and aluminium foil and then placed in a Kühner orbital shaker at 37 °C and 250 rpm. A 1 mL sample of culture was taken every hour, with OD being measured at 600nm to monitor cell growth (Section 2.5.1) and then analysed by HPLC (Section 2.5.3) to quantify the amount of pregallidermin (PGDM) present.

2.2.2 7.5L fermentation of *S.gallinarum* Δp : batch mode

Batch fermentations were performed using 7.5 L BioFlo 110 bioreactors (New Brunswick Scientific Company, Edison, NJ, USA). The bioreactor had a top-driven impeller shaft with two six-bladed Rushton turbine impellers, capable of agitation between 200 rpm and 1200 rpm (Figure 2.1). The bioreactor working volume was 5 L.

The pH probe was calibrated by initial immersion in a buffer at pH 4, followed by a buffer at pH 7. The probe was tested by immersing in a solution of known pH, with the reading confirmed using a bench-top Mettler-Toledo (Leicester, UK) pH probe. The DOT probe (Mettler-Toledo Ltd, Leicester, UK) was calibrated at 0 % air saturation by placing in a stream of pure nitrogen outside the vessel, followed by calibration at 100 % air saturation by leaving the probe exposed to air for at least 30 minutes. The exit gas port from the bioreactor was connected

to a Prima-Pro process mass spectrometer (Thermo Scientific, Waltham, MA, USA).

The BioFlo reactors allow for the automatic control of pH, temperature, DOT and antifoam (polypropylene glycol, PPG) addition. Process media was prepared (as described in Section 2.1.3) and filled into the bioreactor up to 5 L. The media was sterilised by autoclaving the whole bioreactor for 20 minutes at 121 °C in a Getinge H-Series autoclave (Getinge, Sweden). The temperature of the media was adjusted to 37 °C and the pH adjusted to 6.5 using 20 % (v/v) ammonium hydroxide solution and 20 % (v/v) phosphoric acid. Airflow was set to 1 vvm (vessel volume per litre per minute) and impeller speed set to a minimum of 250 rpm and a maximum of 1200 rpm. DOT (dissolved oxygen tension) was set at a minimum of 30 %. A cascade system was operated by which vessel agitation would automatically increase in response to drops in DOT due to cellular growth. PPG addition was done via syringe injection through a septum as opposed to automated control. The antibiotics Kanamycin 20 µg.mL⁻¹ and Tetracycline 10 µg.mL⁻¹ were added prior to inoculation to ensure microbial selectivity.

Inoculation was performed with 10% (v/v) cell culture solution (prepared as described in section 2.1.2). Growth of the cells was charted by taking OD readings of samples at 600nm (section 2.5.1) and PGDM expression analysed by HPLC (section 2.5.3).

Antifoam used in the culture was autoclaved at 121°C for 20 minutes. All connectors used for the addition of substances were sterilised by wiping with 70 % (v/v) ethanol solution.

2.2.3 7.5L fermentation of *S.gallinarum* Δp : fed-batch mode

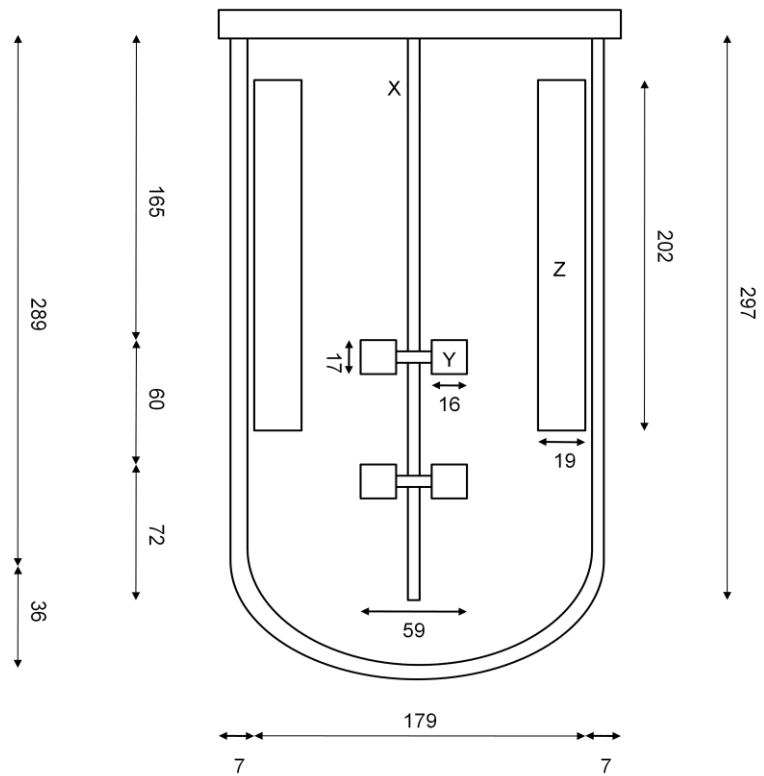
Fed-batch cultures were performed in the same 7.5 L New Brunswick BioFlo bioreactors as used for batch cultures in Section 2.2.2. For fed-batch cultures these were initially filled with 1.8 L of media. One litre each of the feed solutions (500 g.L⁻¹ maltose and 300 g.L⁻¹ yeast extract solution) were attached to the bioreactor using sterile connectors and tubing, with the whole system being sterilised by autoclaving at 121 °C for a minimum of 20 minutes. The system temperature was then adjusted to 37 °C, pH adjusted to 6.5 using 20 % (v/v) ammonium hydroxide and 20 % (v/v) phosphoric acid and DOT set to 30 % with cascade control of agitation between 250 rpm and 1200 rpm. The vessels containing the feed solutions were placed on weighing scales to record feed rates over time with flow rates adjusted using Watson-Marlow 101 U/R peristaltic pumps (Wilmington, MA, USA). Automatic antifoam control was set up for the fed-batch cultures by setting the control system to activate PPG addition if liquid level hit the foam detection probe tip. The antibiotics Kanamycin 20 µg.mL⁻¹ and Tetracycline 10 µg.mL⁻¹ were added prior to inoculation.

Inoculation was performed using a 10 % (v/v) cell culture solution, placed overnight in a 1 L conical flask at 37 °C and 250 rpm in an orbital shaker, grown direct from frozen glycerol stock as described in Section 2.1.2. Cellular growth was determined by taking the OD at 600 nm of cell culture samples (Section 2.5.1), with HPLC analysis used to determine PGDM expression (Section 2.5.3).

Feeding of the 500 g.L⁻¹ maltose solution was initiated at 2 hours post inoculation, with feeding of the 300 g.L⁻¹ yeast extract solution initiated at 4 hours post inoculation in fed-batch fermentations where a two feed setup was used.

Aeration was initially set at 1 vvm; however it was manually adjusted to allow for the changing volume of the bioreactor broth. Where the DOT fell below the minimum 30 % at maximum impeller agitation rate and maximum possible aeration rate, pure oxygen was blended into the vessel air supply to a maximum of 100 % (v/v) to increase DOT back to the set point. The exit gas port from the bioreactor was connected to a Prima PRO process mass spectrometer (Thermo Scientific, Waltham, MA, USA).

A



B

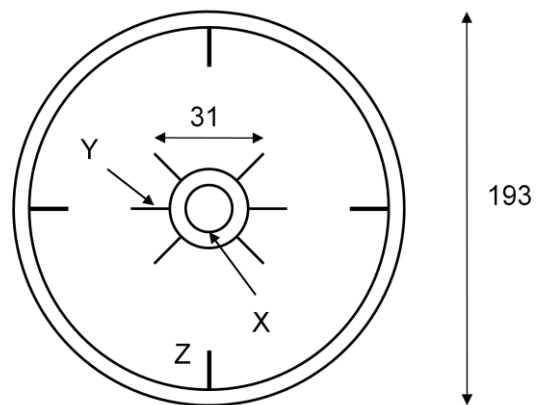


Figure 2.1 The Dimensions of the BioFlo 110 7.5 L bioreactor, with A) showing the vertical cross-section and B) showing the horizontal cross-section. X= the impeller shaft; Y= impeller blade; Z= baffle. All measurements are displayed in millimetres (mm).

2.2.4 30L Fed-Batch fermentation of *S.gallinarum* Δp

Fed-batch fermentations were performed at 30 L scale using a Sartorius Biostat® CPlus bioreactor (Göttingen, Germany). The reactor had a height to diameter aspect ratio of 3:1, with a total internal volume of 42 L and a working volume of 30 L. The reactor has a top-driven impeller shaft with three 6-bladed impellers, allowing agitation up to 1000 rpm. The pH and DOT probes were calibrated as described in Section 2.2.2 and the bioreactor off-gas was connected to the Prima Pro process mass spectrometer (Thermo Scientific, Waltham, MA, USA) for analysis.

The Biostat® CPlus allows for the control of temperature, pH, antifoam addition and DOT control via aeration, agitation and gas blending (with O₂). Additionally, the bioreactor can be programmed to perform exponential feeding via automated control of the flowrates of attached peristaltic pumps.

The feed solutions of either 500 or 600 g.L⁻¹ maltose solution, 300 or 200 g.L⁻¹ yeast extract solution and the antifoam PPG were sterilised by autoclaving at 121 °C for 20 minutes and then attached to the bioreactor. Aqueous ammonium hydroxide 20 % (v/v) and phosphoric acid 20 % (v/v) were connected to the bioreactor prior to process media filling. 9 L of process media was filled into the bioreactor, which was sterilized *in-situ* by steam injection into the vessel jacket raising temperature to 121 °C for a minimum of 20 minutes. The antibiotics Kanamycin 20 µg.mL⁻¹ and Tetracycline 10 µg.mL⁻¹ were added to the sterile media pre-inoculation. The temperature was controlled at 37 °C, pH at 6.5 and DOT set to a minimum of 30 %.

Inoculation was performed with a 1 L cell culture, grown in a 3 L conical flask overnight at 37 °C and 250 rpm, in a Kühner orbital shaker, direct from frozen glycerol stock. Off-gas was analysed for OUR and CER using the process mass spectrometer.

The flowrate of feed solutions was adjusted using Watson Marlow 101 U/R peristaltic pumps (Wilmington, MA, USA).

Maltose feed was started at 3 hours post-inoculation and yeast extract feed was started 6 hours post-inoculation. When pump reached maximum flow rate, the feed rate was maintained at this level until fermentation end.

Aeration was begun with 1 vvm, however it was manually adjusted to account for the changing volume of the reactor, due to feed addition and to maintain DOT at a minimum 30 %.

2.2.5 Fermentation substrate feed strategies

At 7.5L scale substrate was fed into the fermentation using either an exponential feed regimen or a step-up regimen; both these feed profiles are illustrated in Figure 2.2.

For the 'exponential' regimen, it was not possible to use the Watson-Marlow 101 U/R (Wilmington, MA, USA) pumps as the BioFlo 110 bioreactors do not possess an interface that allows external pumps to be controlled. Instead, the BioFlo's built-in pumps were utilised and programmed with an exponential profile.

The 'step-up' feeding regimen required a manual adjustment of the Watson-Marlow 101 U/R to allow a step increase in the feed rate in order to ensure the substrate did not become growth limiting. This adjustment was performed in response to a drop in DOT and subsequent increase in impeller agitation rate, which were used as indicators of increased cellular respiration.

The exponential regime was applied to the feed solutions following the equation:

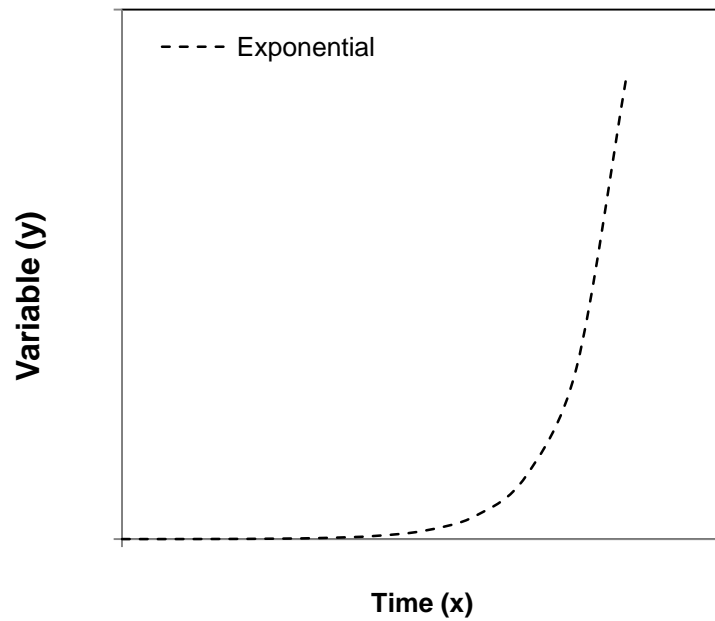
$$Feed(t) = \left(\frac{\mu_{set}}{Y_{x/s}} \right) X_0 \frac{V_0}{S_0} e^{\mu_{set} t} \quad (2.1)$$

where feed (t) in L.h⁻¹ is the feed rate for a single feed, μ_{set} (h⁻¹) is the desired specific growth rate; $Y_{x/s}$ (g.g⁻¹) is the biomass yield per unit of maltose fed, X_0 is cell dry weight (CDW) in g.L⁻¹ i.e. the CDW concentration at the beginning of the feed, V_0 (L) is the liquid volume in the bioreactor at the start of the feed, S_0 (g.L⁻¹) is the concentration of the substrate in the feed solution and t (h) is the time elapsed since feed start (Medaglia, 2009).

In comparison the 30L Sartorius Biostat® CPlus bioreactor (Göttingen, Germany) allows the flow rate of external pumps to be controlled from the main user interface, hence the flow rates of the Watson Marlow 101 U/R peristaltic pumps (Wilmington, MA, USA) was controlled by the bioreactor where an exponential feed regime was applied.

In the case of the 'step-up' feed regimen, the flow rate of the pumps was manually adjusted in response to changes in DOT and impeller agitation rate.

A



B

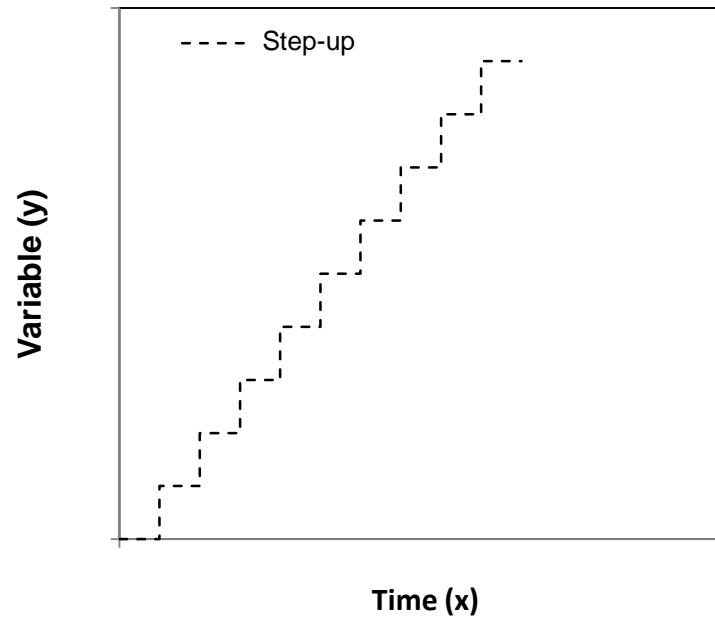


Figure 2.2 The two substrate feed profiles used for the fermentation studies, with A) depicting an exponential feed regime in which an attempt is made to map the feed rate onto the microbial growth curve and B) showing a 'step-up' feed profile, with step changes in the feed rate to ensure the substrate is maintained in excess and does not become growth limiting.

2.2.6 Anti-foaming agent utilised

Polypropylene Glycol (PPG) from Sigma-Aldrich (Dorset, UK) was added either manually or using an automated control system as the anti-foaming agent in all Stirred-tank bioreactions.

2.2.7 Measurement and calculation of off-gas data

The Prima PRO (Thermo Scientific, Waltham, MA, USA) process Mass Spectrometer (MS) is connected to the bioreactor air inlet port and the off-gas port for both the 7.5L scale and 30L scale bioreactors. This allows the instrument to measure the composition of the air being bubbled into the fermentation and the air flowing out. Detection of these quantitative changes allow the MS software to determine the bioreactor OUR and CER, which can then be used to calculate the Respiratory Quotient (RQ). The RQ can be used as an indicator of the substrate being utilised, with different RQ values corresponding to cellular metabolism on different substrates (Winkler, 1990; Arifin *et al.*, 2014).

The calculation of these variables may be done by the use of the following equations:

$$\text{OUR} = \frac{1}{V} (F_{in}(\text{O}_2)_{in} - F_{out}(\text{O}_2)_{out}) \quad (2.2)$$

Where $(\text{O}_2)_{in}$, $(\text{O}_2)_{out}$ are the oxygen concentrations, and F_{in} and F_{out} are the gas flow rates at inlet and outlet respectively.

$$\text{CER} = \frac{1}{V} (F_{out}(\text{CO}_2)_{out} - F_{in}(\text{CO}_2)_{in}) \quad (2.3)$$

Where $(CO_2)_{in}$, $(CO_2)_{out}$ are the carbon dioxide concentrations at the inlet and outlet respectively.

$$RQ = \frac{CER}{OUR} \quad (2.4)$$

In this research, the calculation of the variables for the bioreactor studies (where possible) conducted at 7.5L and 30L scale were performed using the Prima PRO process MS software.

2.3 Purification of Pregallidermin

The purification sequence established for the novel PGDM product comprised the following stages: centrifugation, adsorption/desorption, ion exchange chromatography, salt removal by adsorption desorption and lyophilisation. These are described in detail in the following sections.

2.3.1 Small Scale centrifugation

Small scale centrifugation was performed using an Eppendorf 5810 bench top centrifuge (Hamburg, Germany). Cell culture broth was pipetted into 1.5 mL Eppendorf tubes and spun at 14,000 rpm for 5 minutes, at a temperature of 4 °C. The supernatant was pipetted into another 1.5mL Eppendorf tube and re-centrifuged for another 5 minutes to ensure the adequate removal of cells for supernatant analysis.

2.3.2 Large Scale Centrifugation

Large scale centrifugation was performed using a Beckman-Coulter Avanti® centrifuge (Brea, CA, USA). Cell culture broth was filled into 500 mL centrifuge flasks and spun at 10,000 rpm for 30 minutes at a temperature of 4 °C. The supernatant was decanted into fresh 500mL flasks and the centrifugation repeated for another 30 minutes. The supernatant was then pooled in Duran flasks and stored in the refrigerator at 4 °C for storage and further processing.

2.3.3 Adsorption using XAD-7

The hydrophobic resin, Amberlite® XAD-7, (Sigma-Aldrich, Dorset, UK) was prepared for adsorption by first washing with pure methanol for 60 minutes. The methanol was then replaced with MilliQ water and the beads washed for another 60 minutes. The water was then removed by vacuum filtration and 20 g of beads measured out into 500 mL conical flasks. 100 mL of clarified fermentation broth was poured into the flasks, which were then placed into a Kuhner (Basel, Switzerland) orbital shaker at 25°C and 200rpm for 60 minutes. The supernatant was removed by vacuum filtration with the adsorbed amount of PGDM determined by HPLC (Section 2.5.3) of the fermentation broth, pre and post adsorption.

For prep-scale adsorption of material, 40 g of washed and vacuum filtered XAD-7 was filled into a 3 L conical flask with 1 L of clarified fermentation broth. The conical flask was placed into an orbital shaker at 250 rpm and 25 °C for 120

minutes. Adsorption was determined by comparison of the HPLC (Section 2.5.3) chromatograms prior to and post adsorption.

2.3.4 Desorption

Prior to desorption the XAD-7 beads from section 2.3.3 were washed with 0.5 L of MilliQ water followed by a 0.02 M phosphate buffer solution at pH 6. The wash liquids were examined for PGDM by HPLC analysis Section 2.5.3 and the yeast extract released by the beads was monitored by measuring the change in colour intensity of the wash buffer using a UV spectrophotometer (section 2.5.1). Desorption was performed in two batches using a 100 mL solution of 60%/40% (v/v) Methanol/0.05 M sulphuric acid, placed in an orbital shaker at 250 rpm and 25 °C for 90 minutes. The amount and purity of desorbed PGDM was determined by HPLC (Section 2.5.3) before the batches were pooled and methanol evaporated in a rotary evaporator in preparation for ion exchange chromatography (Section 2.3.5).

2.3.5 Ion Exchange Chromatography

Ion exchange chromatography was performed using a GE Healthcare (Little Chalfont, UK) Sepharose SP FF and SP HP 1mL Hitrap® column on a GE Healthcare ÄKTA Purifier (Little Chalfont, UK) liquid chromatography system. Mobile phases for the chromatography were 0.02 M acetate buffer at pH 4.5 as the load and wash buffer, with 0.02 M acetate buffer at pH 4.5 with 2 M sodium chloride serving as the elution buffer. PGDM from 2 mL of desorbed eluent (Section 2.3.4) was purified using gradient elution from 0 % elution buffer to 15

% elution buffer. The eluted liquid was captured in 1 mL fractions and analysed for PGDM by HPLC (Section 2.5.3).

Scale up was performed using GE Healthcare SP HP, a strong cation exchange resin. An XK-16 (GE Healthcare, Little Chalfont, and UK) column was packed with 15 mL of resin, with packing quality tested by the symmetry of the peak produced by a 1 % (v/v) acetone solution on the chromatogram. Operational flowrate was maintained at 6 mL.min⁻¹. The purified PGDM was analysed using HPLC and then all fractions pooled for removal of sodium acetate and sodium chloride components by XAD-7.

2.3.6 Adsorption/Desorption

The PGDM containing Ion exchange fractions were pooled and 50 mL, product rich solution, poured into 250 mL conical flasks containing 2 g of washed Amberlite® XAD-7 resin (as mentioned in Section 2.3.4). Adsorption was performed by shaking the flasks at 250 rpm and 25 °C, for 60 minutes. The resin was then washed with 0.05 M buffer at pH 7 until no more yeast extract components were released (Section 2.3.4).

Desorption was performed using a 100 mL solution of 60% MeOH and 40% distilled water, at 25°C shaken at 250 rpm, in two batches of 50 mL each. The batches were pooled together with the Methanol removed using a rotary evaporator in preparation for lyophilisation.

HPLC analysis was used to determine yield and purity of the desorbed PGDM (section 2.5.3).

2.3.7 Lyophilization

Lyophilisation of the PGDM solution obtained from Section 2.3.6 was performed by placing 5 mL samples in pre-weighed flasks in a VirTis® (SP Scientific, Ipswich, UK) freeze dryer over 24 hours. Once liquid removal was complete, samples of the powder were weighed and analysed by HPLC (section 2.5.3).

2.4 Trypsinization of PGDM

PGDM (1 mg.mL^{-1}) was trypsinised (Chapter 1.5.1) using $10 \text{ }\mu\text{L}$ of 1 mg.mL^{-1} porcine trypsin buffered at pH 7 using a 0.02 M phosphate buffer, a PGDM to trypsin ratio of 100:1 (w/w), at $25 \text{ }^\circ\text{C}$. Samples were taken every 60 seconds, with the trypsin denatured using $10 \text{ }\mu\text{L}$ of concentrated 10 M sulphuric acid to halt the conversion, and analysed by HPLC to confirm the presence of the mature gallidermin.

Confirmation of the identity of gallidermin and leader sequences was undertaken by Mass Spectrometry (MALDI-MS) as described in Section 2.5.4.

2.5 Analytical Techniques

2.5.1 UV-VIS spectroscopy

The growth kinetics of the *S.gallinarum* variants (Section 2.1.1) during fermentation were determined by UV-VIS spectroscopy at 600 nm, using a Genesys UV-VIS spectrophotometer (Waltham, MA, USA). 1 mL samples of fermentation broth were pipetted into cuvettes for analysis. Dilutions with RO water were performed for high concentration fermentation samples that showed absorbance values beyond the accuracy range specified for the spectrophotometer (0 to 1 absorbance units (OD) at 600 nm).

The amount of yeast extract removed from XAD-7 resin beads during desorption (section 2.3.4) was also determined by measuring the UV-absorbance of 1 mL samples of wash buffer at 600 nm.

2.5.2 Biomass quantification

UV-VIS analysed samples of fermentation broth were filtered using pre-weighed membrane filters (Sartorius, Göttingen, Germany) and then dried overnight in an oven at 60 °C. The filters with the dry cell mass were reweighed and a calibration curve was determined using triplicate samples of each concentration.

2.5.3 Quantification of antibiotic concentration and purity

Gallidermin and PGDM were quantified and identified in broth by analysis on an Agilent 1200-series high performance liquid chromatography system (Agilent Technologies, Santa Clara, CA, USA). The system was equipped with a degasser, quaternary pump, automatic injector and a diode array detector (DAD) capable of detecting multiple wavelengths of visible and ultra-violet light.

The column utilized for the separation was a Nucleosil 100 C-18 column with 5 μ m pore size (125 x 4 mm) and a guard column (Hewlett-Packard, Dortmund, Germany). Sample Injection volume was maintained at 10 μ L and temperature was maintained at 25°C. The wavelength for detection was 204 nm. All samples were run in triplicate.

The mobile phases were composed of 0.1% (v/v) H₃PO₄ (solvent A) and Acetonitrile (solvent B), which followed a linear gradient from 0 to 40% solvent B in 10 minutes. Stripping, regeneration and re-equilibration of column to start conditions were achieved in another 7 minutes.

Identifications were performed by comparing the retention time of samples of PGDM/GDM against the retention time of a sample of commercially purchased pure gallidermin (Enzo-Life Sciences, Farmingdale, NY, USA). Quantification was performed by comparison against calibration curves made using the pure commercially sourced materials (Appendix 2).

Product purity was determined by comparing the total product peak area in mAU, on the HPLC chromatogram, with the total area in mAU of all the component peaks in the analysed sample (including product peak). The purity is thus expressed as a percentage of the sample. The purity is calculated using the equation:

$$Purity = \frac{A_{Prod}}{A_{Tot}} \times 100 \quad (2.5)$$

Where *Purity* is the PGDM or GDM purity in %, A_{Prod} is the total area of the product peak/peaks in mAU and A_{Tot} is the total area of all sample peaks in mAU.

It is noteworthy, that when calculating the purity of pregallidermin, the area of the peaks of both PGDM variant 1 and PGDM variant 2 have to be added.

2.5.4 Mass Spectrometry for product identification

Mass Spectrometry of the samples was performed by the UCL Chemistry Mass Spectrometry service using MALDI-TOF analysis on a Micromass MalDI micro MX system (Waters Corporation, Milford, MA, USA). Purified PGDM dissolved in water and gallidermin from the trypsinization in Section 2.4 were diluted with RO water to a concentration of 0.1 mg.mL^{-1} and provided for analysis. The mass spectra obtained were compared against mass spectra of commercially sourced gallidermin and literature to confirm product identity by molar mass.

2.6 Microscale Methods for product analysis

Microscale methods for the analysis of PGDM and gallidermin properties were initially established using a 24 microwell Eppendorf Thermomixer Comfort® (Hamburg, Germany), with enclosing lid. The thermo-mixer allowed for control of temperature and agitation. 1.5 mL eppendorf tubes were utilized to contain the antibiotic solutions with the plate lid providing an additional barrier to liquid evaporation, control experiments conducted with the setup showed negligible evaporation, allowing it to be ignored. All samples were analysed using HPLC as described in Section 2.5.3.

2.6.1 Temperature stability studies

The temperature stability of PGDM and GDM was determined by pipetting a 1 g.L⁻¹ antibiotic solution, buffered at pH 6, 7 or 8 using a 0.02 M phosphate buffer, into a 1.5 mL eppendorf tube and placing onto a thermo-mixer at 25 °C and 37 °C. Samples from the microwells were analysed via HPLC as described in Section 2.5.3 to determine changes in concentration of antibiotics over time.

2.6.2 pH stability studies

The pH stability of the antibiotics was determined by pipetting 1 mL of 1 g.L⁻¹ antibiotic solution at pH 6, 7 and 8 into 1.5 mL Eppendorf tubes and placing them within the thermo-mixer. The samples were adjusted to pH 6 using 0.02 M acetate buffer and pH 7 and 8 using 0.02 M phosphate buffer. Experiments

were carried out at 25 °C and 37 °C, with mixer shaking set at 1200 rpm. Samples were analysed by HPLC (Section 2.5.3).

2.6.3 Stability at varying ionic strength

The impact of antibiotic concentration on degradation kinetics was determined by pipetting 1 g.L⁻¹ of antibiotic solution; buffered at pH 6, 7, and 8, with ionic strengths of 0.02 M, 0.04 M and 0.06 M, into 1.5 mL eppendorf tubes and placing into a thermo-mixer agitated at 1200 rpm. Experiments were carried out at temperatures of 25 °C and 37 °C with samples taken at regular intervals analysed by HPLC over time.

2.7 Microscale methods for optimisation of product capture

Microscale methods for optimisation of DSP sequences were performed using a 24 well Eppendorf Thermomixer Comfort® (Hamburg, Germany) with enclosing lid. The methods were used to optimise the PGDM primary capture step, product capture by Amberlite XAD-7. 1.5 mL Eppendorf tubes filled with 20 mg of XAD-7 resin were utilized for each experiment. One clarified fermentation broth was filled into the tubes; the temperature was set at 25 °C and agitation rate to 1200 rpm. The quantity of adsorbed and desorbed PGDM was determined by HPLC as described in section 2.5.3. The optimisation experiments are described in the following sections.

2.7.1 Optimisation of product capture on XAD-7

1 mL each of clarified fermentation broth adjusted to a pH of 5, 6, 7, 8, and 9, was pipetted into 1.5 mL eppendorf tubes. 20 mg of Amberlite XAD-7 resin was added to the broth in each Eppendorf tube and shaken on the thermo-mixer at 25°C and 1200 rpm for 90 minutes. Samples of broth were pipetted into HPLC vials and analysed to determine antibiotic uptake (Section 2.5.3).

The Eppendorf tubes were then centrifuged at 10,000 rpm, decanted to remove supernatant and refilled with 1 mL of wash buffer at pH 5, 6, 7, 8 and 9. The resin wash was repeated 3 times, before elution was performed using a 60 % (v/v) Methanol/0.05 M sulphuric acid elution buffer. HPLC analysis as described in Section 2.5.3 was performed on all samples for each wash step and the PGDM elution step. In wash analysis by HPLC, where there was no detectable PGDM present, a sum of the total area for all impurity peaks (in milli-absorbance units, mAU) on the chromatogram was used as a representation of the amount of impurity released by the resin during wash of an individual sample. A comparison between the total HPLC chromatogram impurity peak area, for the various samples, was used to determine impurity removal efficiency of the wash buffer in the individual eppendorf tube.

2.7.2 Optimisation of product elution from XAD-7

1 mL of clarified fermentation broth, adjusted to pH 6, was pipetted into 1.5 mL eppendorf tubes. The tubes were filled with 20 mg of XAD-7 resin each and

adsorption of PGDM was performed by shaking at 25 °C and 1200 rpm as described in Section 2.7.

The beads were then washed with 0.06 M phosphate buffer at pH 7. Once washing was complete, the eppendorf tubes were spun at 10,000 rpm, decanted and refilled with the elution liquid composed of Methanol and a sulphuric acid (H₂SO₄) solution co-solvent. Methanol concentration was adjusted from 0 % (v/v) to 100 % (v/v). The ionic strength of the H₂SO₄ co-solvent was adjusted between nil and 0.005 M. Elution was performed in two batches with samples analysed using HPLC to determine amount and purity of eluted antibiotic (Section 2.5.3).

2.7.3 Optimisation of impurity removal from XAD-7

1 mL of clarified fermentation broth was used for PGDM adsorption onto 20 mg of XAD-7 resin as described in Section 2.7.2.

The beads were then washed with a wash buffer composed of 0 to 10 % (v/v) Methanol and 0.02 to 0.06 M phosphate buffer at pH 7. After 60 minutes of washing, each wash sample was analysed for the presence of PGDM. Where PGDM was not present, the sum of the total area of all impurity peaks was used as representative of impurity removal from the XAD-7 resin beads (Section 2.7.1). A comparison of total impurity removal (total impurity peak area in mAU) from each sample was used to determine the optimal resin wash.

Elution was then performed using 80% (v/v) Methanol/0.05 M sulphuric acid. The purity and concentration of PGDM as determined by HPLC for each sample, (Section 2.5.3) was used to confirm the optimal conditions for XAD-7 impurity removal.

3. Optimisation of Pregallidermin production by Fed-batch fermentation of *S.gallinarum* Δp

3.1 Introduction and Aims

It is important to realise that in order for any useful benefits to be derived from the novel antibiotic candidates under consideration, they must be producible at scale. Scale production of compounds using biological organisms relies on fermentative culture in bioreactors. Large scale bioreactors have environments that differ substantially from lab-scale environments, with completely different engineering parameters and mass transfer methods. Thus for large scale production of any novel compound, the choice of chassis organism and its interaction with the bioreactor environment becomes crucial in the compounds commercial viability (Zhang *et al.*, 2016).

The ability to develop platform processes, that can be used to produce the novel compounds at scale thus become an important component in developing the ability to rapidly deal with outbreaks of novel or multidrug resistant bacteria. To develop such platform processes would require an understanding of the behaviour of the chosen chassis organisms under pilot-scale and large scale fermentation conditions.

Thus in order to optimise the production of a candidate antibiotic compound, it is vital that the various environmental interactions and engineering parameters at which the organism thrives and yields the most antibiotic are studied. In the

following research a genetically modified organism *Staphylococcus gallinarum* Δ *gdmP::aphIII*, a knock-out mutant (Valsesia *et al.*, 2007), which produces the novel antibiotic compound pregallidermin is investigated for the optimisation of antibiotic production with respect to the crucial engineering parameters in scale fermentation.

As described in Section 1.9, the **aim** of this Chapter is to establish a reproducible and scalable fermentation process for the production of PGDM by *S.gallinarum* Δ *p*. The focus is on production of PGDM rather than gallidermin directly because the gallidermin displays host cell auto-toxicity, which limits achievable titres in culture (Section 1.3.9). The specific **objectives** are as follows:

- To characterise PGDM production in batch and fed-batch cultures of *S.gallinarum* Δ *p* in laboratory scale (7.5 L) stirred tank bioreactors (STR).
- To examine the impact of different feeding regimes and aeration control strategies on the efficiency of PGDM production.
- To establish the scale-up of the fed-batch PGDM fermentation process to a small pilot-scale (30 L) fermenter
- To compare PGDM production at various scales to determine critical parameters for fermentation scale-up. PGDM was identified and quantified using HPLC and MS, outlined in section 2.5.3 and 2.5.4. Product identity confirmed by spectra in Figure 4.5.

3.2 Overview of fermentation development strategy

The research presented in this Chapter aims to understand the impact of various engineering parameters on the cellular growth of *S.gallinarum* Δp and production of the novel antibiotic PGDM. The data acquired is intended to illuminate the scalability and reproducibility of *S.gallinarum* Δp fermentations and provide material for study in subsequent parts of this thesis.

The approach to fermentation development and the different scales of fermenter used is summarised in Figure 3.1. Initial experiments were performed in shake flasks to determine cellular batch growth kinetics. Subsequently studies were performed in laboratory scale fermenters to examine feed regimes and aeration strategies to characterise their impact on growth. Finally, attempts are made to replicate cell growth and PGDM production at 30 L scale, with a view to analysing the importance of the characterised parameters on scale up. Table 3.1 summarises the main findings from all the stirred bioreactor studies. These will be described in further detail in the following sections.

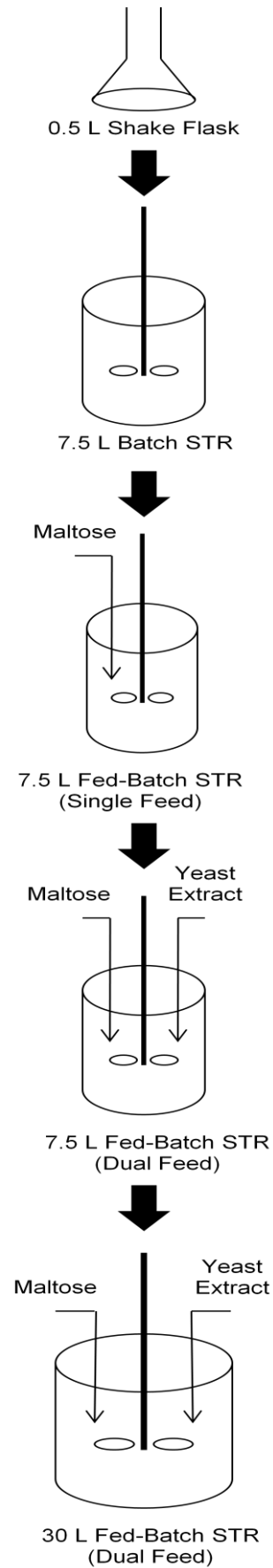


Figure 3.1 Overview of the types of fermentation performed as outlined in Section 2.2.

3.3 Shake Flask culture

In order to understand the initial growth parameters of the *S.gallinarum* Δp , shake flask cultures with a 10 % inoculum were performed. The 1:9 ratio for pre-culture and media were kept uniform for all fermentations. After inoculation, 1 mL samples were taken every hour in order to map the batch growth kinetics. Figure 3.2 illustrates the growth of *S.gallinarum* Δp .

From the growth curves it is visible that *S.gallinarum* Δp is a rapidly growing organism, obtaining maximum biomass in about 11 hours of growth. To determine the fastest period of growth for the organism, it is useful to convert cellular growth to a logarithmic scale. Figure 3.3 illustrates the logarithmic growth of the organism. The period of fastest growth (the exponential growth phase) of the organism is found to be between 1- 4 hours after inoculation. The fastest specific growth rate achieved by the organism is 1 h^{-1} .

The total increase in cell biomass as demonstrated by the data is 4 orders of magnitude within the experimental time. In order to achieve higher cell densities, it would be important to prolong the exponential phase as much as possible, as the lantibiotic gallidermin displays primary metabolite kinetics, and hence maximum biomass would lead to maximum lantibiotic yield (Medaglia, 2009).

Shake flask studies on *S.Gallinarum* Δp have previously been performed by both Valsesia (2008) and Medaglia (2009). In the latter case these studies were briefly done for the preparation of inocula and testing of cellular growth in a

selection of liquid culture media. However, the shake flask studies performed by Valsesia (2008) produced amounts of PGDM detectable by HPLC. Earlier experiments in shake flasks by Kempf *et al.*, 2000 with the wild type *Stapylococcus gallinarum* Tü3928 had also produced detectable quantities of the wild type gallidermin, considering the PGDM is the precursor, it would be expected that expression would follow the same profile as the active lantibiotic. It is worth noting that this was not the case with the current work, which was unexpected as the secretion of a primary metabolite in solution should match cellular growth.

Shake flask cultures are an important tool for the determination of preliminary data on bacterial growth characteristics. However in order to the conditions necessary to achieve optimal bacterial growth over a sustained period, other parameters such as dissolved oxygen, aeration and mixing are required which are beyond the scope of the shake flask setup to determine. These are examined in the following sections.

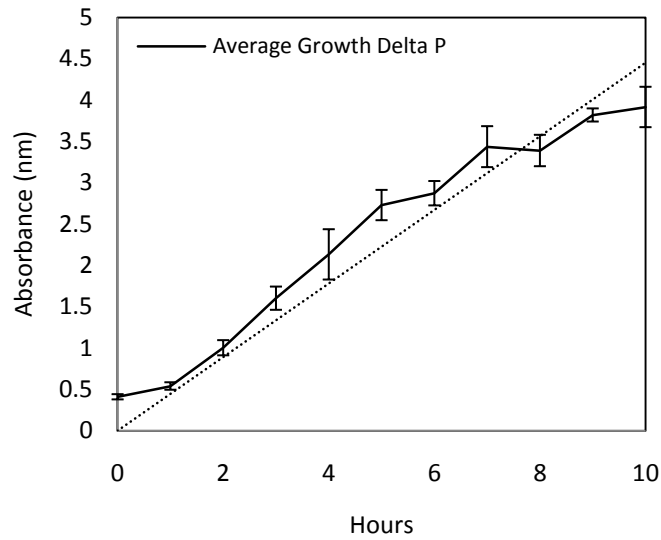


Figure 3.2 Representative shake flask batch growth kinetic profile of *Staphylococcus gallinarum* Δp . The error bars represent one standard deviation about the mean. (n=3, average of 3 fermentations) Experiments performed as described in Section 2.2.1.

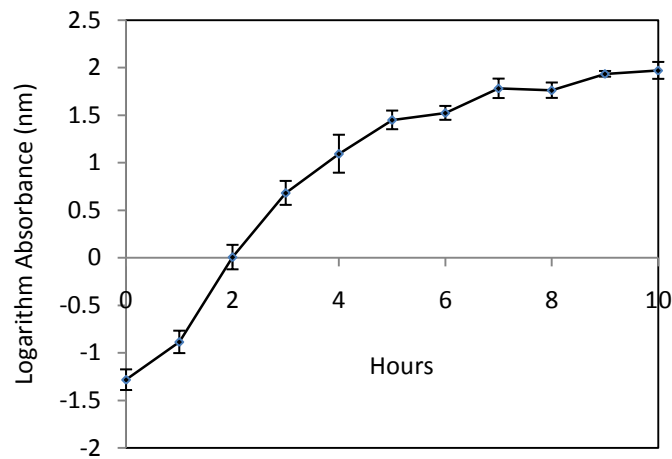


Figure 3.3 Logarithmic growth curve for *Staphylococcus gallinarum* Δp . The error bars represent one standard deviation around the mean. (n=3)

3.4 7.5 L STR Fermentation: *S.gallinarum* Δp growth in batch mode

Batch fermentations were performed at 7.5 L scale with a 10 % inoculation (Section 2.2.2). The 5 L stirred tank bioreactor allows for the control of a larger number of engineering parameters than shake flask fermentations, allowing for a greater degree of control to be exerted on the bacterial growth. The attached mass spectrometer allowed the off-gas to be analysed for CER (carbon evolution rate) and OUR (oxygen uptake rate), allowing for the calculation of the respiratory quotient (RQ) in order to relate the two parameters to cellular growth.

The results in figure 3.4 show that as the cells grow, an increase in the CER and OUR is observed, especially in the exponential growth phase. The agitation rate similarly increases with increasing cellular growth, which is logical as growing cells put greater pressure on the oxygen availability, requiring higher fluid agitation to ensure greater oxygen distribution and maintain DOT. The growth pattern was similar to the shake flask kinetics, with a rapid exponential phase lasting about 5 hours. The OUR and CER follow each other quite closely, both increasing as the exponential growth progressed. However both drop off considerably when biomass increase declines, illustrating the much reduced oxygen requirements for cellular maintenance as opposed to growth. The corresponding drop in agitation rate from about 700 rpm to roughly 300 rpm reinforces this assessment.

Figure 3.5 displays the RQ for the duration of the fermentation and as is visible the value was approximately 1, which suggests that the cells prefer carbohydrate as the main growth substrate. However, it is also visible from figure 3.4 A that cellular growth drops-off with no corresponding drop in RQ, which suggests that in Medium 21B, growth was limited by a nutrient other than carbohydrates.

It is of note that the 21B medium used for the experimental set-up is composed of yeast extract, which is a complex combination of autolysed carbohydrates and proteins. The reason for the choice is the ease of making the media and low-cost of the components, characteristics suitable for platform production processes. However the media complexity means that precise composition by mass of proteins as opposed to carbohydrates is uncertain. This is significant as the RQ indicates carbohydrate to be the preferred growth substrate for the organism, suggesting media with higher sugar content may be a better choice. The data indicates that 21B media containing 50 g.L^{-1} of yeast extract results in a biomass yield of roughly 12.5 g.L^{-1} . This computes to a biomass conversion ratio of roughly 1:4 at a DOT of 40 %.

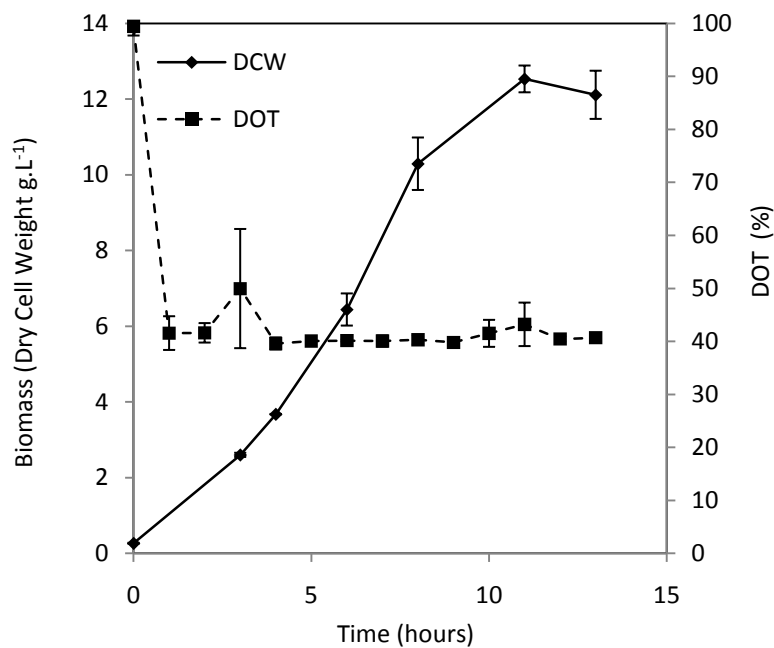
It is however interesting to note that when the batch process was tested for the presence of the lantibiotic pregallidermin (Section 2.5.3), it was found that none was present. Considering that pregallidermin has been shown to display primary metabolite kinetics (Valsesia *et al.*, 2007), this was unexpected. It has been suggested previously that lantibiotic production is initiated by quorum sensing (Heinman & Panke, 2006; Kleebezem, 2004); hence it is possible that the cellular biomass concentration is simply not high enough for a quorum to

form. Work by Kempf *et al.* (1999) with the wild-type strain had determined that the use of an appropriate feeding strategy was important to maximise the production of lantibiotic. Studies by Medaglia (2009) on the use of various substrate feeds to *S.gallinarum* Δp had demonstrated a culture that had not been fed any substrate (i.e. essentially a batch culture) produced very little detectable PGDM during the exponential growth phase, which later disappeared from solution during the stationary phase. It is also notable that Medaglia's (2009) fermentation had a biomass yield of about 20 g.L⁻¹, which is significantly higher than the 12.5 g.L⁻¹ generated in this work. This difference may potentially be due to differences in aeration and agitation strategy, though this is difficult to determine as Medaglia (2009) did not characterise these parameters.

Additionally, Medaglia (2009) showed that PGDM degraded much faster in media that had low sugar content; hence it is possible that even if a small amount of PGDM was produced, it degraded rapidly.

Also of note is the initial reduction in the OUR and CER after 3 hours of fermentation. As the two parameters closely map the growth of *S.gallinarum* Δp , it is suggested that some kind of metabolic shift takes place, possibly from the preferred media substrate to the second substrate. An examination of the RQ provides no clue as to what happened, experimentation with defined media would be suggested to establish the organism's preference; however such experimentation is beyond the scope of this research.

A



B

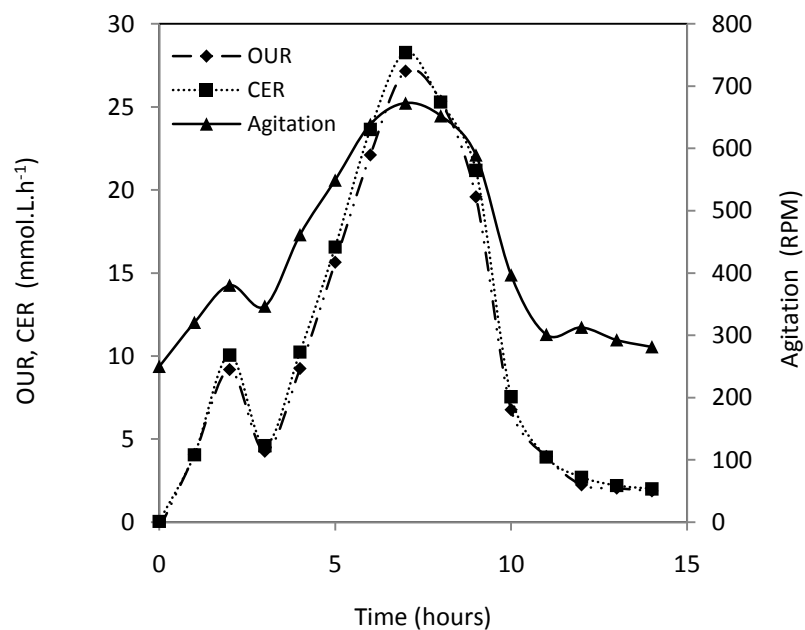


Figure 3.4 Batch growth kinetics of *Staphylococcus gallinarum* Δp at 7.5 L scale. (A) Biomass increase with DOT maintained at 40% (B) the corresponding OUR, CER and Agitation profiles. Error bars represent one standard deviation around the mean ($n=3$, average of 3 fermentations). Fermentations performed as described in Section 2.2.2. A summary of fermentation performance is provided in Table 3.2.

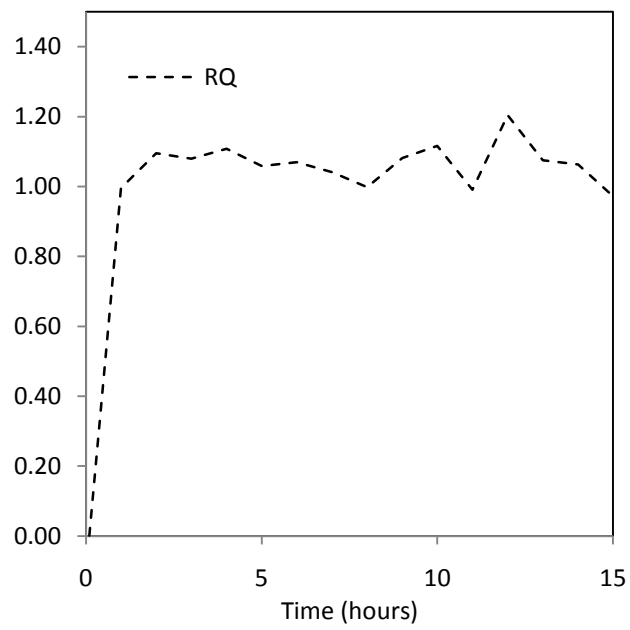


Figure 3.5 RQ profile for the 7.5L scale batch fermentation of *Staphylococcus gallinarum* Δp

3.5 7.5 L STR Fermentation: *S.gallinarum* Δp growth in fed-batch mode

The data from the 7.5 L STR in Figure 3.4 illustrates the substrate limitations to growth and lantibiotic production in batch mode. It also appears that the biomass achieved was insufficient to initiate lantibiotic production. In order to achieve a higher biomass and subsequently initiate pregallidermin production, a fed-batch mode of operation was pursued with a 500 g.L⁻¹ maltose solution chosen as the feed (Section 2.2.3). Maltose offers the highest pregallidermin production out of a selection of simple sugars (Medaglia, 2009).

After running a fed-batch culture using a maltose feed only (Figure 3.6), it again became apparent that there was a limiting reactant present in the media and feed combination. The continued feeding of maltose did not lead to any increase in biomass beyond 30 g.L⁻¹, a result consistent with previous studies by Medaglia (2009). This led to the assumption that a nitrogen source (protein) or a different medium nutrient had become growth limiting. As yeast extract is a complex combination of proteins, carbohydrates and other simple components, a yeast feed of 300 g.L⁻¹ was used as the nitrogen source. This dual feed method was applied in order to achieve high lantibiotic production, which seemingly necessitates a high cell density culture.

3.5.1 Fed-batch – Maltose feed

As shown in Figure 3.6, the use of a maltose feed resulted in a total biomass of 30 g.L^{-1} , in comparison to 12.5 g.L^{-1} achieved in batch mode. Engineering parameters such as temperature, pH and DOT were maintained at the same levels as the batch fermentations. It is important to note that the maltose feed resulted in the production of pregallidermin, which indicates a cell density high enough to activate quorum sensing. Additionally, it could also suggest that the addition of a concentrated maltose feed prevents the pregallidermin from degrading in culture (Medaglia, 2009).

It is also notable that the growth kinetics, of the fed-batch culture, were similar to batch culture and the provision of extra-nutrients did not prolong the exponential growth phase. Similarly increasing the amount of maltose in solution further did not result in a corresponding increase in biomass above 30 g.L^{-1} . Additionally, as in the batch fermentation (Figure 3.5), the RQ for the fed-batch fermentation (Figure 3.7 B) stayed at approximately 1, indicating that the cells continued to use carbohydrate as the principle substrate and providing further evidence that some other medium component was limiting growth.

When the biomass achievable in batch mode (12.5 g.L^{-1}) is accounted to the fermentation media alone, the new biomass accountable to maltose addition alone is determined to be 17.5 g.L^{-1} from the addition of 70 g.L^{-1} maltose. The resultant biomass to substrate conversion ratio achieved overall is 1:4; however it is visible that conversion efficiency was greater at the start of exponential phase as opposed to the late exponential phase and stationary phase. Hence it

could be assumed that prolonging the exponential phase would result in utilization of the carbon source more efficiently.

What does however, become clear from the fed-batch growth of *S.gallinarum* Δp is that achieving high cell density fermentations requires certain key variables to be adjusted at an exponential rate. The agitation rate in Figure 3.6 C, mirrors cellular growth (Figure 3.6 A), with increasing agitation signalling growth and decreasing agitation indicating the slowing of cellular growth and the beginning of stationary phase for cell maintenance. The cascade system involving agitation rate and DOT was adequate to maintain the DOT at 30 %.

It is notable though that the aeration rate must also be increased with the cellular growth rate. This was unexpected as it was assumed that maintaining a DOT set-point of 30 % would be sufficient to cater to the oxygenation and aeration needs of cellular growth. However as is apparent, aeration was manually adjusted to mirror the cellular growth in the exponential phase, starting at 3 L.h^{-1} (1 vvm of the starting volume of the culture) and ending at 9 L.h^{-1} , triple the initial aeration rate (and roughly 2 vvm of final bioreactor volume).

The feed-regime (Figure 3.7A) also maps the growth of *S.gallinarum* Δp , however the bioreactor utilized for the culture did not possess the ability to employ an exponential feed regime. In order to map the growth rate of the organism with the feed regime, feeding was started once the dry cell weight became 1 g.L^{-1} and manually adjusted to follow growth by adjusting the feed rate every hour in a step-up pattern.

The final feed rate broadly follows the equation:

$$Feed(y) = 0.94(x) \quad (3.1)$$

Where y is the feed rate in $\text{g.L}^{-1}.\text{h}^{-1}$ and x is the time in hours.

Equation 3.1 seems to indicate a very linear relationship between the feed requirements and cellular growth.

Pregallidermin production began once the cellular dry cell mass approached 25 g.L^{-1} and continued with the growth in mass (Figure 3.6 A). However, lantibiotic production stopped as soon as growth slowed down, demonstrating primary metabolite kinetics, and did not restart with an increase in the maltose concentration.

The average cellular growth profile of multiple ($n=3$) fed-batch fermentations was consistent with a maltose based fed cultivation performed by Medaglia (2009) and Valsesia *et al.* (2007). However, it is notable that the present work produced significantly lower PGDM; a maximum of 0.1 g.L^{-1} in comparison to almost 0.6 g.L^{-1} in both previous studies. This was unexpected and it is unclear exactly why this happened. A possible explanation is variability in the aeration and agitation regimes, Medaglia (2009) ensured the DOT was maintained above 20%, however in both cases details were not provided on the adjustments made to achieve this. Thus it is difficult to ascertain the cause of the reduced yield without characterisation of these parameters.

However, the results were consistent in showing that there is a limit to biomass yield based on just maltose addition, and further feeding did not coerce any more cellular growth.

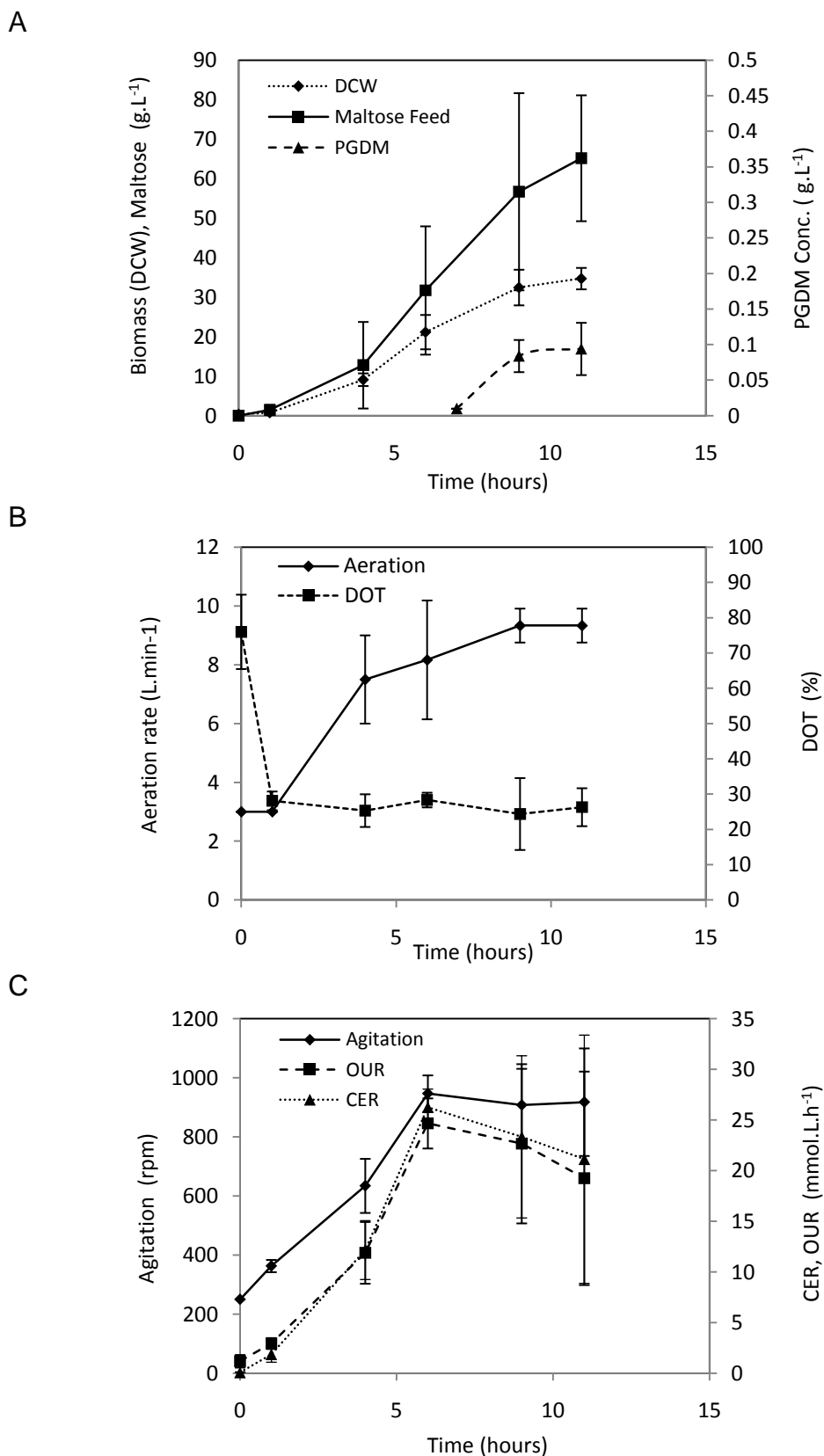
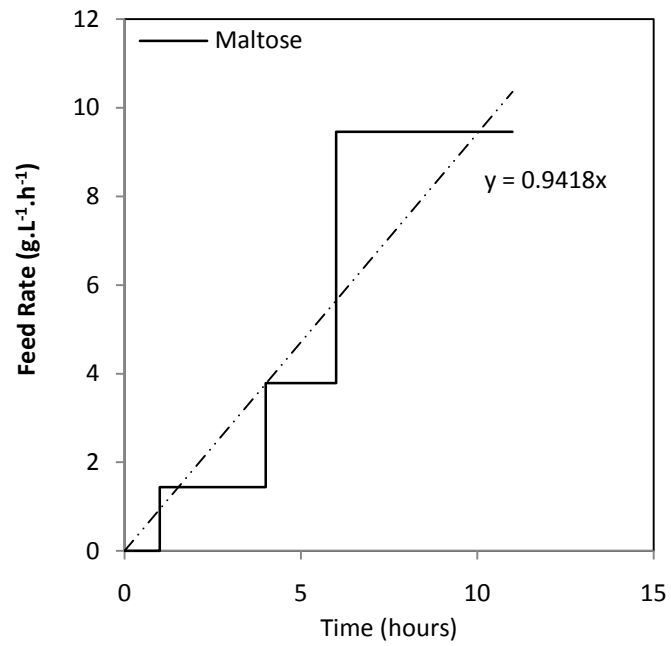


Figure 3.6 Fed-batch growth kinetics of *Staphylococcus gallinarum* Δp at 7.5L scale using a maltose feed.(A) showing cell growth, the maltose feed and PGDM production. (B) DOT and the aeration rate. (C) Agitation, CER and OUR (Off-gas analysis) as fermentation progresses. The error bars represent one standard deviation about the mean ($n= 3$, average of 3 fermentations). Fermentations performed as described in Section 2.2.3. A summary of fermentation performance is provided in Table 3.1.

A



B

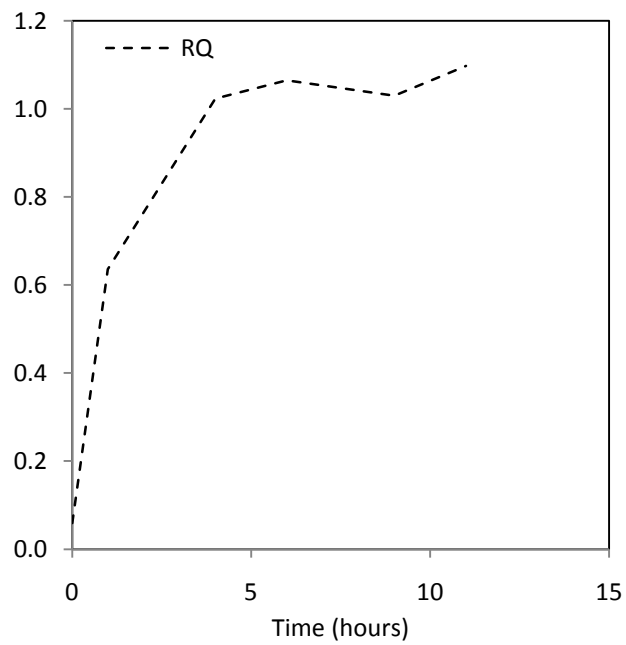


Figure 3.7 Fed-batch growth of *Staphylococcus gallinarum* Δp on 21B medium and 500g.L⁻¹ maltose feed at 7.5L scale with A) showing the maltose feed rate and feed profile applied to the culture and B) showing the RQ.

3.5.2 Fed Batch- Maltose and yeast extract feed

The culture of *S.gallinarum* Δp in fed-batch mode with only maltose as the additional carbon source did not reach very high cell densities and subsequently did not produce correspondingly high levels of lantibiotic. Yeast-extract (300 g.L⁻¹) was introduced as a secondary feed with a view to providing a protein source and ensuring that growth is not limited by the absence of a nitrogen source or any other component in the medium (Section 3.5).

Figure 3.8 illustrates the use of a dual feed fed-batch system (Section 2.2.3), which allowed the dry cell mass to reach around 120 g.L⁻¹. The corresponding yield of PGDM from the fermentation was around 350 mg. The provision of a protein source in the form of a yeast-extract feed allowed for an extension in the exponential growth phase from 3 hours to roughly 6 hours. The results confirm the nitrogen substrate limitation placed on a fed-batch system with only maltose as an additional carbon source.

The trends from the dual feed setup reconfirm the importance of mirroring the cellular growth pattern with the process inputs such as aeration and the feed streams. The parameters all map the growth pattern of *s.gallinarum* Δp in its exponential growth phase, indicating that to prolong cellular growth, a dynamic bioreactor environment must be provided where any of the carbon source (maltose), nitrogen source (yeast-extract protein) and airflow rate cannot be limiting to growth.

The system generated about 110 g.L^{-1} of additional biomass (compared to the 7.5 L batch fermentation, with no added maltose in Section 3.4) using 120 g.L^{-1} of maltose. This translates to a yield of biomass on substrate of 0.9 g.g^{-1} for the complete fermentation as opposed to 0.25 g.g^{-1} in cultures without the presence of yeast-extract. PGDM production also tripled, however at quadruple the total cell biomass of the single feed fed-batch culture.

The aeration rate was increased to map the growth pattern of *S.gallinarum* Δp , notably this was done even without a corresponding drop in the DOT set-point. It appears that to promote high cell density culture with *S.gallinarum* Δp , the aeration becomes a critical factor indicating that the bacteria is highly aerobic. The data indicates that a doubling of the airflow rate corresponds to roughly a doubling of the biomass during the organisms' exponential growth phase.

It is also notable that in order to maintain the DOT set-point, gas blending was performed on the air flowing into the bioreactor. The gas-blending operated in a cascade mechanism synchronised with the agitation, where any fall in DOT upon reaching the maximum agitation rate would initiate pure oxygen to be blended into the air supply. The initiation of pure oxygen blending meant that the concentration of oxygen exiting the bioreactor in the off-gas was higher than in the air inlet, hence at this time the OUR readings became unreliable (this occurred at the end of the cellular exponential growth phase, as can be seen by the agitation rate flattening and hitting a maximum in figure 3.9 B, as a result only the CER readings for these fermentations have been provided).

However, it is still possible to compute the fermentation RQ profile by excluding the time period with unreliable OUR values (data not shown). The RQ values for the dual-feed fed-batch culture are illustrated in Figure 3.9 C. The data suggests that the primary substrate for the fermentation was no longer carbohydrate, rather as the RQ is roughly between 0.7 - 0.8, it appears that a mixture of nutrients is being utilised by the cell. As the culture resulted in a very high level of biomass, it would appear to support the suggestion made earlier in section 3.5.1 that high cell density cultivations of *S.gallinarum* Δp require the presence of additional nutrients present in the yeast-extract to continue cellular growth.

The maltose and yeast extract feeds were manually adjusted (using separate Watson-Marlow 101 U/R pumps) in a 'step-up' feeding regimen (Figure 3.9 A). The maltose feed was started earlier as in Section 3.5.1, when dry cell mass approached 1 g.L⁻¹. In comparison, yeast-extract feeding was only started once the cells were in early exponential phase and stepped-up hourly until the maximum achievable (Figure 3.9 A). The final maltose feed profile broadly follows the linear equation:

$$Feed(y) = 1.96(x) \quad (3.2)$$

Where y is the feed rate in g.L⁻¹.h⁻¹ and x is the time in hours.

It is notable from Equation 3.2, that in comparison to the fed-batch culture utilising only maltose as the feed in Equation 3.1, the dual-feed system uses twice as much maltose per hour. This was likely because the dual feed system successfully prolonged the cells exponential growth phase, meaning higher substrate requirements for longer. It also provides further evidence that

S.gallinarum Δp requires certain additional nutrients, which are present in the yeast-extract to maintain cellular growth. Thus, high cell density cultures cannot be grown using just an additional carbon source.

It was also notable that during cellular exponential growth phase, on average the feed rate of the maltose was roughly 3 times the feed rate of yeast-extract (Figure 3.9 A), suggesting that a ratio of 3:1 maltose to yeast extract could provide suitable substrate requirements for fast growing cells and thus enable an elongation of the exponential growth phase by maintaining a dynamic nutrient microenvironment within the bioreactor.

Additionally, the CER closely mapped the production of PGDM (Figure 3.9 B). This suggests that PGDM is a normal by-product of cellular respiration for *S.gallinarum* Δp .

Kempf *et al.* (1999) had studied the growth of the wild-type *S.gallinarum* and found that improving the production of lantibiotic required the addition of a source of peptides. As the 21B medium component yeast-extract is a mixture of proteins and carbohydrates, it is reasonable to suggest that the use of a yeast-extract feed provides this additional nutrient requirement. Biomass yield for the dual-feed approach was comparable to similar studies conducted by Medaglia (2009), however as in the case of the maltose-only fed-batch cultivation, the yield of PGDM for the present study was significantly lower, 0.35 g.L^{-1} compared to 1.2 g.L^{-1} for the previous study.

As in the previous instance, Medaglia (2009) did not characterise the aeration strategy and agitation strategy and thus, there it is not possible to compare these parameters to spot potential differences. However, a notable difference is Medaglia's (2009) use of an exponential feeding strategy as compared to a step change or step-up strategy in the current work. It is suggested that an exponential feed strategy better predicts the growth profile of the cells in exponential growth phase, and hence is better able to emulate the nutrient requirements. Thus, the varying feed-strategies could be the source of the difference in product titres.

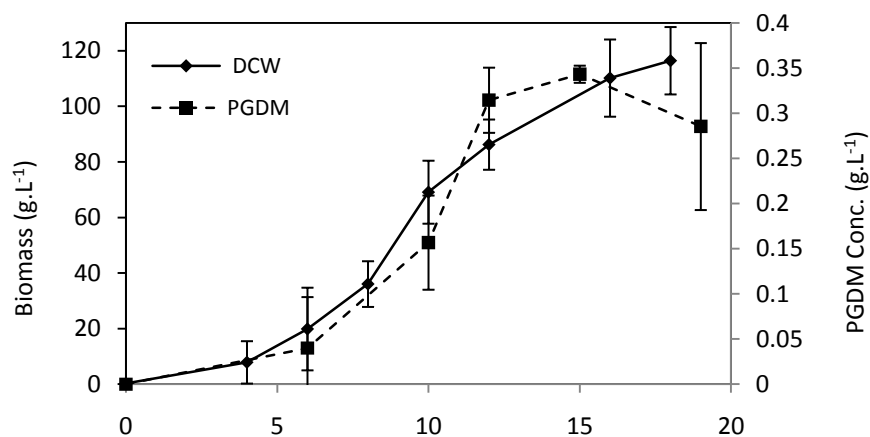
However, it is notable that a step-up profile is simpler to reproduce than an exponential profile, in cases where the bioreactors and pumps cannot be easily programmed or lack the capacity to use exponential regimes. Thus, from the perspective of developing a platform process, being able to easily reproduce results may be of greater importance for the initial antibiotic production to enable optimization studies that allow simultaneous process development.

Another difference between this work and studies by Medaglia (2009) was the lack of excessive foaming that was observed by the latter. Foaming in the present fermentation was easily controlled by the addition of anti-foam via bioreactors automated control system and provided no impediment to the continuation of fermentation.

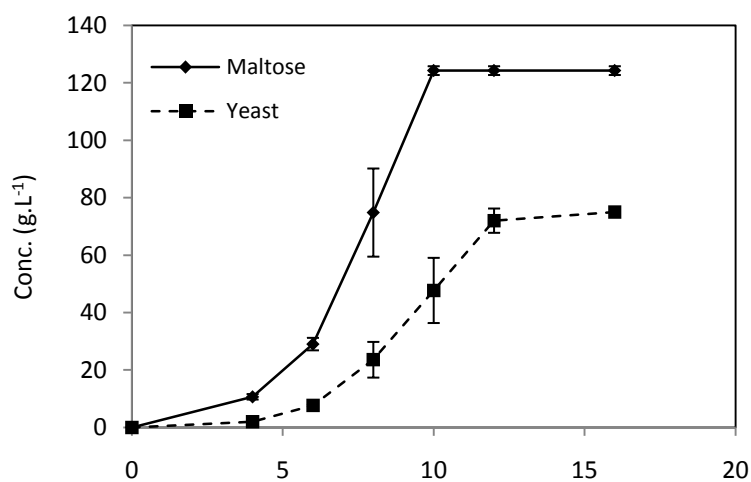
The results also demonstrate that high cellular growth requires all key parameters to map each other, creating a dynamic bioreactor environment.

Such conditions have previously been demonstrated to increase productivity and product quality (Spadiut *et al.*, 2013).

A



B



C

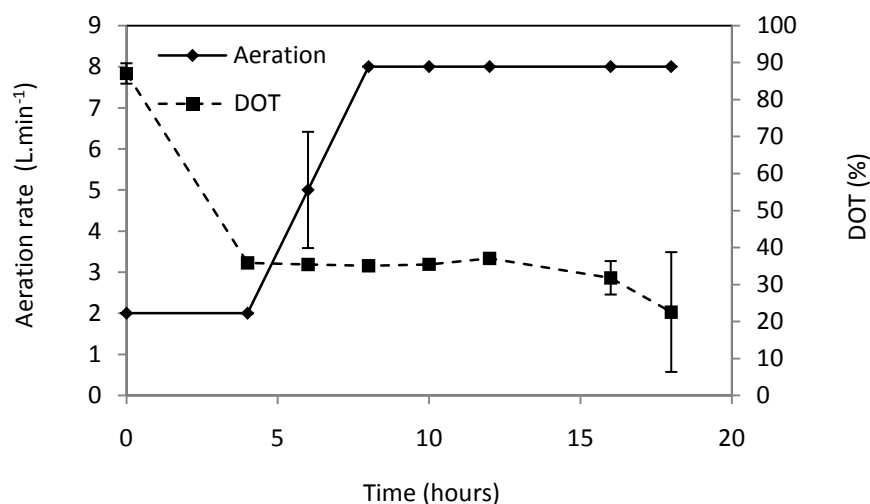


Figure 3.8 Fed-batch growth kinetics of *Staphylococcus gallinarum* Δp at 7.5L scale using dual Maltose and yeast extract feed. (A) Biomass and pregallidermin production. (B) Cumulative maltose (500g.L^{-1}) and yeast extract (300g.L^{-1}) feed addition. (C) Aeration and DOT (set-point minimum 30%). Error bars represent one standard deviation around the mean. ($n=2$). Fermentations performed as described in Section 2.2.3. A summary of fermentation performance is provided in Table 3.2.

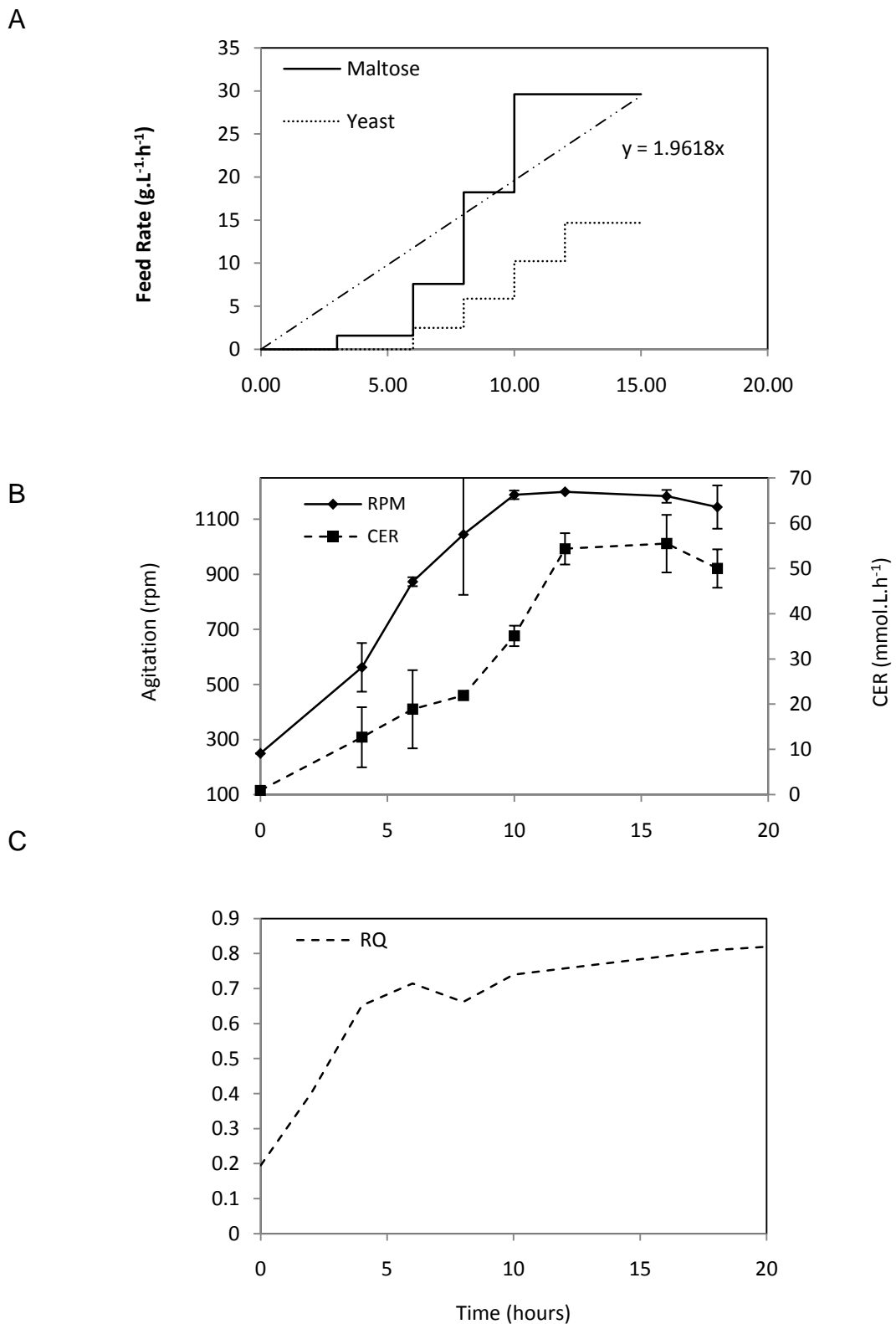


Figure 3.9 Fed-batch growth of *Staphylococcus gallinarum* Δp at 7.5L scale using dual maltose and yeast extract feed with A) showing the feed rates of the 500g.L^{-1} maltose feed and 300g.L^{-1} yeast-extract feed B) the agitation rate and CER and C) the RQ. Error bars represent one standard deviation around the mean. ($n=2$). Fermentations performed as described in Section 2.2.3.

3.6 30 L STR Fermentation: Scale up of pregallidermin production

In order to produce enough material for subsequent purification studies in Chapter 4, the fermentation process was scaled-up to 30 L scale (Section 2.2.4). Figures 3.10 and Figure 3.11 show the results of the fermentation along with the critical parameters outlined in previous fermentations. The dry cell weight achieved by the *S.gallinarum* Δp was 105 g.L^{-1} , while PGDM yield was 0.7 g.L^{-1} , more than twice the yield at 7.5 L scale.

It is clearly visible that the trends outlined by experiments at 7.5 L scale are displayed at 30 L scale, suggesting reproducibility at scale by ensuring that parameters such as feed regime and aeration closely map the cellular growth pattern. As suggested at 7.5 L scale in Section 3.5.2, the ratio of maltose to yeast extract feed solutions was modified to 3:1, with a maltose feed of 600 g.L^{-1} and a yeast-extract feed of 200 g.L^{-1} . This change benefits the process by making the experimental set-up simpler i.e. by using a constant ratio between the feeds; a single pump can be used for both, discarding the necessity of having to make manual adjustments to two individual pumps in an effort to closely map cellular growth. Instead, a gate clamp can be used on the yeast-extract feed tube until the beginning of exponential growth phase to ensure the feed is pumped into the broth at the correct time.

The step-up feeding regime from Section 3.5.2 was replicated for the culture and the exponential growth phase of the cells was successfully elongated to 6 hours. The importance of maintaining the nutrient balance between maltose and yeast-extract was illustrated by the fact that when yeast-extract feed ran out

after a total cumulative addition to the broth of 40 g.L^{-1} (Figure 3.10 B), bacterial growth slowed dramatically and entered stationary phase (Figure 3.10 A), the addition of extra maltose did not coerce any more increase in biomass. The 30 L scale fermentation generated an additional 93 g.L^{-1} of biomass (as compared to the batch fermentation in Section 3.4), for the addition of about 110 g.L^{-1} of maltose. This translates to a yield of biomass on substrate of about 0.84 g.g^{-1} compared to 0.9 g.g^{-1} at 7.5 L scale.

Aeration was manually adjusted to map growth patterns, however, when aeration was maintained at 16 L.min^{-1} , a sharp drop in the off-gas carbon dioxide concentration from 3 % to 2 % was noted. Unfortunately, as the oxygen detector malfunctioned shortly into the fermentation, the OUR rates could not be obtained, meaning the RQ could not be calculated. However, previous fermentations in Section 3.5 had demonstrated that the CER closely mapped cellular growth in the exponential phase; hence a drop in this rate suggested a potential slowdown in cell growth.

The subsequent increase in aeration to 20 L.min^{-1} (Figure 3.11 A) caused a jump in bacterial growth, suggesting that aeration had become growth limiting at that stage, reinforcing the highly aerobic nature of *S.gallinarum* Δp . A provision was made for gas blending, however at no point did DOT dip significantly enough below the set-point to activate the oxygen blending cascade. This was unexpected as gas blending had been necessary in all the 7.5 L scale fermentations using the dual feed mode of operation.

The production of lantibiotic pregallidermin closely mapped the bacterial exponential growth phase, with additional expression appearing to halt in the stationary phase. It is however notable that PGDM expression starts earlier at 30 L scale as opposed to 7.5 L scale, at a time of 3 hours post inoculation as opposed to 6 hours respectively. This could potentially be explained by the total biomass present in culture, meaning the total biomass required to activate quorum sensing could be achieved earlier at larger scales.

The minimum agitation rate at 30 L scale was 400 rpm (bioreactor cascade setup requirements) and the maximum was 1000 rpm, as opposed to a maximum of 1200 rpm at 7.5 L scale. The agitation rate never hit maximum (Figure 3.11 B), this could be due to the differences in mass transfer rate impacted by vessel geometry and impeller radii, however those parameters are beyond the scope of this work to investigate.

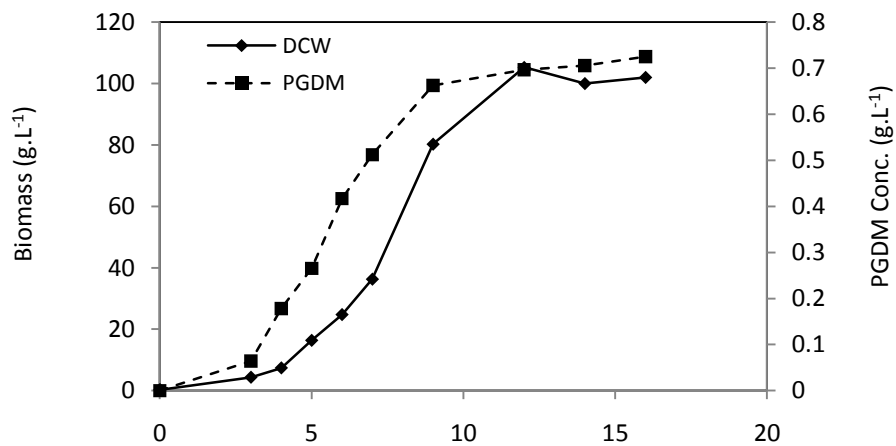
The application of the aeration and feed strategy developed at 7.5 L scale to a 30 L fermentation was successfully able to replicate the previous cellular growth profile. However, in comparison to the smaller scale fermentation, the 30 L culture yielded twice the amount of pregallidermin per litre. This suggests that there could be a link between the total overall mass of cells in culture and the yield of product. However, this is still significantly lower than that achieved by Medaglia (2009) at smaller scale. Possible reasons for the lower yield have been suggested in Section 3.5.2.

Pilot scale fermentations for active lantibiotic production have previously been conducted by Arias *et al.* (2013) and Kempf *et al.* (2000). In both studies, the

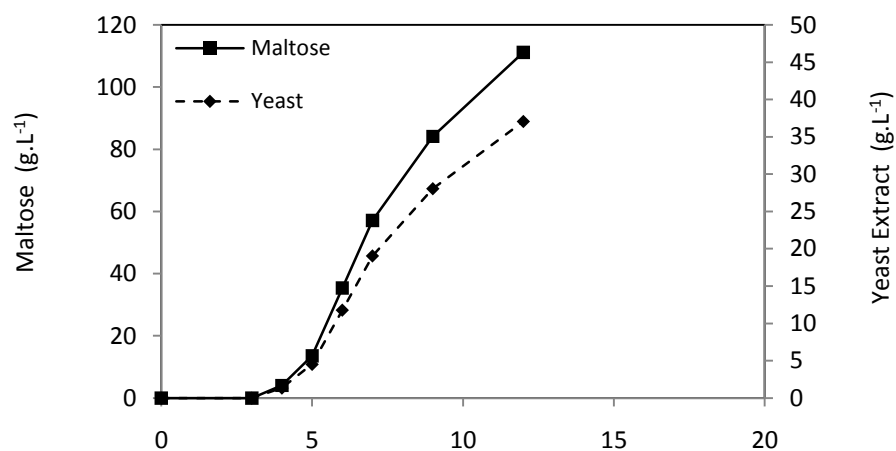
authors did not characterise the bioreactor microenvironment or the engineering parameters used.

However, in the study by Kempf *et al.* (2000), where fermentations were performed in a 20 L pilot scale bioreactor and a simulated 200 L bioreactor, it is notable that the highest yield of wild-type gallidermin was 0.33 g.L^{-1} , less than half the 0.7 g.L^{-1} of pregallidermin (which equates to 0.45 g.L^{-1} of active gallidermin) produced in the present study. This suggests that production of lantibiotic precursors in fermentation is a viable step in an overall production process for active lantibiotics.

A



B



C

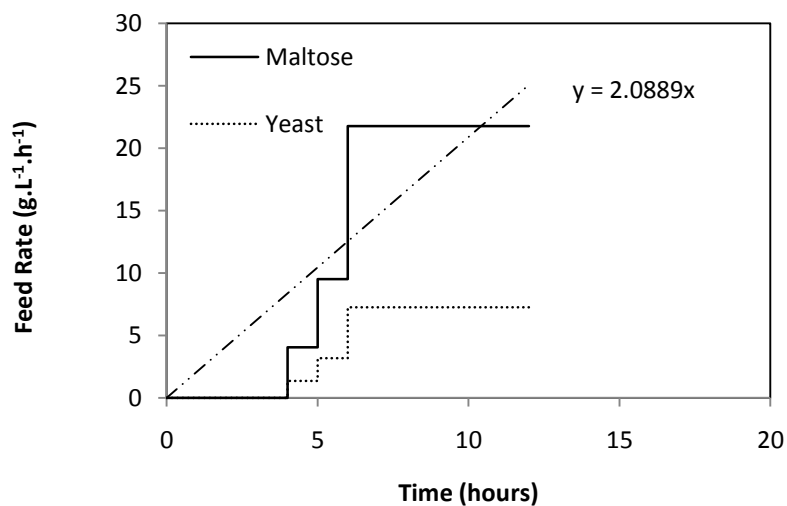


Figure 3.10 Fed-batch growth kinetics of *Staphylococcus gallinarum* Δp at 30L scale using dual feed of maltose and yeast extract. (A) Biomass and pregallidermin production. (B) Cumulative total maltose (600g.L^{-1}) and yeast extract (200g.L^{-1}) feed added to culture and (C) showing the feed rates. Fermentation performed as described in Section 2.2.4. A summary of fermentation kinetics is provided in Table 3.2

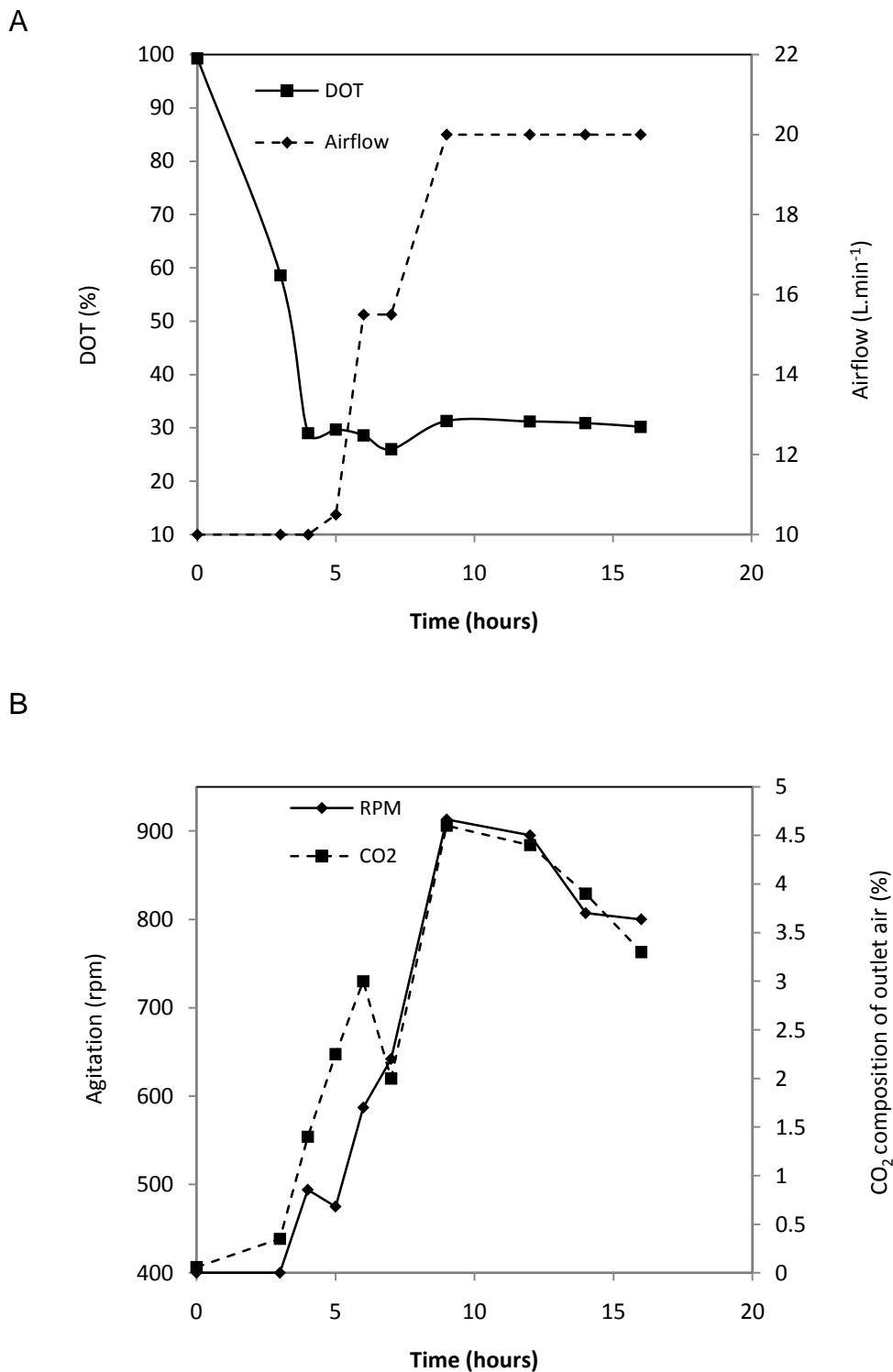


Figure 3.11 Fed-batch growth of *Staphylococcus gallinarum* Δp at 30L scale using dual feed of maltose and yeast extract with A) showing aeration and DOT (set-point 30%) and B) showing Agitation and CER (Determined by the BIOSStat C-Plus as a percentage of total exit gas). Fermentation performed as described in Section 2.2.4. A summary of fermentation kinetics is provided in Table 3.2

3.7 Factors influencing the oxidative production of PGDM by *S.gallinarum* Δp

3.7.1 Aeration

The aeration regime of the bacterial culture appeared to have a significant impact on growth and antibiotic production. The growth rate appeared heavily linked to aeration strategy, specifically the vessel airflow rate. This was unexpected as the maintenance of DOT above the set-point implies that the dissolved oxygen concentration of the culture should be sufficient for bacterial growth as suggested by Medaglia, (2009). However it was clearly visible that even when the DOT was sustained at 30 %, increases in airflow rates led to increases in cell biomass.

The DOT or the available dissolved oxygen in the fermenter broth can be linked to the K_{LA} , an oxygen mass transfer coefficient through the cellular OUR and OTR (Klöckner *et al.*, 2013, Garcia-Ochoa *et al.*, 2010). To achieve cellular growth, the available oxygen in solution must exceed the critical level required for cellular maintenance. However the introduction of higher input airflow rates increases the absolute mass of oxygen made available, notably in this case without an impact on DOT, contrary to the expected spike in DOT, it is sustained at the set point. This could possibly indicate that the added mass of oxygen is being consumed for cellular respiration and the cells require a minimum DOT above 30 % to maintain growth rates. Studies using the wild type *S.gallinarum* Tü3928 indicate that oxygen saturation during cellular growth phase is important to achieve high cellular biomass (Kempf *et al.*, 1997).

It is also possible that in a high cell density environment, the high rates of agitation rate required to maintain DOT prevents the cells in culture from adequately utilising the oxygen, indeed high rates of agitation have been demonstrated to have a negative impact on cellular growth in certain cell cultures (Ducros *et al.*, 2009). Thus, it is possible DOT is maintained purely because a large amount of the oxygen is unconsumed, requiring an increasing mass of oxygen to meet cellular respiration needs. Indeed the drop in carbon dioxide evolution noted at the 30 L scale when the input airflow was sustained at $16 \text{ L}\cdot\text{min}^{-1}$ would seem to indicate that it is the additional oxygen being consumed for cellular growth.

In order to gain a better understanding of the impact of airflow rate versus DOT on cellular growth, it is useful to examine a study conducted under a constant aeration rate. Batch cultures where DOT was sustained purely by changes in agitation rate under constant airflow did not achieve high cell densities (Section 3.4). However it is beyond the scope of this work to perform a detailed analysis on the impacts of both these parameters on the mass transfer efficiency in solution.

Consistent with previous studies by Medaglia, (2009) and Valsesia *et al.* (2007) involving fermentation of *S.gallinarum* Δp , the aeration rate was maximised in order to ensure high cellular growth. However, contrary to the both previous studies, it was found that the aeration rate needed to be increased in concert with agitation rates to achieve high cell density cultures, even when no fall in

DOT was observed. This suggests a crucial role for aeration strategy in process reproducibility.

3.7.2 Feed

Maximum cellular growth was obtained by emulating cellular growth patterns with the dual component feed setup. The high cell density dual feed fermentation was performed using a 'step-up' feed strategy, with the feed rate manually adjusted through the duration of the fermentation. The maltose feed rate profile for high cell density fermentation can be described by the linear equation:

$$Feed(t) = 2(x) \quad (3.3)$$

Where t is the feed rate in $\text{g.L}^{-1}.\text{h}^{-1}$ and x is the time in hours.

It must be noted that feeding was only started after 1 g.L^{-1} of cell density had been attained; this was used as a signal that cells had started growing steadily post inoculation (typical fermenter cell density immediately post inoculation was 0.3 g.L^{-1} , data not shown). Equation 3.3 indicates that high cell density cultures require the feed rate to be doubled every hour, a simple correlation which should be easy to calculate and replicate.

However, it is worth mentioning that using a linear feeding regimen means that cellular growth patterns can be replicated with less precision, as such regimes have a tendency to overfeed in the initial stages when growth is slow and underfeed in the latter stages, when growth is high. This also applies to step-up feeding regimes, however step-up regimes allow a capacity for adjustment to

the feed rate based on observation of other parameters such as agitation rate and RQ. This capacity for reacting to changes in fermentation parameters means that a step-up feed regime can maintain dynamic conditions in the bioreactor (Spadiut *et al.*, 2013).

While using a linear feed is much easier in terms of setting up the system and it requires fewer calculations in determining a feed pumping rate, the reduced dynamism inherent in the strategy may prevent it from achieving high cell density cultures and as a consequence reduce the antibiotic yield. Data from the fermentations performed in Sections 3.5 through Section 3.6 demonstrate the importance of all fermentation parameters mapping the growth profile of the organism in its exponential phase, which a linear feed would be incapable of doing.

In comparison, an exponential feed was suggested by Medaglia, (2009) as the optimal feed strategy to achieve high cell density cultures with a high yield of pregallidermin. An exponential regimen was attempted at the 30 L scale; however the attempts failed to produce high cell density cultures (Appendix 3, page 211). It was notable when using an exponential feed; employing a reduced specific growth rate in order to slow down the rapidly growing cells by limiting carbon source, a method often utilised to optimise antibiotic production (Flickinger, 1979), failed to yield high biomass. Thus, the step-up feeding regime was utilised for subsequent 30 L scale fermentation.

Section 3.5.2 suggested a ratio of 3:1 between maltose and yeast to optimise cellular growth. This allows both feeds to be pumped into the culture

simultaneously without having to programme separate feed equations into two separate feed pumping setups. This eliminates the need of making adjustments to individual feed rates when an adjustment to the feed rate is required.

Kempf *et al.* (1999B) initially recognised the requirement for the addition of extra yeast extract components in culture to optimise growth of the wild type *S.gallinarum* Tü3928. A subsequent study also suggested the use of a maltose feed when scaling-up the process (Kempf *et al.*, 2000). Work by Valsesia *et al.* (2007) confirmed a maltose feed also led to optimal pregallidermin production using the modified *S.gallinarum* Δp . However, it was Medaglia, (2009) from the same research group that determined the optimal feed strategy for lantibiotic production involved using a dual feed system of maltose and yeast extract fed to the culture using an exponential regime. In contrast, the present study utilised a step-up feed regime, due to its ease of operation. *S.gallinarum* Δp fermentations at 30 L scale showed good reproducibility with those conducted at 7.5 L scale, using the same process conditions. However, it is notable that final pregallidermin yield was significantly lower than that achieved by Medaglia, (2009) at equivalent biomass concentrations; it is possible that the difference in feed regimes had a role in this outcome.

3.7.3 Agitation

The agitation rate of the fermentations closely followed the growth trends. This is logical as agitation rate correlates closely with mixing and mass transfer of various substrates and gases in culture to the growing cells (Gill *et al.*, 2008).

In the current work, the bioreactors used allowed the agitation rate to be slaved to the cellular oxygen demand. This reduces the complexity of the fermentation as manually adjusting agitation rates would entail predicting and calculating cellular oxygen demand at various biomass concentrations, a procedure non-conducive to rapid setup and difficult to use. This would also entail recalculations if unexpected changes occur in cellular growth kinetics.

It is clear however that, higher rates of agitation lead to higher rates of cellular growth. What cannot be said conclusively from the current experimentation is whether manually adjusting agitation to high values from the beginning would result in a prolonging of exponential growth. Artificially manipulating agitation to high rates could possibly subject cells to high levels of shear and stress early in the growth phase, negatively impacting the growth rate (Ducros *et al.*, 2009). Investigations into the shear and stress tolerance of *S.gallinarum* Δp was beyond the scope of this work.

No previous study involving the fermentation of *S.gallinarum* Δp or any other lantibiotic producing cell strain has attempted to characterise the impact of agitation on cell growth. While Valsesia *et al.* (2007) and Medaglia, (2009) have mentioned agitation as important in maintaining DOT levels, no data has been provided to demonstrate its' impact on fermentation. The present research has demonstrated that the stirrer agitation rate closely follows cellular growth and high agitation rates signify high growth rates. This is intuitive as previous studies have shown agitation as one of key parameters determining the oxygen mass transfer (Gill *et al.*, 2008) and nutrient distribution to the cells (Garcia-Ochoa *et al.*, 2010).

3.7.4 OUR, CER and RQ

The CER and OUR both mapped the cellular growth rate in the fermentations where off-gas analysis allowed the values to be obtained. OUR also relates to the volumetric oxygen transfer coefficient (Klöckner *et al.*, 2013, Garcia-Ochoa *et al.*, 2010) indicating that a higher OUR means more oxygen being transferred to the cells. The CER and OUR can both act as a guide to cellular respiration, as it is logical for actively growing and multiplying cells to demand more oxygen and produce more carbon dioxide.

The RQ of >1 demonstrated that for *S.gallinarum* Δp in batch and fed-batch fermentation with only maltose feed, a carbohydrate source was the preferred substrate for respiration (Slavov *et al.*, 2014; Arifin *et al.*, 2014). This was in the absence of other nutrients necessary for cellular growth. In the dual-feed mode of operation, the RQ value dropped below 1, signifying a mixture of substrates was being used for respiration. However, this lower RQ coincided with much higher cellular growth and the generation of more biomass. The RQ from the dual-feed cultures suggests that there are certain nutrients present in the yeast-extract, which become growth limiting if not present in adequate amounts within the media.

The RQ appears to reaffirm the assessment by Medaglia, (2009) and Kempf *et al.* (1999B) that using just maltose feed is not sufficient for optimal growth. However, as no other study has attempted to analyse and characterise the fermentation off gas, more research is needed to gain a better understanding of the cellular respiration and substrate preferences.

3.8 Summary

The aim of this chapter was to perform high cell density culture in 7.5 L STRs of *S.gallinarum* Δp reproducibly and replicate the fermentations at 30 L scale, by first characterising the parameters critical to PGDM production at 5 L scale. The results illustrate that the key parameters to consider when replicating fermentation and performing scale-up are: feeding regimes, aeration and agitation. Ensuring these parameters map cellular exponential growth allowed the production of 0.7 g.L^{-1} of PGDM per 100 g.L^{-1} biomass, at 30 L scale, a 2-fold increase on the PGDM produced in 7.5 L fed-batch fermentations. However, industrial scale production of the lantibiotic would require gram or multi-gram yields to be obtained (Islam *et al.*, 2007), which requires further optimisation studies.

Analysing the different feeding strategies; the data illustrates that using dual-feed fed-batch fermentation while focusing on the key parameters identified (aeration, feed-regimes, substrate-ratios, agitation) allows both scalability and reproducibility. It has been demonstrated that reproducibility is achievable using automated DOT control and impeller agitation coupled with step-up substrate-feed and aeration regimes, a setup that reduces the complexity of the fermentation in comparison to exponentially adjusting the parameters.

The process is also rapid, with no fermentation exceeding 20 hours. This allows for multiple fermentations to be run during the course of a week, increasing research and development efficiency in a time-limited environment. The cell biomass achieved was comparable to previous dual feed fed-batch studies by

Medaglia, (2009) at lab scale using the same organism. However, both Medaglia (2009) and Valsesia *et al.* (2007) were able to obtain significantly higher quantities of PGDM at lab scale in comparison to the present study. This appears to be due to the different feeding regimes applied, with the previous studies indicating exponential feed is optimal for growth.

However, the successful translation of cellular growth and precursor production using *S.gallinarum* Δp from lab to pilot scale demonstrates that it is viable process for the production of lantibiotics. Additionally, the inexpensive media, rapid process completion and relatively simple operation, characteristics that have been deemed important for the development of platform processes in previous studies (Liu *et al.*, 2010), demonstrate its potential to serve as a platform for large-scale and optimisation studies.

In the next chapter a downstream purification process sequence will be developed to recover the PGDM produced in Section 3.6 at pilot scale.

Table 3.1 Summary of Fermentation Strategy

| Operation | Feed 1* (g.L ⁻¹) | Feed 2+ (g.L ⁻¹) | Feed Strategy | DOT Control Strategy | Scale | Aeration | Max Biomass (g _{DCW} L ⁻¹) | PGDM HPLC peak |
|-----------|---------------------------------|---------------------------------|---------------|---|-------|-------------|--|----------------|
| Batch | None | | NA | rpm | 7.5L | Constant | 10 | No |
| Batch | None | None | NA | rpm | 7.5L | Constant | 12 | No |
| Batch | None | None | NA | rpm | 7.5L | Constant | 12 | No |
| Fed-Batch | 500 | None | Step-up | rpm | 7.5L | Constant | 12 | No |
| Fed-Batch | 500 | None | Step-up | rpm | 7.5L | Constant | 16 | No |
| Fed-Batch | 500 | None | Exponential | Q _{Air} → rpm | 7.5L | Exponential | 30 | No |
| Fed-Batch | 500 | None | Step-up | Q _{Air} → rpm | 7.5L | Linear | 37 | No |
| Fed-Batch | 500 | None | Step-up | Q _{Air} → rpm | 7.5L | Exponential | 28 | Yes |
| Fed-Batch | 500 | None | Step-up | Q _{Air} → rpm | 7.5L | Exponential | 30 | Yes |
| Fed-Batch | 500 | None | Step-up | Q _{Air} → rpm | 7.5L | Exponential | 38 | Yes |
| Fed-Batch | 500 | 300 | Step-up | Q _{Air} → rpm | 7.5L | Exponential | 61 | Yes |
| Fed-Batch | 500 | 300 | Step-up | ††Q _{Air} → rpm → O ₂ | 7.5L | Exponential | 127 | Yes |
| Fed-Batch | 500 | 300 | Step-up | Q _{Air} → rpm → O ₂ | 7.5L | Exponential | 140 | Yes |
| Fed-Batch | 500 | 300 | Exponential | Q _{Air} → rpm → O ₂ | 30L | Exponential | 35 | Yes |
| Fed-Batch | 500 | 300 | Exponential | Q _{Air} → rpm → O ₂ | 30L | Exponential | 45 | Yes |
| Fed-Batch | 600 | 200 | Step-up | Q _{Air} → rpm → O ₂ | 30L | Exponential | 100 | Yes |

*Maltose Feed

†Yeast Extract Feed

†† Q_{air} → rpm → O₂ : represents the strategy where airflow rate (Q) is manually adjusted to emulate cellular growth, in order to prevent Oxygen from becoming growth limiting, agitation is then allowed to control DOT at the enhanced airflow rate.

Table 3.2 Summary of Average Fermentation Kinetics

| Fermentation Type | Scale | Final Biomass | Final Product Concentration | Yield of Biomass on Substrate (Maltose) | Yield of product on Biomass |
|-------------------------|-------|-------------------|-----------------------------|---|-----------------------------|
| | L | g.L ⁻¹ | g.L ⁻¹ | g.g ⁻¹ | g.g ⁻¹ |
| Batch | 7.5 | 12.5 | None | 0.25 | None |
| Fed-Batch (Single feed) | 7.5 | 30 | 0.10 | 0.25 | 0.004 |
| Fed-Batch (Dual feed) | 7.5 | 120 | 0.37 | 0.90 | 0.003 |
| Fed-Batch (Dual Feed) | 30 | 100 | 0.73 | 0.84 | 0.007 |

4. Downstream Process Design for recovery and optimisation of pregallidermin

4.1 Introduction

In Chapter 3 the parameters responsible for optimising the production of the novel pre-antibiotic PGDM using *S.gallinarum* Δp were identified. From fed-batch fermentation, it was possible to produce a broth which at harvest contained 0.7 g.L⁻¹ PGDM and 100 g.L⁻¹ biomass. The next stage in evaluating options for manufacture of the novel antibiotic is the downstream purification processes. In order for any novel antibiotic to become usable by humans, it must first reach adequate purity levels using processes described in Section 1.5.2. Additionally, for any new product to become commercially feasible the purification process must be cost effective (Ongey & Neubauer, 2016; Liu *et al.*, 2010), i.e. the desired purity should be achievable via a high yield process that limits the amount of product losses.

In order to design a purification process, it is first necessary to understand the product specification required. The product is an antibiotic compound produced in its inactive form PGDM which possesses a leader sequence of 12 or 14 amino acid residues (Valesia *et al.*, 2007) as described in section 1.3.4. In order to achieve the active, usable form, the PGDM must undergo trypsinization to cleave the leader sequence resulting in formation of the antibiotic gallidermin. Gallidermin with a small size (Ottenwalder *et al.*, 1995) is an ideal candidate for manipulation by synthetic biology techniques in order to change its properties

and antimicrobial characteristics, thus allowing the creation of antibiotic libraries using *S.gallinarum* as the host organism.

The design of any downstream process for these antibiotic candidates must consider the activation by trypsinization and the impact this will have on the downstream process. Figure 4.1 illustrates the various possible options for downstream process design. At the present time there exists no lantibiotic based clinical product for humans (Section 1.3.10), even after they have shown promise in the treatment of various bacterial infections (Valesia, 2008). Thus there exists no industrial manufacturing scale process for purification of these compounds. A variety of purification techniques have been suggested including HPLC (Arias *et al.*, 2013; Fiedler *et al.*, 1988) and immuno-affinity chromatography (Suarez *et al.*, 1997), however the cost and complexity of these methods means they might prove unsuitable for large scale lantibiotic purification.

The cationic nature of these molecules (gallidermin and PGDM, Section 1.3.4) has resulted in a preference for ion exchange purification (Barbour *et al.*, 2013; AlKhatib *et al.*, 2014) usually along with hydrophobic interaction chromatography as a capture step (Barbour *et al.*, 2013; Parente & Ricciardi, 1999). These processes are lower cost alternatives to the higher performance techniques suggested previously and are already utilized at scale for the purification of various clinical compounds e.g. monoclonal antibodies (Liu *et al.*, 2010).

4.1.1 Aim

As described in Section 1.9 the **aim** of this chapter is to establish a downstream purification sequence suitable for the large scale manufacture of the novel antibiotic gallidermin from PGDM. The various process options that will be examined were described in Fig 4.1. The specific **objectives** of this work are:

- To examine the use of centrifugation for pilot scale solid-liquid separation.
- To examine the use of solid-liquid adsorption/desorption processes for primary recovery of PGDM.
- To explore the use of ion exchange chromatography for purification of the crude PGDM obtained from the adsorption/desorption process.
- To confirm the identity of the purified PGDM and mature gallidermin obtained post trypsinization.
- To demonstrate the operational performance of the established DSP sequence in terms of product recovery yield and purity at each stage

As described in Section 2.5.3 analytical HPLC using a 5 μm pore size, C-18 Nucleosil column will be used to quantify the recovery and purity of PGDM at each process stage and GDM post trypsinization. Here purity is defined as the area on the HPLC chromatogram, in mAU, of the product peaks in comparison to the area of all sample peaks. Confirmation of the identity of the PGDM and GDM will be performed by MALDI-MS as described in Section 2.5.4.

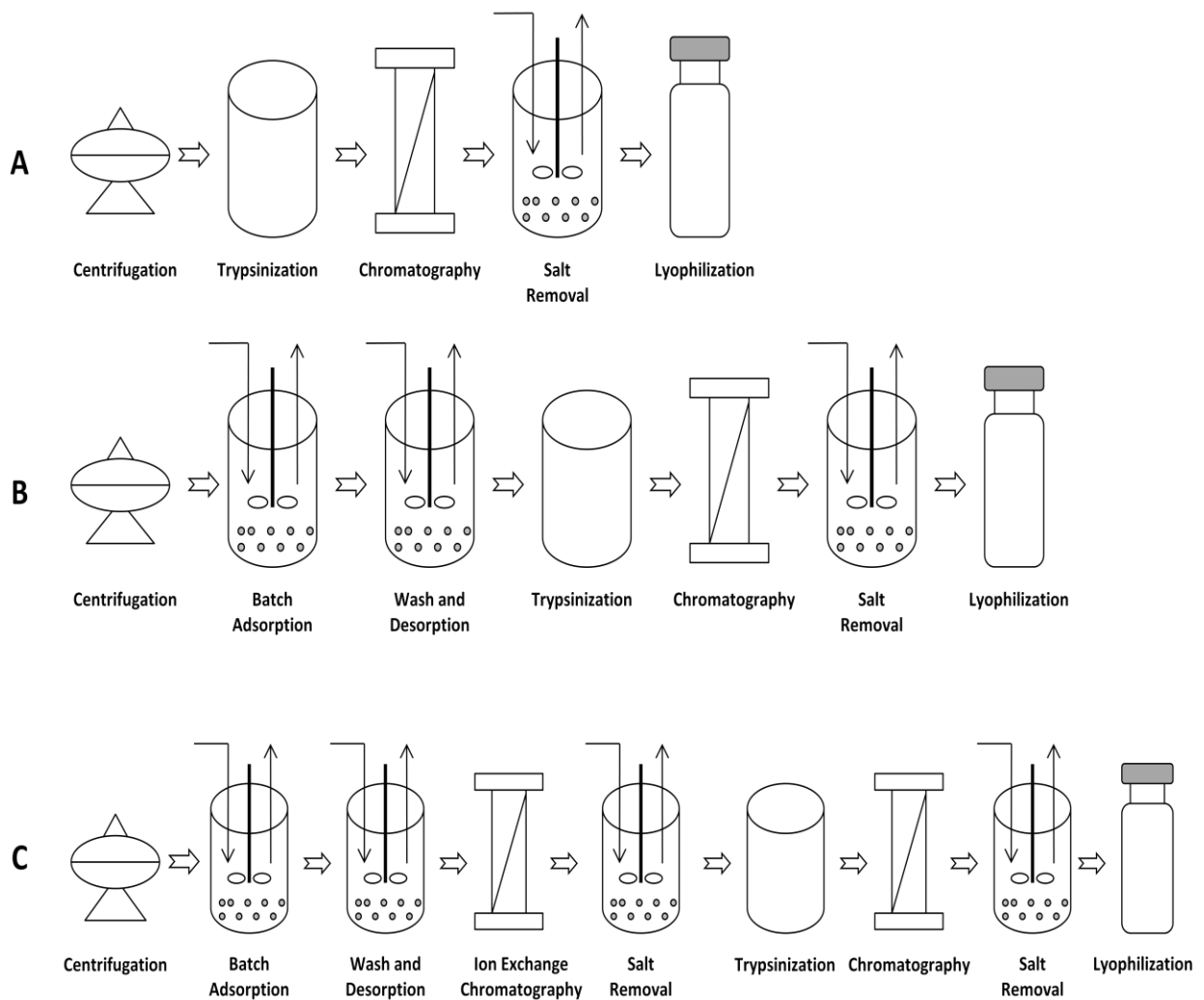


Figure 4.1 Downstream processing options for the purification of pure gallidermin from the PGDM. (A) trypsinization in-situ after cell removal. (B) trypsinization of crude PGDM directly after initial capture from solution. (C) showing the DSP sequence for trypsinization after purification of PGDM.

4.2 Overview of Downstream Process Sequence

The stated aim of this chapter is the development of a DSP sequence for the manufacture of PGDM at Scale. Hence the DSP sequence utilised will isolate and purify PGDM, which corresponds to the sequence in Figure 4.1 C. The polishing chromatography required to remove the cleaved leader peptide from gallidermin post trypsinization is not investigated, as it is beyond the scope of this work.

4.3 Solid-Liquid separation by centrifugation

Centrifugation was chosen to perform broth clarification because of the difficulty in using membrane filtration on broth containing yeast extract compounds. Culture broth that had been pre-clarified with centrifugation was still capable of clogging membrane filters with pore sizes of 0.2 μm , 0.4 μm and 0.7 μm . Hence for cell removal of culture broth containing yeast extract components at scale, membrane filtration proved inefficient. However, as pregallidermin is an extracellular product which dissolves in solution, a small mass of cells left in culture broth did not interfere with the adsorption of PGDM to the hydrophobic resin. Thus two rounds of centrifugation at 10,000 rpm for 30 minutes at pilot scale removed sufficient cell mass for batch adsorption requirements.

When the clarified cell broth was analysed by HPLC (Section 2.5.3), no detectable difference was noticed in PGDM concentration. Thus PGDM recovery using centrifugation is almost 100%.

4.4 Hydrophobic Interaction: Batch Adsorption

The clarified broth produced as in Section 4.3 was next used for study of PGDM adsorption by the hydrophobic resin Amberlite XAD-7 an acrylic ester resin, with a surface area for adsorption of $450 \text{ m}^2.\text{g}^{-1}$. The resin had already been previously demonstrated to adsorb pregallidermin in lab scale processes by Medaglia, (2009). The resin beads are porous, with an average pore diameter of 90 \AA and a pore volume of 1.14 mL.g^{-1} . The manufacturer (Sigma-Aldrich, Dorset, UK) recommended XAD-1180 and XAD-7 for antibiotic recovery; however XAD-1180 costs twice as much per unit weight. Hence XAD-7 was selected as the cost effective alternative for a large scale process.

The adsorption was performed in batch mode, with the XAD-7 resin simply mixed into the clarified fermentation broth. The effect of XAD-7 concentration on the adsorption of PGDM from culture broth is illustrated in Figure 4.2. Each gram of XAD-7 was shown to adsorb roughly 10 mg of PGDM from broth. However after adsorption the resin beads underwent a notable colour change to dark-red orange, a similar colouration to the yeast extract used in the fermentation media (Section 2.5.1). This would suggest that along with the hydrophobic absorption of PGDM, a selection of the hydrophobic culture broth and media components were also being adsorbed. These components would clearly impact the capacity of the XAD-7 resin to optimally adsorb PGDM per unit mass of resin, as well as impact the purity of the feed stream to purification processes downstream.

However analysis by HPLC (Section 2.5.3) determined that despite the adsorption of unwanted media components, all the PGDM present in broth was effectively removed from solution. Culture supernatant post adsorption had no detectable levels of PGDM.

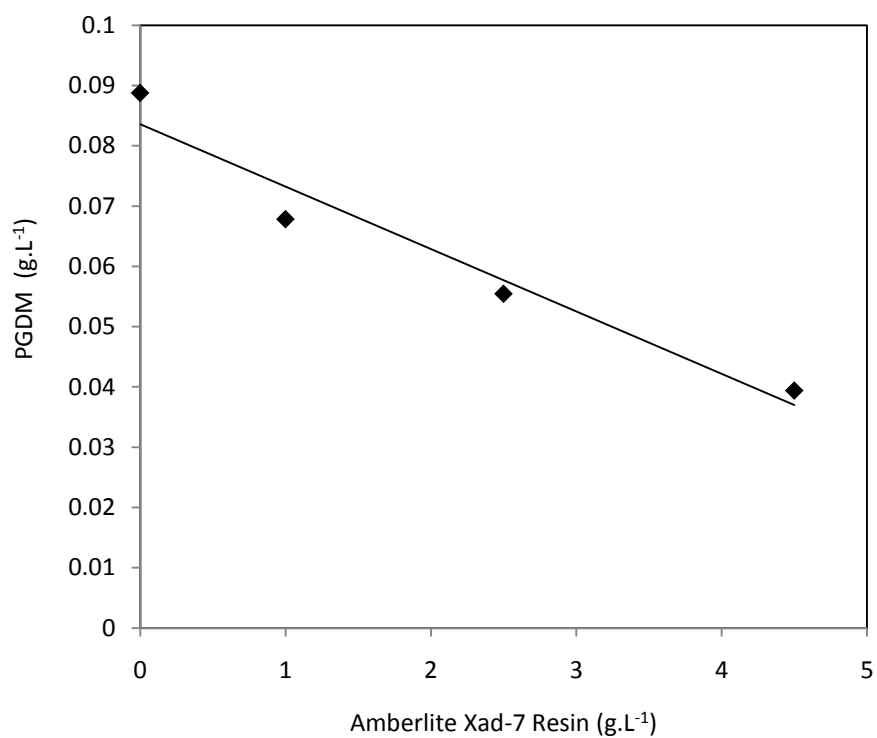


Figure 4.2 The adsorption profile of PGDM from clarified culture broth on Amberlite XAD-7. Adsorption performed as described in Section 2.3.3. A summary of the DSP sequence and the performance for each component process is provided in Table 4.2.

4.5.1 Hydrophobic Interaction: Wash

The Amberlite XAD-7 beads adsorbed media components along with the PGDM in solution as clearly demonstrated by the colour change undergone by the beads after an adsorption carried out as described in Section 2.3.3. In order to achieve a high purity PGDM desorption, washing of the beads becomes necessary to remove the bound yeast extract to reduce the eluted impurity for the subsequent chromatography process.

Washing the resin beads with distilled water, as described in Section 2.3.4, removes some of the impurities; this is visible by the colour change of the wash supernatant. However certain impurities such as yeast protein will have hydrophobic characteristics, meaning they will be more tightly bound to the XAD-7 resin and washing with water is not enough to remove them. In order to improve the removal power of the wash, solutions buffered at various pH values were evaluated. In general, increases in pH weaken hydrophobic interactions. (Hjertén, 1973) The results are illustrated in Figure 4.3, presence of impurity in solution was determined by OD at 600 nm, as described in Section 2.5.1.

As is visible from Figure 4.3 A, a relatively basic buffer solution at pH 8 was most effective at desorbing the bound yeast extract impurities. The trend indicates that increasing pH leads to an increase in the removal of unwanted impurities. However HPLC analysis of the wash buffer to determine product losses showed the presence of PGDM at pH 8, as opposed to no losses of PGDM at pH 4 or 6. The PGDM eluted by the pH 8 wash solution amounted to

2% w/w of the total mass in the starting clarified fermentation broth. Potentially significant losses at manufacturing scale.

The data also demonstrates that increasing the number of washes (performed in batch mode) will result in increased amounts of impurity removal, however the quantity removed diminishes for each wash cycle. The highest amount of impurity was always removed in the first wash cycle, with all washes beyond the third having a minimal impact on further impurity removal. This indicates the remaining impurities are very tightly bound to the resin. Increasing the volume of wash buffer, from 200 mL to 500 mL per 10 g of resin, did result in an increase in impurity removal. However, increasing the duration of the wash by doubling the wash time resulted in no observable increase in impurity removal, with specifically increasing the duration of the 2nd wash cycle in an attempt to enhance impurity removal resulting in no change in OD readings at 600 nm. It was noted that 30 minutes proved sufficient for maximal impurity removal in that particular batch.

It was also noted that increasing the molarity of the pH 8 buffer solution from 0.02 M to 0.05 M increased the removal of yeast extract impurity, however it also resulted in an increase in the desorption of PGDM from 2% in wash solution to 5% as determined by HPLC (Section 2.5.3), possibly due to an additional 'salting out' effect. Hence further increases in molarity were not pursued. A summary of the buffer wash data is presented in table 4.1. The optimal wash conditions based on the data is a 0.02 M buffer at pH 6.

4.5.2 Hydrophobic Interaction: Desorption

Desorption of the bound PGDM was performed with a solution of Methanol and acidified water (0.005 M sulphuric acid). The acidified water is added to enhance the solubility and stability of PGDM in the elution buffer, as low pH has been indicated to do this for Type A lantibiotics (Rollema *et al.*, 1995). A comparison of desorption performed with 100% methanol and 60% Methanol/40% acidified water is illustrated in figure 4.3 (B). As is demonstrated a 60% MeOH solution resulted in substantially higher PGDM obtained as opposed to 100%. This is attributable to the minimal solubility of PGDM in methanol (40 mg.L^{-1}) as opposed to water ($>3\text{g L}^{-1}$). It is noteworthy, that the recovered PGDM at 60% methanol represented 57 % of the total PGDM in clarified culture broth as determined by HPLC (Section 2.5.3). Thus the PGDM desorption was optimal at 60/40 % (v/v) Methanol/5 mM H_2SO_4 .

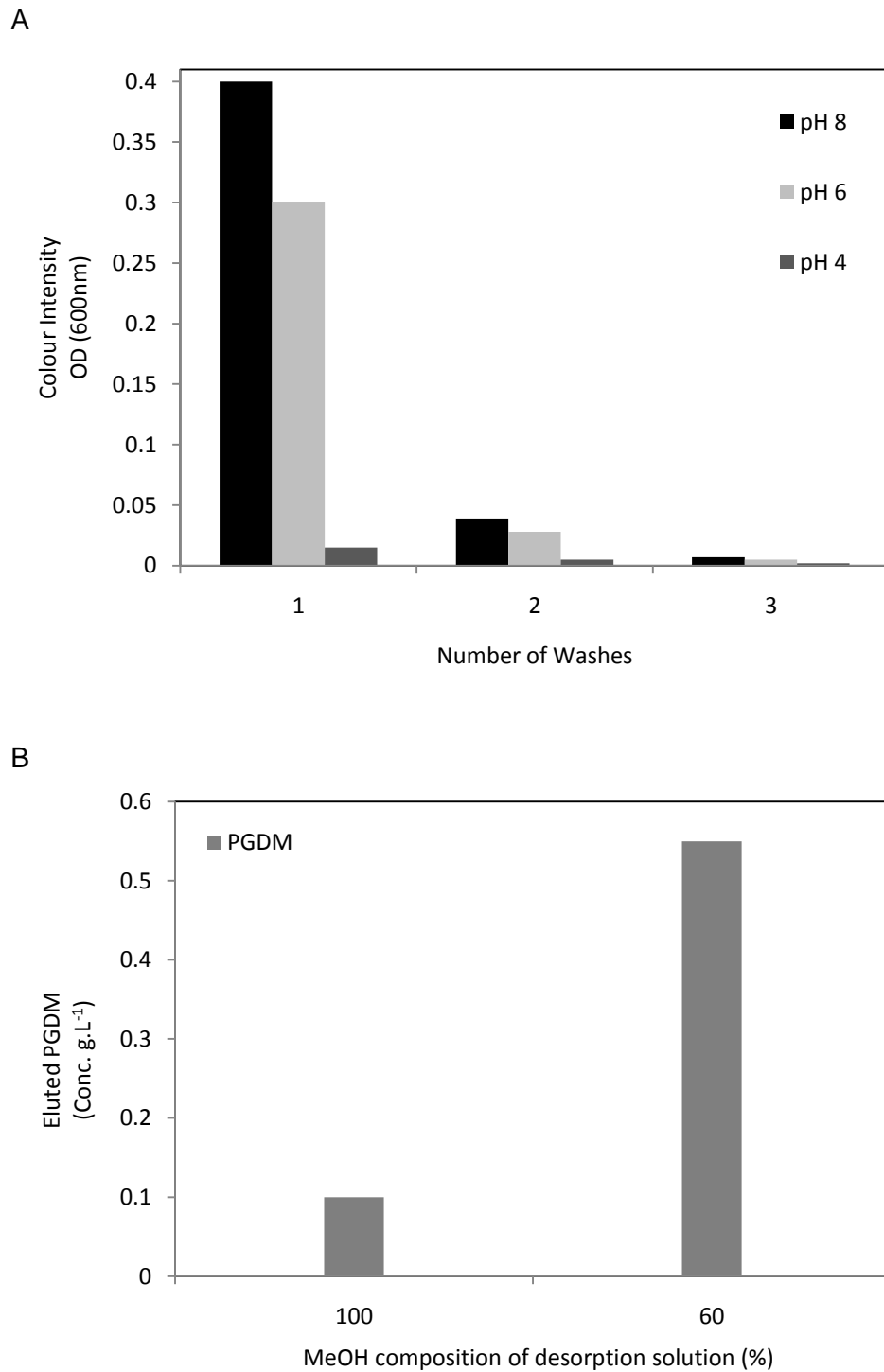


Figure 4.3 Washing and desorption of PGDM from Amberlite XAD-7 resin with A) representing the yeast extract impurities removed by each successive wash and B) the PGDM captured in solution when eluted with 100% methanol and 60% methanol. Wash and desorption performed as described in Section 2.3.4. A summary of the DSP sequence and the performance for each component process is provided in Table 4.2.

Table 4.1 Summary of wash variation data

| Impact of varying wash conditions on impurity removal | | | |
|--|------------------|-------------------------------|--------------------|
| Wash condition | Variation | Impact | PGDM Losses |
| Duration | Increase | No change | None |
| Volume | Increase | Marginal Increase | None |
| pH | Increase | Increase | Yes |
| Number of washes | Increase | No improvement after 3 washes | None |
| Molarity | Increase | Increase | Yes |
| Methanol Content | Increase | Increase | Yes |

4.6 Ion Exchange Chromatography

The PGDM solution from the batch adsorption/desorption process described in Sections 4.4 and 4.5.2 provided the feed stream for the subsequent chromatographic separation. This is intended to be the high resolution step in the purification sequence, enhancing the purity of the recovered PGDM. An XK-16 column (diameter 16 mm) was packed with the strong cation exchange resin SP HP (SP sepharose high performance) as described in Section 2.3.5. The column was first equilibrated using buffer A (0.02M acetate buffer at pH 4.5, common for both equilibration and feed loading) with the PGDM feed stream then loaded onto the column.

Figure 4.4(A) demonstrates the ion exchange chromatograms at various dilutions of the feed material. Elution was performed by increasing buffer B gradient from 0 % to 15 % (Section 2.3.5), with the two variants of PGDM referred to as PGDM 1 and PGDM 2, based on the length of their leader sequences (Figure 4.5), eluting at 12.5 % buffer B and 9.5 % buffer B

respectively. The identity of the PGDM peaks was confirmed by analytical HPLC as described in Section 2.5.3, followed by MALDI-MS as described in Section 2.5.4.

It is visible from Figure 4.4 B that a higher dilution, results in a smaller volume of unwanted yeast extract capture; the first peak in the chromatogram is the yeast extract component peak and the size diminishes with increasing feed dilution. This would imply higher product purity when the PGDM peaks are captured by fractionating the PGDM product stream. However, yeast extract components were still present in the PGDM fractions at 20 dilutions, but PGDM purity increased from 28.5 % without any dilution to 72 % with 20 dilutions as determined by HPLC (Section 2.5.3). The PGDM variants were recovered for further processing by capturing the eluent fraction from 250 mL to 350 mL at 20 dilutions.

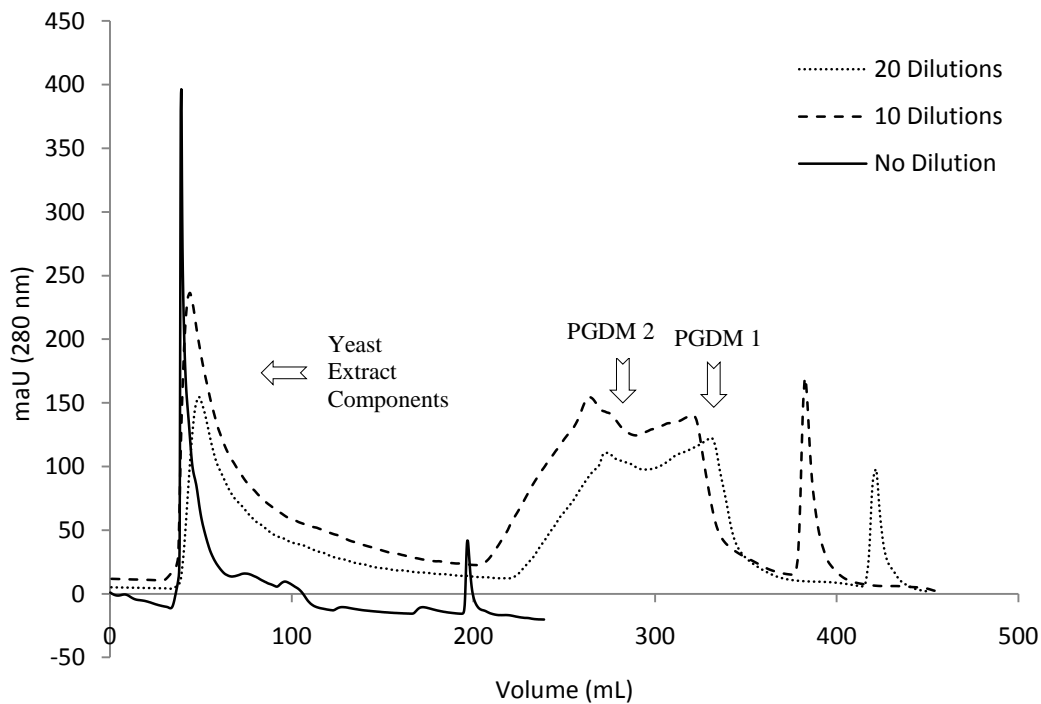
The removal of all yeast extract components proved extremely challenging using the SP HP resin, this is clearly demonstrated by the final yeast extract component peak eluting well after the two PGDM variants at a Buffer B gradient of 15 %. The implication being that some impurities from the fermentation broth possess a strong positive charge, causing them to bind very strongly with the resin, thus in order for the process to achieve very high purity, it might be necessary to determine a method to remove these components from the overall production process.

The chromatograms of feed loading in Figure 4.4 B demonstrate the break-through curves of the PGDM feed, i.e. the amount of PGDM feed being loaded

onto the column that is not attaching to the resin and flowing straight through. PGDM possesses a net positive charge, as described by Medaglia (2009) hence it is expected to attach strongly with the resin, allowing media components possessing an opposite charge to flow through. However as yeast extract is a complex mixture of autolysed yeast components, it is expected that certain charged yeast extract components will attach to the resin. As is demonstrated by Figure 4.4 A the pure undiluted feed stream onto the column will result in very high material breakthrough, 550 maU as opposed to less than 50 maU when the feed is diluted 20 times (1 volume feed: 19 volumes buffer).

The high breakthrough in the load phase implies that most of the feed stream including product and media components is flowing through unattached, resulting in lower productivity and process yield; cation exchange of the undiluted feed stream resulted in a process yield of only 20% PGDM as opposed to about 50% yield with 20 dilutions as determined by HPLC (Section 2.5.3). It is noteworthy that the undiluted feed stream had to be loaded as an injection into the mobile phase, which also implies smaller volumes have to be processed in a given cycle. Injecting larger volumes of PGDM feed results in higher breakthroughs resulting in high product wastage. The pressure drop across the column created by large impurity molecules saturating the top of the matrix could potentially compromise column packing integrity.

A



B

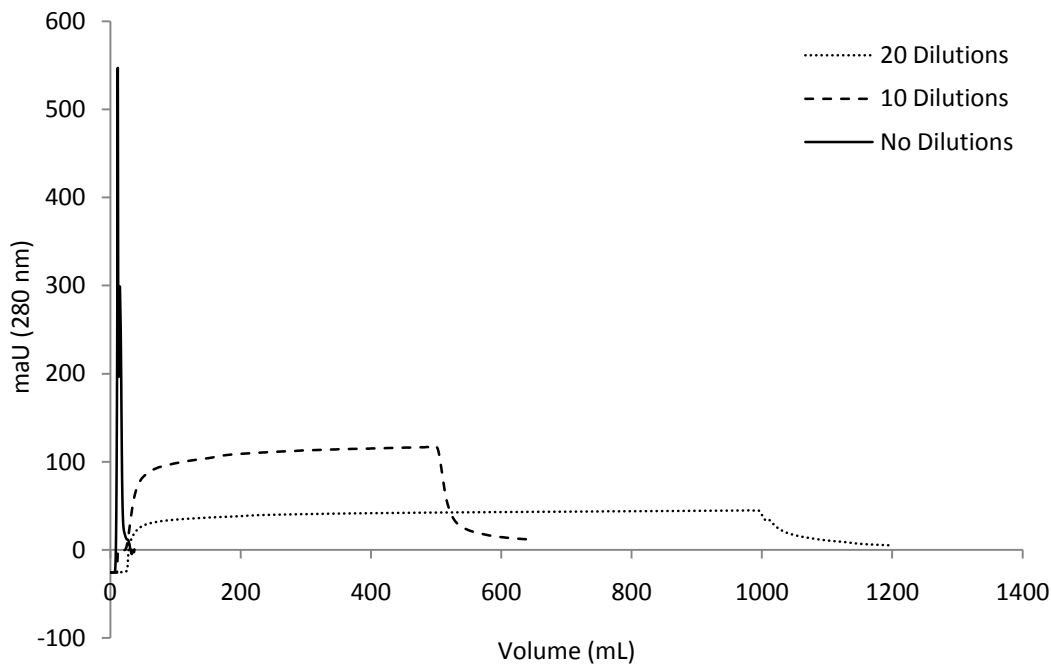


Figure 4.4 Chromatograms for ion exchange of pregallidermin product. A) elution profiles of the PGDM solution at 20 dilutions, 10 dilutions and no dilution. B) load profiles of the PGDM solution at 20 dilutions, 10 dilutions and no dilution (raw solution injection). Ion exchange chromatography performed as described in Section 2.3.5. A summary of the DSP sequence and the performance for each component process is provided in Table 4.2.

4.7 Salt removal from eluted product stream

The eluted PGDM in buffer B (2 M NaCl dissolved in 0.02M acetate buffer at pH 4.5) contained high concentrations of NaCl, requiring removal prior to further processing and trypsinization. Salt removal was performed by using the same batch adsorption/desorption process as described in Section 4.4 and Section 4.5, with only a single wash step utilised. The batch process resulted in an increase in purity from 72 % to 80 % and the step yield increased to 76 % as opposed to 57 % in the original batch process using the cell free supernatant. The methanol fraction in the desorption eluent was evaporated *in-vacuo* and the remaining solution was lyophilised to obtain the powdered PGDM.

It is however noteworthy that the desorption solution had to be modified, as the original desorption involved the use of 5 mM H₂SO₄. When lyophilized with the original desorption solution containing 5 mM H₂SO₄, the gradual removal of water left behind an increasingly concentrated acid which it is assumed denatured the PGDM, resulting in a black, discoloured powder. Thus in order to prevent this and provide unaltered PGDM for tryptic digestion, desorption from XAD-7 during salt removal was performed with a solution of 60 % (v/v) MeOH / 40 % MilliQ water.

4.8 Trypsinisation of pregallidermin to produce mature gallidermin

Once PGDM was obtained in powdered form after lyophilisation, it was weighed and re-dissolved in distilled water for trypsinization. Trypsinization was performed in pH 7 phosphate buffer as described in Section 2.4. The trypsinization cleaves off the PGDM leader sequence, leaving behind mature gallidermin. Every 1 g of PGDM produced 0.6 g of mature gallidermin when trypsinised, a step yield of 60 %. The identity of PGDM and gallidermin was confirmed by HPLC (Section 2.5.3) and MALDI-MS (Section 2.5.4) as described in the following section.

4.9 Identification of pregallidermin and gallidermin

In order to confirm the presence of both PGDM and gallidermin, off-line HPLC analysis was performed as described in Section 4.6 analysis of the ion exchange chromatograms. However the retention time from HPLC chromatograms confirms identity only in relation to the retention time of commercial standards, and provides no other physico-chemical evidence to confirm identity. A combination of the HPLC chromatogram with the molecular mass of the compound in question provides much stronger evidence for positive identification. Thus the mass of the product compounds pre and post trypsinization along with their HPLC chromatograms were used to positively identify PGDM and gallidermin in solution.

Figure 4.5 shows the chromatogram and mass spectrum of the product fraction obtained from the Ion exchange chromatography stage shown in Figure 4.4.

The mass spectrum confirms the presence of the two variants of PGDM detected by Valsesia *et al.* (2007). It is also notable that *S.gallinarum* Δp appears to have a much higher preference for the production of PGDM variant 1 as opposed to PGDM variant 2, a fact confirmed by Medaglia (2009). The peaks on the chromatogram left unidentified are thought to be various buffer solution and cell culture broth components eluted along with the PGDM.

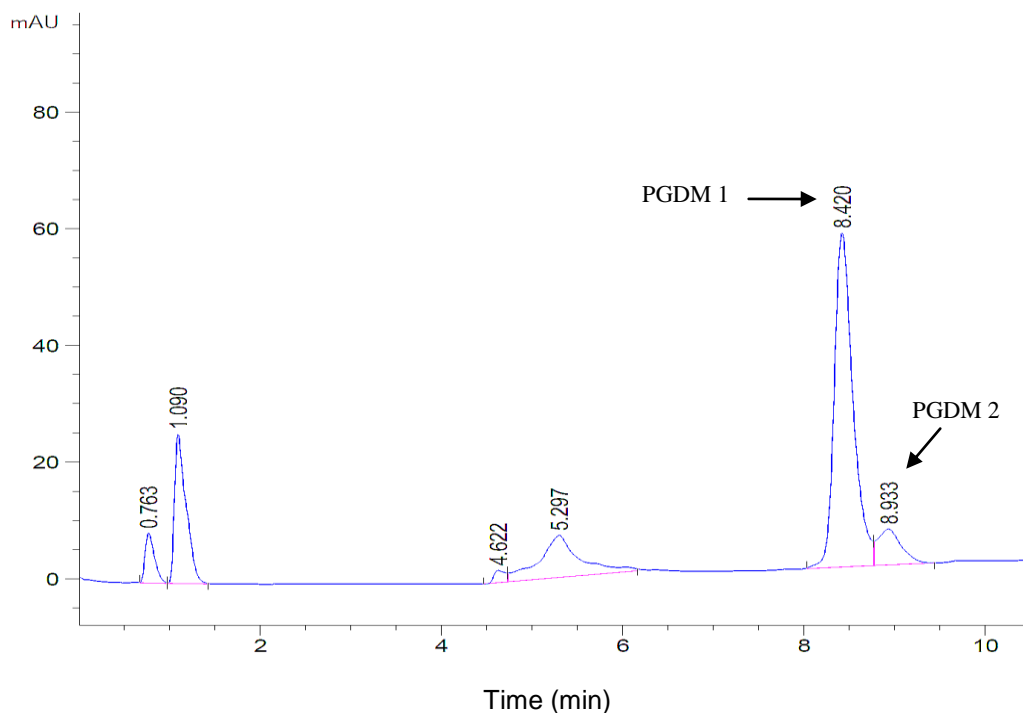
Figure 4.6 A shows the HPLC chromatogram and 4.6 B the mass spectrum of the PGDM sample in Figure 4.5, post trypsinisation. The presence of the gallidermin peak at 9.1 minutes is notable, which can also be confirmed by the mass spectrum at 2166.5 m/z (relative mass of ions). The data would also suggest that PGDM 2 is cleaved in preference to PGDM 1; however that may just be observable due to the difference in concentration between variants, resulting in PGDM 2 being completely utilized quicker.

The data does however confirm the production of the novel antibiotic PGDM by *S.gallinarum* Δp , which is then trypsinised to gallidermin, as demonstrated by the presence of both in solution compared to the complete absence of Gallidermin from figure 4.5 B.

In order to confirm the identity of the gallidermin produced by trypsinisation from the PGDM variants, the mass spectrum of a sample where the PGDM had been completely trypsinised was compared to a sample of commercially available Gallidermin (Enzo Life Sciences, East Farmingdale, NY, USA). The mass spectra in Figure 4.7 determined using MALDI-TOF (Section 2.5.4); indicate

identical masses for both samples at 2168 m/z (molecular mass of Gallidermin is calculated at 2165 g.M⁻¹).

A



PGDM 1 Mass 3408 Da AKESNDSGAEPR- Gallidermin

PGDM 2 Mass 3621 Da VNAKESNDSGAEPR- Gallidermin

B

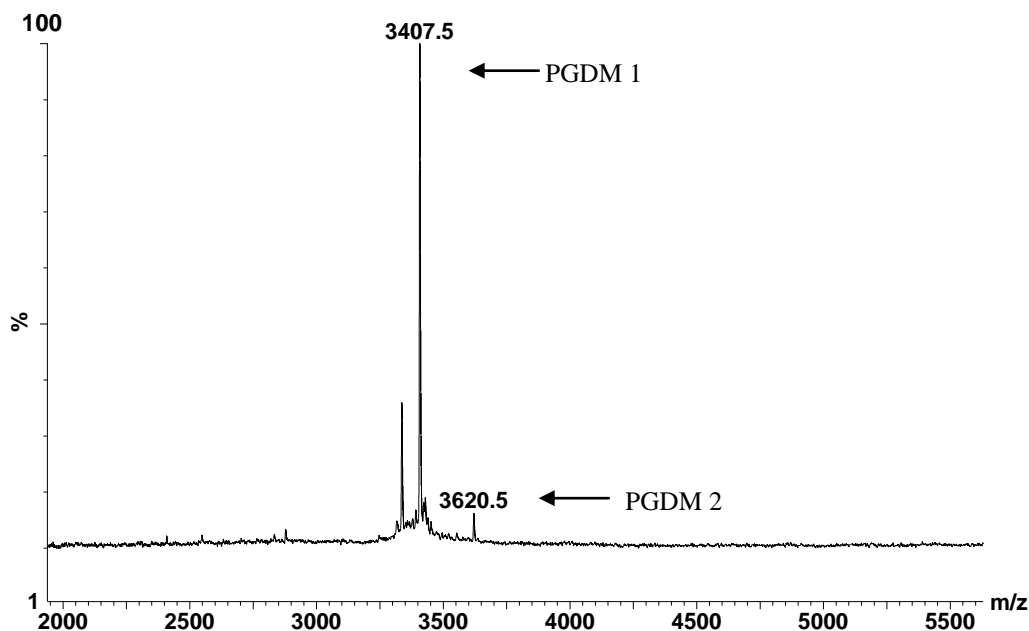
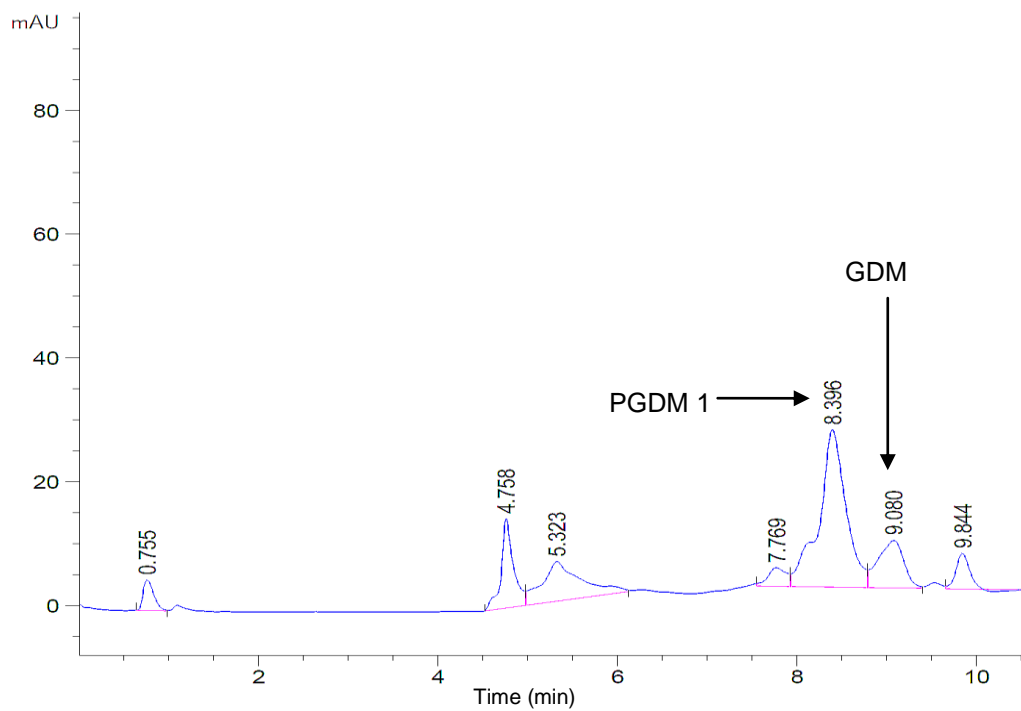


Figure 4.5 Identification of PGDM. A) HPLC chromatogram of the PGDM product solution obtained from Ion Exchange chromatography show the retention times 8.4 min and 8.9 min for variants PGDM 1 and PGDM 2 respectively. B) Mass-spectrum of the same product solution using MALDI-MS, the spectrum shows the relative abundance of ions (%) relative to the mass of ions (m/z). The molecular masses obtained correspond to values obtained by Valsesia *et al.* (2007).

A



B

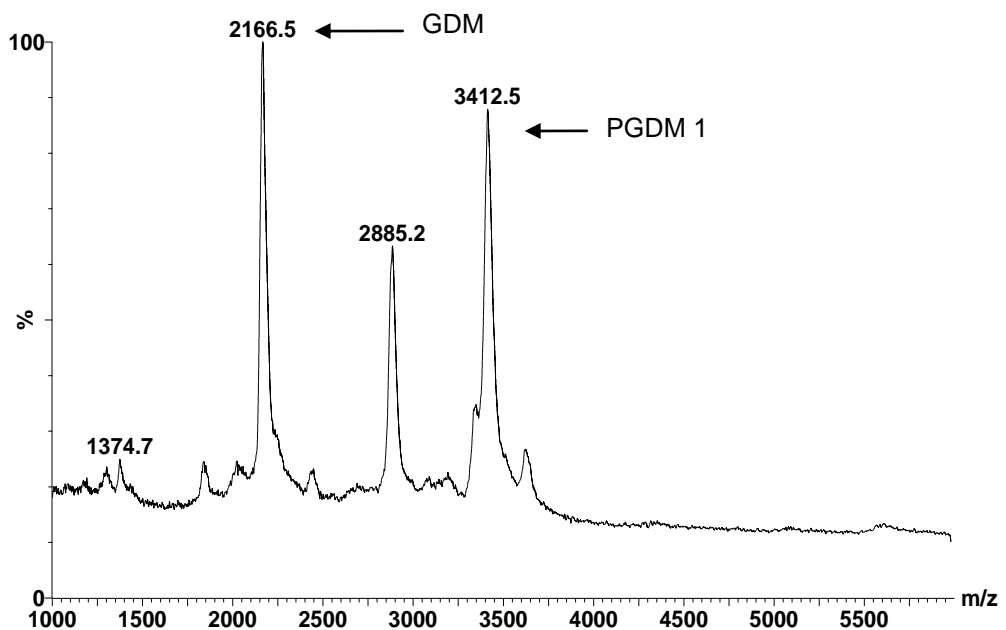


Figure 4.6 The trypsinization of PGDM to produce gallidermin. A) HPLC chromatogram of the PGDM product solution 6 min after the introduction of Porcine Trypsin, the presence of Gallidermin with a retention time of 9.1 minutes is notable, indicating the conversion of PGDM to active Gallidermin. B) Mass Spectrum of the same sample, confirming the presence of Gallidermin (mass: 2166) along with PGDM variant 1. The MalDI-MS spectrum shows the abundance of the ions (%) relative to the mass of ions (m/z).

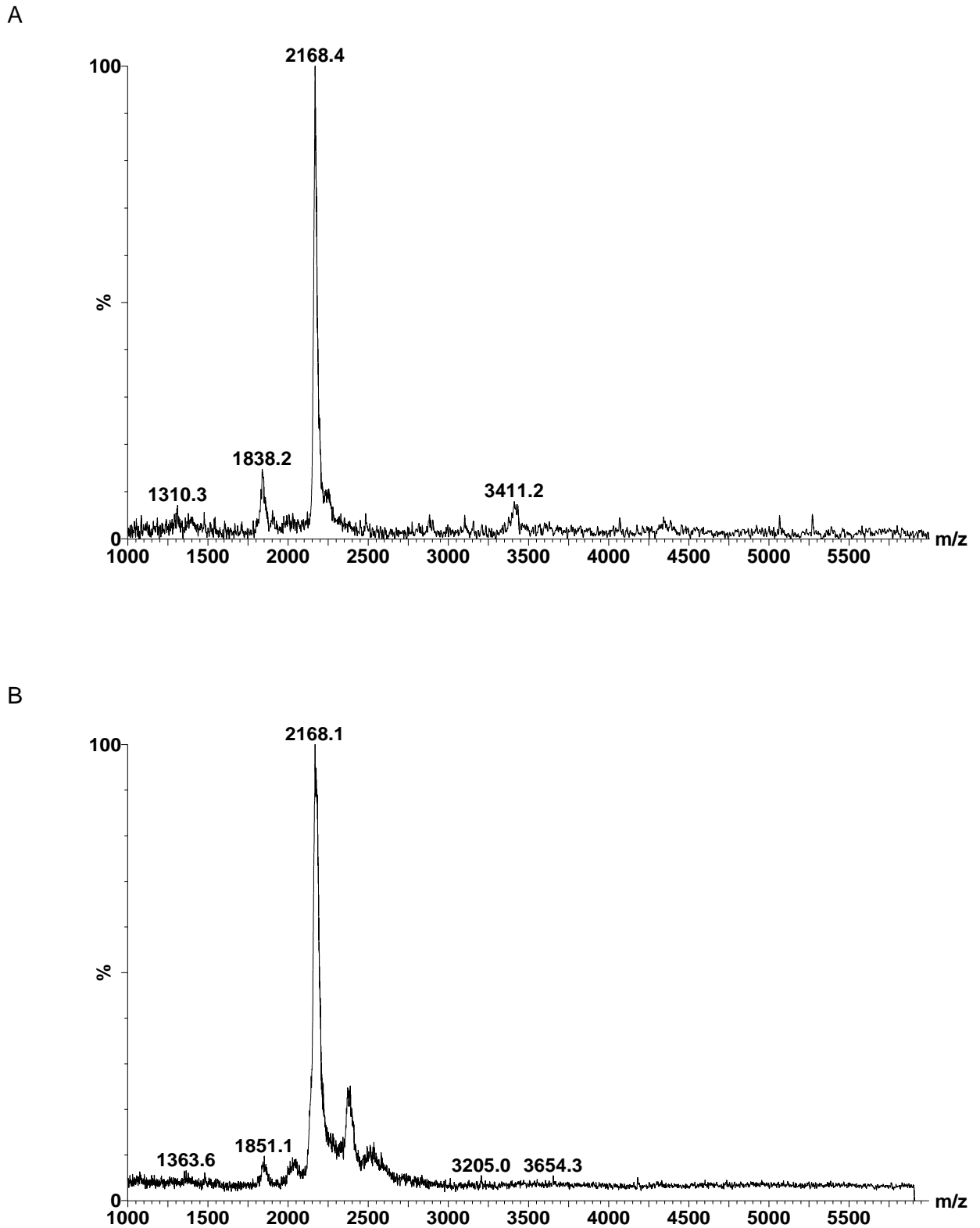


Figure 4.7 MALDI-TOF mass spectrum of Gallidermin) Gallidermin (2168.1) obtained from the near-total trypsinization of PGDM product solution, note the presence of small traces of PGDM variant 1 (3411.2). B) commercially produced gallidermin, from Enzo Life Sciences. The Maldi-MS spectrum shows the abundance of the ions (%) relative to the mass of ions (m/z).

4.10 Assessment of overall downstream process performance

Having examined the selection and performance of potential downstream processing steps in Section 4.3 to 4.8, the whole process sequence was performed on a batch of PGDM produced as described in Section 3.6. The culture broth was harvested at 15 h, when PGDM concentration was 0.7 g.L^{-1} (Figure 3.10 A). Table 4.1 shows a purification table summarising the recovery yield and purity of PGDM/GDM at each stage and for the overall process. The PGDM was quantified at each process stage using HPLC analysis as described in Section 2.5.3. The purity for each process stage was calculated using Equation 2.5.

The DSP sequence utilised for PGDM purification and the activation of GDM was initially proposed by Medaglia, (2009), in their work on *S.gallinarum* Δp . However, it was noted in that study that the sequence needed to be tested with an actual purification run in order to determine step yields and increases in purity. Table 4.2 illustrates the results of using the sequence at pilot scale. Overall process yield from the sequence is 13.5%, while the active GDM obtained after trypsinization had a purity of 70%. Previous studies have reported lab-scale methods to obtain GDM purities of above 90% (Allgaier *et al.*, 1991); however there are no reports of pilot-scale studies involving the purification of a lantibiotic precursor. The reduction in purity of GDM post trypsinization noted in Table 4.2 is accountable to the presence of both trypsin and the cleaved PGDM leader sequence.

It is also noted that the maximum purity obtained for PGDM was 80%. This can be accounted to the presence of some residual media components. The yeast extract based fermentation media is complex and the use of an optimised defined medium would improve the purification process allowing greater PGDM purity to be achieved (Medaglia, 2009).

Table 4.2 Purification table summarising PGDM step yield and purity for the whole downstream process sequence

| Process | Total Mass of PGDM (g) | Overall Yield (%) | Step Yield (%) | Concentration (g.L ⁻¹) | Purity (%) |
|----------------------|------------------------|-------------------|----------------|------------------------------------|------------|
| Fermentation | 14 | 100 | 100 | 0.7 | 0.56 |
| Centrifugation | 14 | 100 | 100 | 0.7 | 0.56 |
| HI* | 8 | 57 | 57 | 0.4 | 28 |
| IEX Chrom. † | 4.1 | 29 | 51 | 0.2 | 72 |
| HI | 3.1 | 22 | 76 | 0.15 | 80 |
| Lyophilization | 3.1 | 22 | 100 | 0.15 | 80 |
| Trypsinization | 1.9 | 13.5 | 60 | 0.09** | 70 |
| Total Process | 1.9 | 13.5 | NA | 0.09** | 70 |

*Hydrophobic Interaction

†Ion exchange Chromatography

**Galliderimin

4.10.1 Solid-Liquid separation by centrifugation

Centrifugation proved capable of removing adequate cell mass to allow the operation of the subsequent hydrophobic interaction resin adsorption/desorption stage. The fermentation broth was spun at 10,000 rpm, the literature shows ranges for centrifugation from 9,000g to 16,000g (Barbour *et al.*, 2013; Valsesia *et al.*, 2008). However, it seems that a process temperature of 4°C is consistent to every study. This is possibly in order to reduce potential lantibiotic degradation from occurring at higher temperatures in the culture media. Centrifugation was performed for 30 minutes, longer than for previous studies as pilot-scale volumes of fermentation broth were being clarified.

HPLC analysis found no detectable difference in PGDM concentration pre and post centrifugation; a product yield of 100%. This is most likely because the PGDM is extra cellular and dissolves in the solution, hence the removal of cells does not impact its presence in solution. Additionally due to the subsequent adsorption/desorption step happening in batch mode, the presence of a small number of cells is expected to have a negligible effect on adsorption efficiency.

Centrifugation has been used frequently as a method to obtain cell-free supernatant with dissolved lantibiotics (Souza *et al.*, 2017; Zhou *et al.*, 2016; Barbour *et al.*, 2013). There are also reports in literature of other methods such as cross flow filtration (Arias *et al.*, 2013) However, centrifugation may prove beneficial in a manufacturing scale process by being a lower cost alternative to clarification by membrane filtration. It is also a process that allows high throughput of product solution, which could potentially reduce the processing times of product batches at manufacturing scale.

4.10.2 Hydrophobic Interaction

The use of batch adsorption as an initial capture step is beneficial due to its relatively simple operation in comparison to column separation procedures. There are also economic benefits to utilizing mixing tanks and resin beads, as opposed to the capital investment required at industrial scale to install a large scale column rig. The resins used are in-expensive in relation to chromatography resins. Additionally due to the robustness of resin beads such as Amberlite XAD-7, the same resins can be used multiple times.

The resin adsorption process is also beneficial due to its ability to adsorb the PGDM from a feed stream that is fairly impure; it contains all the components of the fermentation minus the cells removed by centrifugation. In comparison a column separation step for initial capture, would require a purer feed stream in order for the resins to last longer. This aids in the processing of large volumes of culture broth quickly, which can subsequently be desorbed into smaller volumes of buffer for further processing by column separation techniques, something which could prove useful for manufacturing at large scale, where thousands of litres of culture broth needs to be processed in a single batch (Garcia-Ochoa *et al.*, 2010).

However, desorption of the captured product from the resin beads resulted in a process yield of only 57 % and a product purity of 28 %. This is attributable to the complex medium, composed of yeast extract proteins. Yeast proteins are also adsorbed onto the resin along with the product, with many yeast compounds much larger than the PGDM molecule (2000 Da). It is reasoned that

the reduced yield may be due to the larger yeast extract compounds blocking the resin pores by attaching strongly under the conditions required for PGDM desorption, along with some of the PGDM attaching irreversibly to the resin beads. This is indicated by the increase in step yield achieved by the secondary batch adsorption for salt removal (Section 4.7), where the much purer product stream from the Ion Exchange chromatography resulted in step yield increasing to 76 %. However, the interaction of medium components to resin beads is beyond the scope of this work to determine.

The use of resin based product capture finds common use in literature involving the purification of antibiotics. The preferred are all of the 'Amberlite' XAD series, with XAD-16 and XAD-1180 used frequently (Arias *et al.*, 2013; Barbour *et al.*, 2013; Krismer *et al.*, 2012; Medaglia, 2009). However, when Valsesia *et al.* (2007) originally created the *S.gallinarum* Δp cell strain, XAD-7 was used for initial product capture. Thus, for the present work, XAD-7 was utilised. Additionally, XAD-7 is a cheap resin, a characteristic suitable for a material to be used in platform processes.

4.10.3 Ion Exchange Chromatography

Ion exchange chromatography is a suitable high resolution purification step due to the PGDM possessing a net positive charge (Section 1.3.4). The strong cation exchange resin SP HP (high performance) by GE Healthcare (Little Chalfont, UK) is used in a capture and elute mode, to allow all non-charged and negative charged particles to flow through. The product purity increases to 72 %, from an initial 28 % after the batch adsorption. However, purity grades of above 90 % have been reported in the literature (Medaglia, 2009; Allgaier *et al.*,

1991) and hence there is substantial room for improvement. It is suggested again that the purity achievable is impacted by the feed stream containing undefined yeast extract components, which proved difficult to remove and elute simultaneously with the PGDM under the gradient elution conditions (Figure 4.4 A).

A potential solution to achieve purer product fractions could be allowing a shallower gradient, giving the impurities a larger amount of time to elute off. However in a manufacturing environment increasing process times might not always be suitable as it leads to reduced chromatography cycle efficiency and productivity. Another possibility is the use of higher dilution levels for the product solution beyond 20 times to ensure lower feed solution breakthrough, however at large scale that could lead to problems with handling large quantities of buffer and also increase the process time. However, there remains much scope for further optimization work to determine suitable conditions to enhance PGDM purity.

The process yield also leaves room for further improvement, with the step yield at 51 % as shown in Table 4.2. The ion exchange data indicates that increasing the product dilution reduces the feed breakthrough (Figure 4.4A), thus increasing the amount of PGDM capture. However there is a limit to the amount of dilutions that are feasible at manufacturing scale as this could substantially affect plant productivity and process efficiency. An alternative could be using multiple column rigs; however that leads to large increases in capital and operational costs. Thus in order to optimise the yield and purity of the Ion exchange process, a relatively pure feed stream could provide advantages,

something that becomes difficult when using complex media composed of undefined yeast extract components. It is intuitive that reducing the concentration of impurity would allow more PGDM to bind, as opposed to saturating the column with media components and allowing PGDM to breakthrough.

Ion exchange chromatography has been used frequently in studies that involve lantibiotic purification (Zhou *et al.*, 2016; Zhou *et al.*, 2015; Barbour *et al.*, 2013). This is due to the cationic nature of the lantibiotics that have been most extensively studied. Work by Medaglia, (2009) demonstrated that PGDM was also a cationic peptide, although possessing less positive charge than the wild-type gallidermin. This provided the reasoning behind the selection of the cation exchange resin for the process in this study.

Medaglia, (2009) indicated that at lab scale, the purity of PGDM after cation exchange was 86%, whereas the present work achieved product purity of 70% using a pilot scale process (Table 4.2). This difference in purity can be accounted to Medaglia's use of a defined medium resulting in fewer complex yeast extract components in the purification feed stream.

4.11 Discussion and Summary

The aim of this chapter was to establish a downstream purification sequence suitable for the large scale manufacture of the lantibiotic gallidermin from PGDM. The DSP utilised to achieve this is summarised in Figure 4.8. The process outlined to achieve this aim uses centrifugation for the removal of the

producer cells from fermentation broth. Centrifugation proved suitable to rapidly provide material of a sufficient clarity to allow the subsequent hydrophobic interaction process. No PGDM losses were detected by HPLC after broth clarification (Table 4.2); meaning centrifugation provides a cheap, scalable and high throughput process option, characteristics that are suited to manufacturing scale production.

The hydrophobic interaction adsorption/desorption process provided the primary product capture step of the DSP sequence. Although rapid, cheap and scalable, the product yield of 57 % and purity of 28 % has room for improvement (Table 4.2). The use of a complex medium for cellular growth was suggested as a reason for the lower product recovery and purity, meaning improvements in yield and purity would be possible by using a defined media, as demonstrated by Medaglia, (2009) and optimising the removal of media impurities from the resin during the wash stages.

Ion exchange chromatography was able to increase the purity of the desorbed PGDM 2.5 fold to 72 % (Table 4.2). However PGDM recovery was low at 51 %, which illustrated room for process optimisation. Although the process was rapid, the scalability of ion exchange chromatography is questionable without a process input stream of higher purity. The DSP was able to produce PGDM which was successfully trypsinised to gallidermin. The identities of the products were confirmed initially by HPLC, followed by Mass Spectrometry (Section 4.9).

As demonstrated in Table 4.2, the process provides a DSP platform that can produce material of a sufficient quality to allow trypsinization of the PGDM, allowing the mature gallidermin to be obtained. This is done rapidly; each

process step in the sequence was concluded in less than 24 hours using low complexity processes. However the results shown in Table 4.2 underline the importance of optimising individual processes to achieve high total process yield and purity.

All processes utilised in this DSP sequence have been used in previous studies for the purification of other lantibiotic compounds. Although the complete sequence may differ between studies e.g. Arias *et al.* (2013) utilised a cross-filtration step rather than centrifugation for cell removal, there is a high degree of similarity (Alkhatib *et al.*, 2014; Barbour *et al.*, 2013; Arias *et al.*, 2013; Medaglia, 2009).

Although no study has been conducted on pilot scale DSP sequences for lantibiotics, there are lab-scale sequences that utilise HPLC as a final purification step (Zhou *et al.*, 2016; Zhou *et al.*, 2015). Replicating these at pilot and large scale may prove costly and unsuitable for commercial operations.

It is notable that PGDM yield and purity is not very high, however platform processes are meant to rapidly and cheaply provide usable quantities of material for clinical, further developmental and optimisation studies and may be non-optimal in terms of yield, process economics and throughput (Liu *et al.*, 2010). Thus, the existing process may not translate to commercial production without further optimisation work. The present study has demonstrated that the identified DSP sequence is a viable method of PGDM capture and purification. Lantibiotics have similar biosynthesis pathways (Medaglia, 2009) hence, the process may be generic enough to be utilised with other molecules.

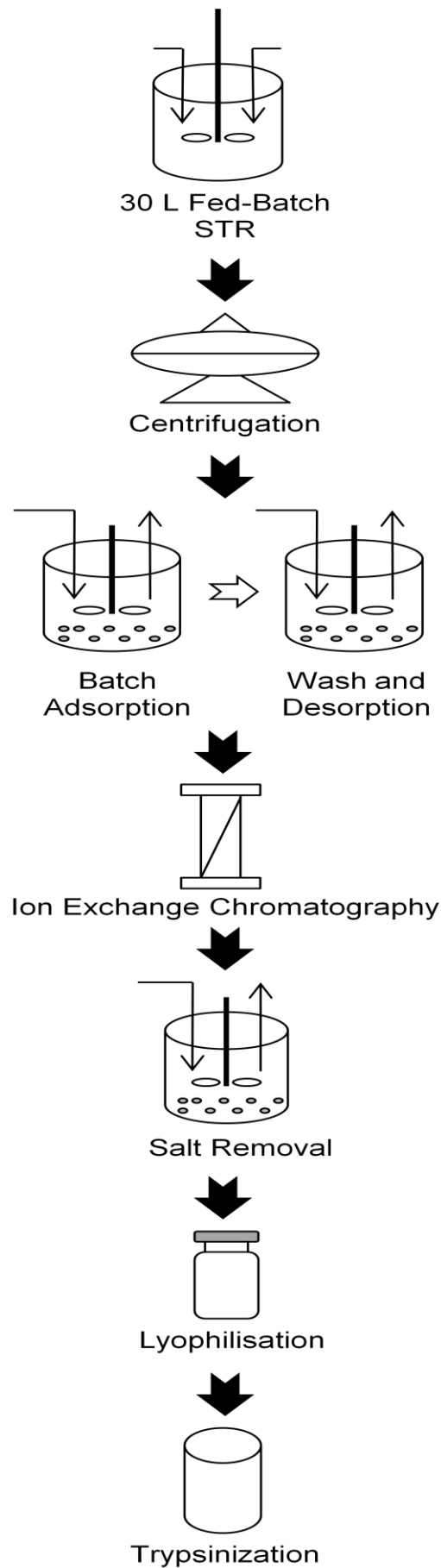


Figure 4.8 Summary of the final overall process used for the production of PGDM, including the finalised DSP sequence that was used to achieve the PGDM yields and purity outlined in Table 4.2

5. Microscale Methods for Rapid Analysis

5.1 Introduction

The development of the DSP sequence for pregallidermin manufacture, described in Chapter 4, facilitates the commencement of process optimisation studies. The major cost drivers in the manufacture of modern biotech compounds are the downstream purification processes utilized and the number of steps required to meet regulatory requirements (Marr *et al.*, 2006; Kelley, 2006). Purification technologies such as chromatography involve both high set-up costs along with expensive consumables such as the resins utilized (Arauz *et al.*, 2009). In the development of novel lantibiotic candidates (Section 1.3.10), once a compound is identified with the required antimicrobial profile, optimization studies to identify suitable process parameters for purification at the manufacturing scale are required. These can be both time consuming and costly. Conducting optimization studies at pilot-scale also requires product quantities that are uneconomical to produce with non-optimized processes; an approach that diverts resources from the development of other potential drug candidates.

Microscale processing techniques offer a potential solution in reducing both cost and time required for performing optimization studies on the chosen candidate (Voulgaris *et al.*, 2016; Micheletti and Lye, 2006). The use of microscale techniques allows the generation of quantitative process data in parallel with initial pilot scale production runs, as the required quantity of material for each

microscale investigation is in milligrams or less. In terms of downstream processing operations microscale methods already exist for a number of unit operations. These include depth filtration (Jackson *et al.*, 2006), centrifugation (Hutchinson *et al.*, 2006), adsorption (Lye and Woodley, 1999), liquid-liquid extraction and chromatography. In the case of lantibiotic downstream process synthesis there remains a requirement for microscale methods to acquire the relevant physic-chemical property data.

5.1.1 Aims

Hence the **aim** of this chapter is to use microscale analysis techniques to develop a comprehensive set of data on the PGDM product physico-chemical characteristics. This would enable informed process design choices that would impact the DSP operations, enabling the optimization of the downstream processes in pursuit of higher product recovery and purity. The **specific** objectives of this chapter are:

- To develop microscale optimization studies for the hydrophobic interaction based capture of PGDM from culture broth by Amberlite XAD-7. It is employed as the primary capture step as shown in Table 4.2; with a step yield of 57% and purity of 28%. Improvements at this stage of the process would allow for improvements in all subsequent steps.
- To demonstrate a substantial improvement in yield and purity of the primary capture step at microscale, which will inform the redesign of the follow-on DSP sequences.

- To develop microscale methods to enable the rapid acquisition relevant physico-chemical data.

It will be suggested that the microscale analytical methods aid design of the manufacturing process for the production of novel antibiotics by proving their usefulness in the collection of data that would enable a comprehensive analysis of the suitability of the candidate antibiotic to existing DSP processes.

As described in Section 2.5.3 Analytical HPLC will be used to determine the purity and quantity of the antibiotics pregallidermin and gallidermin. For this work, purity is calculated using Equation 2.5 in Section 2.5.3.

5.2 Overview of the microscale methods

The microscale methods development aims to inform process design, hence these optimisation studies will focus on the primary capture step; PGDM capture by adsorption/desorption. Thus all the methods developed aim to gather process data that could enhance the yield and purity of PGDM obtained by the XAD-7 Adsorption/Desorption process. A 'one-factor-at-a-time' optimisation strategy was used to develop the methods, as each set of experiments gave rise to data that needed answering with a follow on sequence of experiments (Sequential Analysis). The results from the optimisation experiments are presented as contour plots.

5.3 Impact of pH on impurity removal

The primary capture step suggested for a PGDM manufacturing process is hydrophobic interaction chromatography, as previously shown in Section 4.4, hydrophobic interaction allows for the complete adsorption of PGDM onto the resin Amberlite XAD-7 from clarified fermentation broth. Upon elution this allows a recovery of 57% (w/w) PGDM at 28% purity, a 50 fold increase compared to the culture broth (Table 4.2). It is however worthwhile to investigate the scope for optimization of the primary PGDM capture, with factors such as pH variation influencing PGDM uptake from broth (Yang *et al.*, 1992).

Microscale experiments were conducted to investigate the interaction of multiple parameters on product recovery and impurity removal. Broth pH was adjusted from acidic at pH 5 to more alkaline at pH 9 to determine the impact on the adsorption of impurities along with the PGDM product. Once the adsorption phase was complete (Section 2.7.1), the resin beads were washed with wash buffers at pH ranging from 5 to 8 in an attempt to determine a set of conditions that resulted in the highest amount of impurity removal as determined by HPLC.

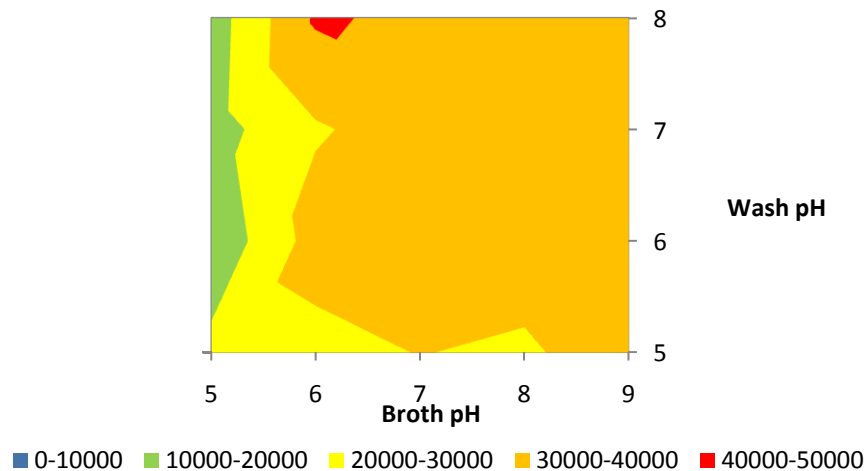
Figure 5.1 A) shows the impurity removal efficiency using wash buffers at various pH values. The data indicates that adsorption at higher pH ranges (alkaline) results in higher impurity removal from the resin when combined with a basic wash at pH 8. The least impurity removal occurred when batch adsorption was performed under acidic conditions and followed up with an acidic wash at pH 5. However the highest amount of impurity removal occurred when batch absorption occurred at pH 6, with a wash buffer at pH 8 (40,000

mAU of impurities detected in wash). This would suggest that post-adsorption resin washes be performed with alkaline wash buffers to achieve higher purity PGDM.

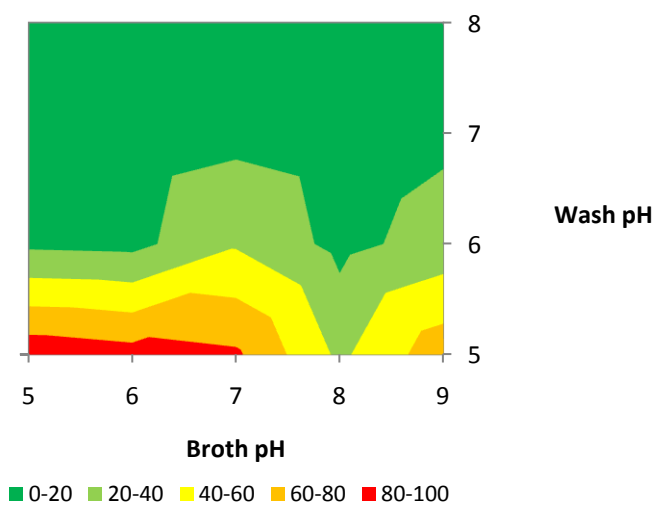
When elution was performed with a buffer of 60% (v/v) Methanol/40% (v/v) 5mM H₂SO₄, the highest PGDM recovery was achieved when the broth was adjusted to an acidic pH along with a resin wash at acidic pH (Figure 5.1 B). The highest PGDM yield of over 80 mg/L was obtained when broth was adjusted to pH 5 with the resin washed at pH 5. Increasing the broth pH for batch adsorption negatively impacted PGDM recovery as did increasing the pH of the resin wash for impurity removal.

Similarly to product yield, Figure 5.1 C shows the highest PGDM purity of 15% was achieved under acidic broth/wash conditions. This was contrary to the expectation that the highest impurity removal during the wash would result in the highest purity product. In contrast to the removal of broth impurity bound to the XAD-7 resin, alkaline pH resin washes resulted in reduced product purity. It is also notable that none of the purity values achieved for the microscale experiments could emulate the 28% PGDM purity achieved at the pilot scale process. This may be due to the degradation of the PGDM under the broth/wash conditions being used, reducing the amount of PGDM in comparison to impurities, or at such small scales some PGDM may be tightly bound to the beads.

A



B



C

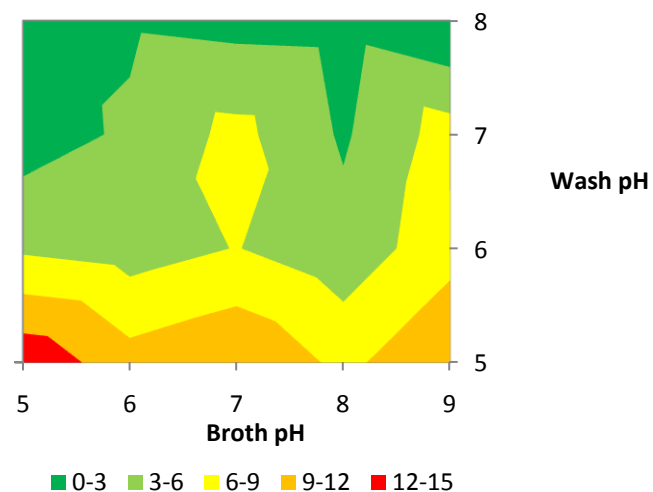


Figure 5.1 Contour plots of microscale XAD-7 adsorption/desorption data at different broth pH values for adsorption and wash pH values for elution: (A) the amount of impurity removal, the colour bands represent the sum of all impurity peak areas in mAU on an HPLC chromatogram; (B) the concentration of eluted PGDM with colour bands representing the eluted PGDM in mg.L^{-1} and (C) the purity of the eluted PGDM with the colour bands displaying the percentage purity (%) of the PGDM. Microscale method performed as described in Section 2.7.3

5.4 Stability of PGDM and Gallidermin

5.4.1 pH

The purity and yield results from the microscale wash experiments were unexpected. The PGDM recovery in batch adsorption at microscale was a maximum 95 mg out of a broth product concentration of 400 mg.L⁻¹, a yield closer to 25 %, as opposed to 57 % achieved at pilot scale. A potential reason for the low product recovery could be the impact on PGDM stability of varying pH levels. Prior to the microscale elution in section 5.3, the resin was subjected to 3 wash cycles of a minimum 8 hours. With the additional time taken to perform HPLC analysis on multiple samples, (each HPLC run being completed in 18 minutes) the PGDM wash exposed to the wash buffer for a minimum 12 hours for each wash. Thus it is proposed that low yields and purity might be due to product degradation.

Figure 5.2 compares the microscale stability data of pure PGDM and gallidermin buffered at pH 6, 7 and 8 at 25 °C. Each experiment was performed at 100 µL scale and required just 1 mg of PGDM in total. As is visible, increasing pH results in increased degradation for both PGDM and gallidermin, however gallidermin (Figure 5.2 B) degrades at a higher rate as compared to PGDM. In the case of stability at pH 8, gallidermin was found to degrade 5 times faster than PGDM. This result corresponds to studies on the stability of Nisin, another Class I lantibiotic, which displayed maximal stability at low pH values (Rollema *et al.*, 1995).

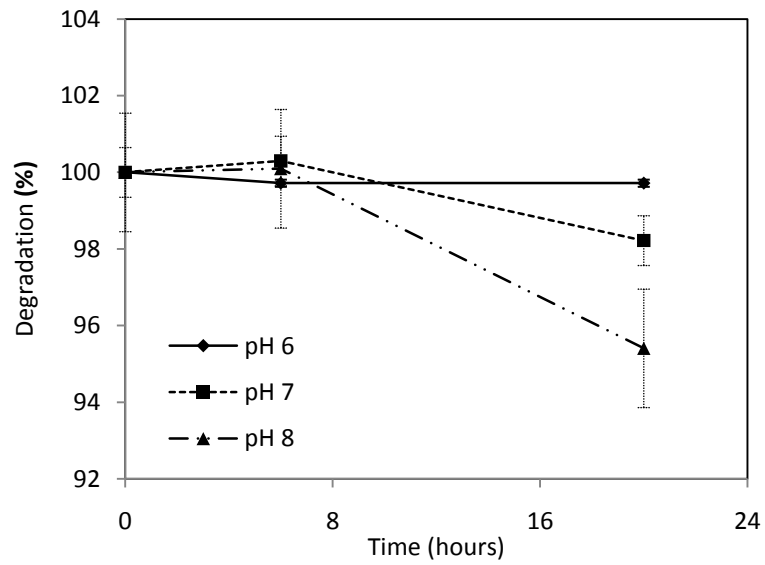
It is worth noting, however that the stability experiments were conducted with pure antibiotic product, as opposed to the PGDM in culture broth. The culture broth contains undefined components from yeast extract and potentially cellular components and enzymes released by *S.gallinarum* Δp that were not removed by centrifugation. Varying the pH on these cellular components may impact the stability of PGDM, possibly accelerating degradation. Indeed it is found that when PGDM is left in un-clarified culture broth post fermentation, it begins to degrade (Medaglia, 2009).

Later studies by Arias *et al.* (2013) on a Type B lantibiotic and Barbour *et al.* (2013) on a novel potentially Type A (the structural grouping was under investigation and not made completely clear) lantibiotic demonstrated that they were stable at high temperatures between a pH range of 2 to 9 and 2 to 10 respectively. Those results are very different from what has been observed in the present study, providing further evidence that the structural variety of lantibiotics may lead to significant differences in their physico-chemical properties (van Heel *et al.*, 2013).

5.4.2 Ionic Strength

The impact of varying ionic strength was investigated by performing microscale experiments with pure gallidermin and PGDM buffered at pH 7, in microwells shaken at 1200 rpm and maintained at 37 °C. Ionic strength of the buffer was varied from 0.02 M to 0.06 M. No change was observed in the rate of degradation for both PGDM and GDM by variation of the buffer ionic strength. This suggests that using a wash buffer at high ionic strength should remove maximal impurity without negatively impacting the PGDM recovery.

A



B

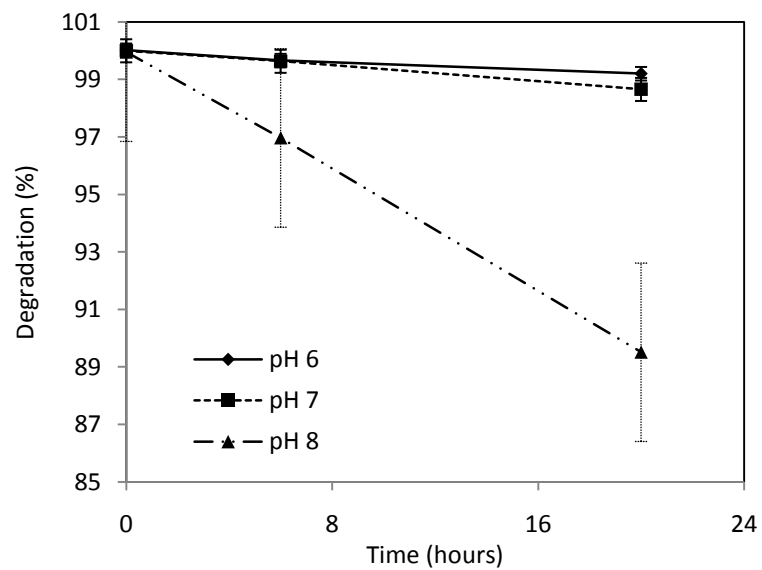


Figure 5.2 The Stability of PGDM and GDM under varying pH. (A) PGDM and (B) GDM in microwells buffered at pH 6, 7 and 8 over a 24 hour time span, maintained at 25°C and shaken at 1200 rpm. Microscale studies performed as described in Section 2.6.2. Error bars represent standard error.

5.4.3 Temperature

Temperature is known to have an impact on lantibiotic stability (Rollema *et al.*, 1995), especially at extremes of pH. It is therefore important to consider the impact of temperature on lantibiotic stability over a range of conditions. The microscale method described in Section 5.4.1 to examine the influence of pH on lantibiotic stability was also used to investigate the effect of temperature on stability.

The adsorption of PGDM onto Amberlite XAD-7 in Section 5.3 was carried out overnight at 25 °C and 1200 rpm from broth buffered at the various pH values. The subsequent resin washes were also performed at 25 °C for 8 hours. However it is notable that between washes, when replacing buffer or waiting for the sample to be analysed by HPLC (Section 2.5.3) on the equipment tray, the samples may have been exposed to higher ambient lab temperatures for a period of a few hours. These process 'waiting' times could be magnified at the manufacturing scale, where thousands of litres of product solutions may require holding at certain conditions between process steps.

Thus, it becomes relevant from a process efficiency viewpoint that the amount of product loss by degradation is minimized due to these process 'gaps'. An investigation into the impact of increasing temperature is shown in figure 5.3. Both PGDM and gallidermin are shown to be increasingly unstable with an increase in temperature. It is notable that gallidermin degrades quicker than PGDM, with degradation at 37 °C five times faster for gallidermin in comparison to PGDM. Stability for the lantibiotic products is higher at 25 °C, however it is again notable that gallidermin degrades 2 times faster than PGDM. As in the

case of pH, it is suggested that certain undefined components of the complex media and cell-culture broth could exacerbate product degradation further.

The stability data suggests that when designing a manufacturing process for PGDM based modified antibiotics, it would be prudent to keep the antibiotic in its inactive form for as long as possible during the process to minimise losses associated with active gallidermin instability. The enhanced stability of PGDM, if a generic feature of lantibiotic precursor peptides, could support a wider adoption of this approach to lantibiotic purification and production.

No previous studies have been conducted on the physico-chemical properties of pregallidermin, to the knowledge of this author. A search of the wider literature did not reveal any comprehensive studies on the physico chemical properties of gallidermin either. Lantibiotics have often been referred to as attractive compounds based on their stability against proteases, heat and oxidation, as well as their antimicrobial activity (Dischinger *et al.*, 2014). Studies by Arias *et al.* (2013) on a novel type B lantibiotic, Amylolysin, showed it to be stable between temperature ranges of 25 to 100 degrees Celsius and a pH range of 2 to 9. A separate lantibiotic, Salivaricin 9 also retained biological stability at temperatures of 90 to 100 degrees Celsius for a pH range of 2 to 10 (Barbour *et al.*, 2013). The current results are contrary to these studies, as both PGDM and GDM start degrading, with GDM degrading significantly, at physiological temperature and pH.

However, earlier studies by Rollema *et al.* (1995) on the stability and solubility of Nisin, showed trends consistent to those elucidated in the present study.

Nisin was shown to have low stability at physiological pH and temperature, while the stability was a little greater at pH 7 and 20°C. Equivalent data for Nisin precursors is not available. This suggests that the physico-chemical properties are related to lantibiotic structure and synthesis pathway, as both Nisin and Gallidermin are type A (I) lantibiotics. Additionally, it suggests that similar production processes and DSP sequences might be applicable to lantibiotics belonging within the same structural grouping.

It is also notable that while the properties for GDM showed consistency with Nisin, PGDM showed enhanced stability at physiological pH for both temperatures. This information could be useful when making process choices e.g. the data suggests that any DSP sequences at high temperatures should be performed prior to the proteolytic cleavage of PGDM leader peptide.

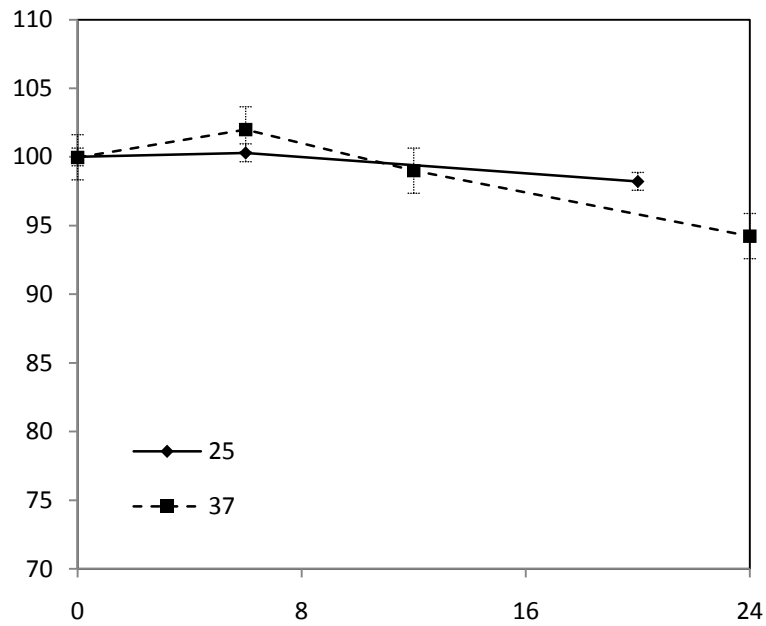
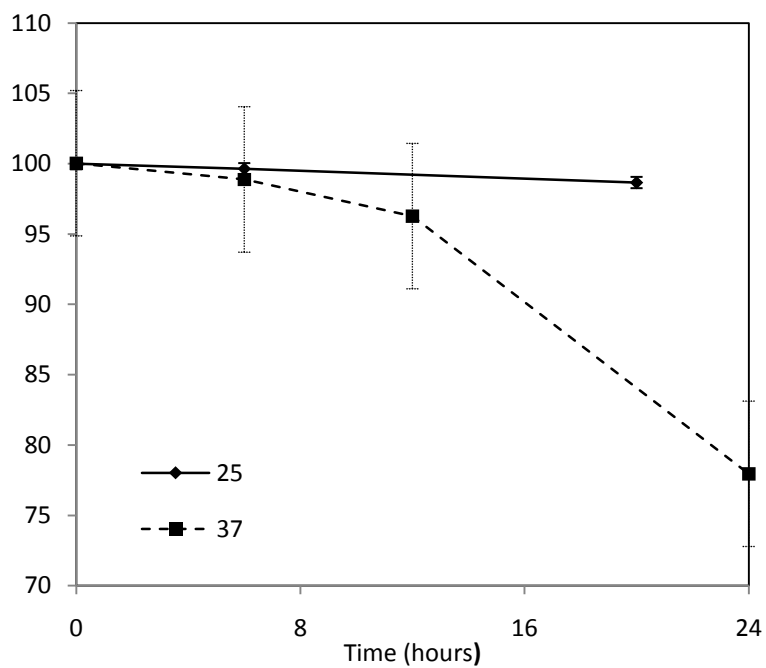
A**B**

Figure 5.3 The Stability of PGDM and GDM under changing temperature. (A) PGDM and (B) pure GDM in microwells at 25 °C and 37 °C, buffered at pH 7 over a 24 hour time span and shaken at 1200 rpm. Microscale studies performed as described in Section 2.6.2. Error bars represent standard error.

5.5 Impact of Methanol and co-solvent ionic strength on elution

The protocol used for PGDM elution from XAD-7, as described in section 2.3.6, was based on work by Medaglia (2009) where a 60/40 % (v/v) methanol to acidified water elution buffer is suggested. Different authors have suggested various compositions for the elution buffer with some using up to 90 % methanol (Kellner *et al.*, 1988). However, as demonstrated in the overall PGDM purification table in Chapter 4 (Table 4.2), with a yield of 57 % and purity of 28 %, there is scope for optimisation. It is worth investigating the optimal elution conditions for PGDM adsorbed to the XAD-7 resin, which could potentially increase primary capture efficiency, improving overall process yield. A DoE sequential analysis approach was adopted for these experiments.

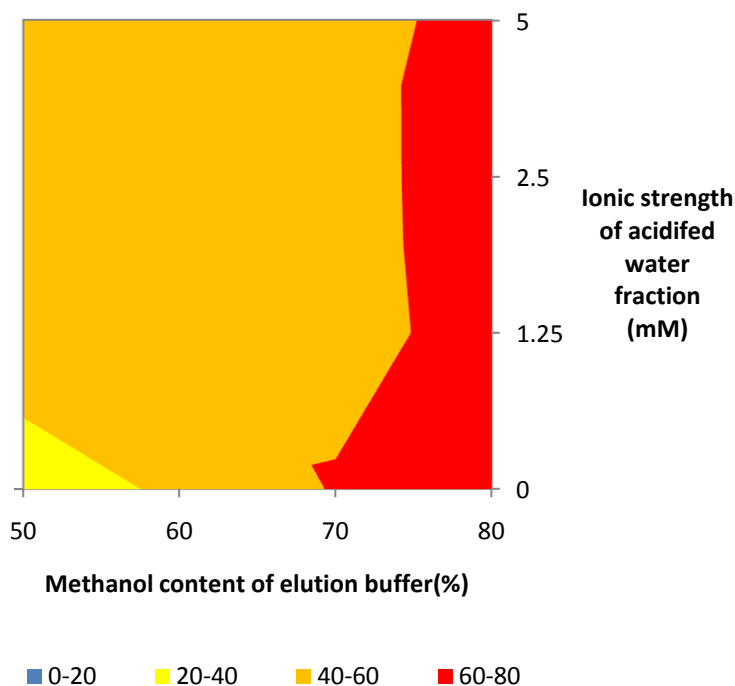
Figure 5.4 displays the effect of varying the methanol fraction of the elution buffer while increasing the ionic strength of the acidified water on PGDM elution from XAD-7 under uniform broth pH and wash conditions. Figure 5.4 A) demonstrates the impact on product purity, with a high methanol content of 70 to 80% seemingly the most suitable to optimise PGDM purity. The ionic strength of the acidified water (H_2SO_4 based) does not apparently have as substantial an impact on purity as methanol content, which is understandable as a lower pH promotes PGDM solubility and stability (Rollema *et al.*, 1995) rather than having any impact on the removal of culture broth impurities.

In comparison, ionic strength of the acidified water plays a larger role in PGDM recovery (figure 5.4 B), with higher ionic strength promoting desorption of

PGDM from the resin by promoting solubility and in turn enhancing the hydrophilic characteristics of the product.

Thus, the highest product yields are obtained with a high methanol fraction and higher ionic strength of the acid fraction, with the highest PGDM elution occurring at 80 % methanol and 2.5 mM H₂SO₄. In terms of product recovery, this translates to 0.37 g.L⁻¹ out of a process broth concentration of 0.5 g.L⁻¹, a primary product recovery greater than 70 %. In comparison, Medaglia, (2009) found the optimal elution buffer for use with Amberlite XAD-1180 to be composed of 60% methanol, which resulted in a PGDM recovery of 90%. This difference in recovery indicates selecting the most suitable resin to be used in the DSP sequence is crucial to ensure process optimisation and that a single resin may not be suitable for all antibiotic variants.

A



B

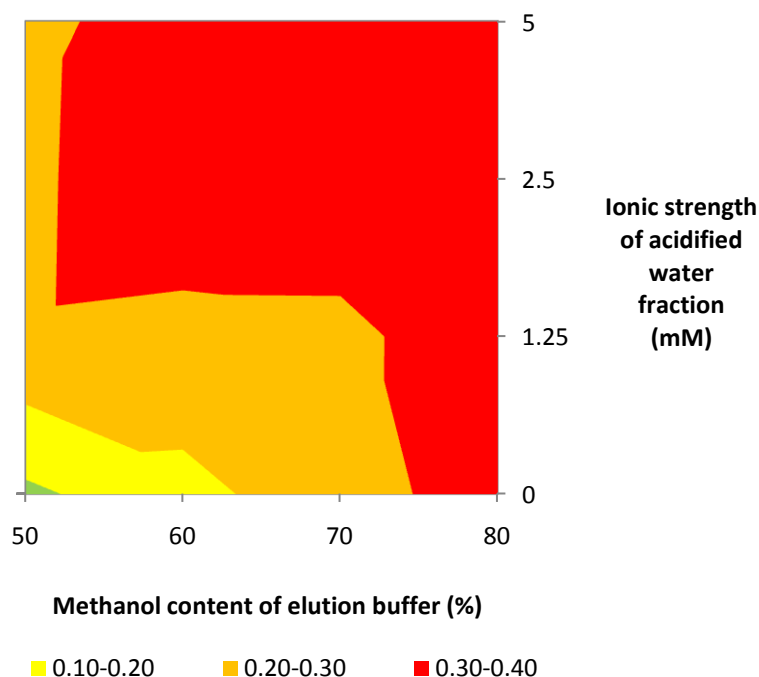


Figure 5.4: Contour plots of microscale XAD7 product elution data at different values for elution buffer methanol content and ionic strength of H₂SO₄ in the acidified water fraction. (A) Showing the impact on PGDM product purity. The coloured bands represent the percentage purity (%) of the recovered PGDM product in comparison to the all eluted components. (B) Illustrates the impact on product recovery with the coloured bands representing the concentration of recovered PGDM in g.L⁻¹. Microscale method performed as described in Section 2.7.2

5.6 Impact of Methanol and ionic strength on wash impurity removal

The data from Figure 5.4 suggests that PGDM adsorbs strongly to XAD-7 and requires a high fraction of methanol in the elution buffer to be recovered from the resin. Hence in pursuit of optimal removal of cell culture impurities adsorbed along with product, it is worth investigating the impact of including methanol in the resin wash buffer. It is proposed that if methanol is included, the wash buffer might enable the removal of culture broth impurities that possess a slight hydrophobic nature and will not otherwise be removed by the alkalinity of the basic wash buffer.

Figure 5.5 A) suggests that the maximum culture broth impurity is removed from the resin when the methanol fraction of wash buffers is 10 % (v/v) and the buffer ionic strength is increased. Maximum culture broth impurity of 26800 mAU (as determined by HPLC analysis of wash fraction) was removed using a wash that contained 10 % methanol and had a buffer ionic strength of 0.02 M, with high impurity removal at 0.06 M also noted. The general trend displayed was increasing impurity removal with an increasing methanol fraction in the wash buffer.

Similarly figure 5.5 B) shows maximum PGDM purity obtained with high methanol content and a high buffer ionic strength, which is logical considering the highest impurity was also removed under these wash conditions. This seems to be confirmed by the comparatively low purity of the PGDM eluted from XAD-7 after wash buffers containing 0 % methanol. It is again notable that the

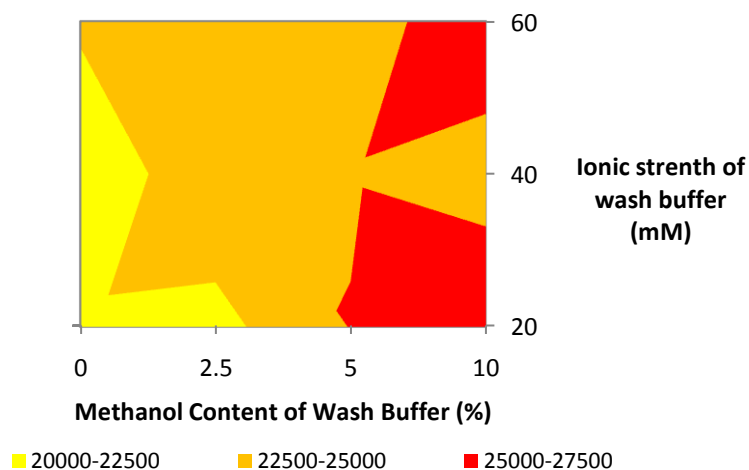
ionic strength of the wash buffer seemingly has a lower impact on purity in comparison to methanol content.

However, conversely, as shown in Figure 5.5 C) a buffer wash with increasing methanol content resulted in lower PGDM yield. The highest PGDM elution was recorded after the resin was washed with 0.02 M buffer which included no methanol. This outcome is logical as the methanol would have removed small amounts of PGDM from the resin; however the methanol concentration does not reach the threshold where all PGDM gets eluted during the wash.

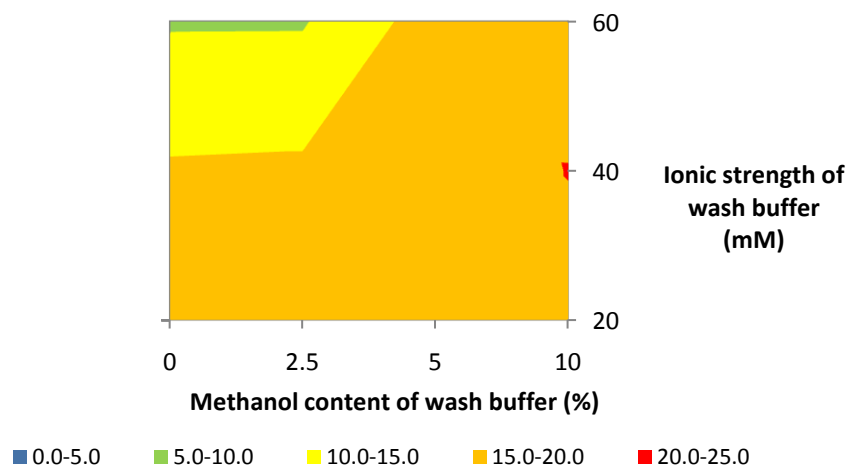
There are no studies in the literature that examine the impact of the wash buffer on desorption of media impurities. To the knowledge of the author, the present study is the first that examines this relationship in the interests of DSP sequence optimization for lantibiotic production. Previous work by Medaglia, (2009), Kellner *et al.* (1988) and Kempf *et al.* (1999) has made use of Amberlite resin adsorption/desorption for product capture, however none of them have characterised the resin wash stage. Medaglia, (2009) does not even use a wash step between steps, eluting the PGDM from resin straight after adsorption.

However, it is notable that Medaglia, (2009) does perform optimisation studies on the elution buffer, which indicates that at low methanol concentrations, a majority of the PGDM remains adsorbed to the resin. This is consistent with the results of the current study, where a wash buffer with a 10% methanol fraction does not elute a majority of the PGDM.

A



B



C

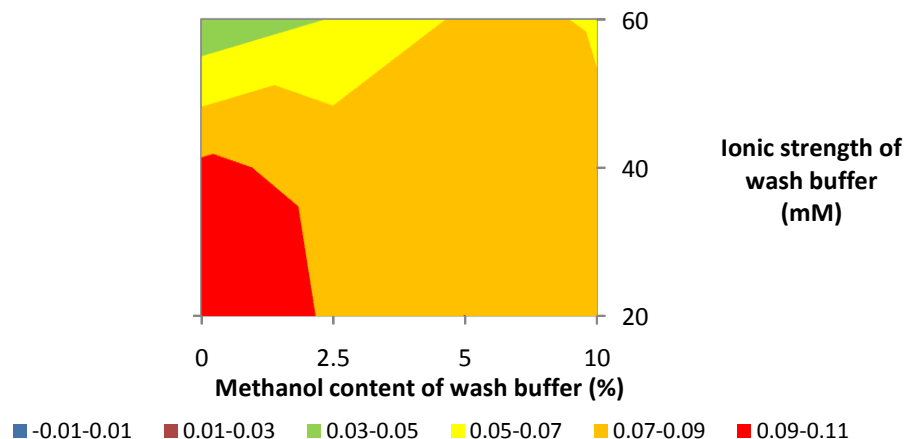


Figure 5.5 Contour plots of microscale XAD-7 adsorption/desorption data on the impact of increasing the ionic strength of the wash buffer and including methanol. A) impurity removal from the XAD-7 resin beads, with the coloured bands representing the sum of impurities removed in mAU as determined by HPLC, B) the purity of PGDM product eluted after the Methanol/high ionic strength buffer wash, the coloured bands represent percentage purity (%). C) the PGDM product yield upon elution after resin wash with the Methanol/high ionic strength buffer, the coloured bands represent PGDM concentration in g.L⁻¹. Microscale method performed as described in 2.7.1

5.7 Selection of optimised downstream process conditions

5.7.1 Impact of pH on antibiotic recovery and processing

The variation of pH during various stages of the adsorption/desorption primary capture process was found to have a significant impact on PGDM recovery and purity as described in Section 5.3. In general, it appears that adjusting broth to an acidic pH results in the highest recovery of PGDM, as opposed to an alkaline environment. This is similar to work by Yang *et al.* (1992) who managed to adsorb maximum antibiotic product onto the producer cells in acidic environments. Alkaline pH was found to negatively impact recovery, possibly due to a reduction in the amount of PGDM adsorbing to the resin.

However the recovery of PGDM could also depend on product stability at different pH values. In particular it was noted that alkaline conditions greatly increased the product degradation rate as compared to neutral or acidic conditions; which displayed the highest antibiotic stability (Rollema *et al.*, 1995). Thus it is possible that the reduced PGDM recovery when culture broth pH is adjusted to above 7 could be attributable to product losses from degradation in solution along with reduced adsorption onto the resin beads.

In contrast to the negative impact of alkaline conditions on PGDM adsorption, high pH values were most effective in removing fermentation impurities adsorbed to the resin during the resin wash before PGDM elution (Section 5.3). Increasing wash buffer pH resulted in increasing impurity removal, however the

highest amount of impurity removal occurred when the culture broth was adjusted to pH 6 pre-adsorption and a pH 8 buffer was used to perform the resin washes. This could be due to higher amounts of broth components adsorbing onto the resin beads at pH 6 as opposed to alkaline culture broths, and subsequently more impurities being removed with the pH 8 washes.

The use of alkaline pH washes, while enhancing adsorbed impurity removal, negatively impacted the purity of the recovered PGDM. The highest product purities were obtained where fermentation broth was acidic and the wash buffers were acidic as well. This result could potentially be caused by the product losses due to degradation under alkaline conditions, with a lower concentration of recovered product reducing the purity in comparison to other eluted components.

The data generated by the microscale experiments in Figure 5.1 show that the optimal production process will operate with a pH range for adsorption and wash buffers that represent a trade-off between product purity and recovery. Priority at the primary capture stage should be product recovery; hence adjusting broth to pH 6 and performing resin washes with a buffer around pH 7 is suggested to achieve optimal results. However, other operating parameters such as processing time, that impact PGDM stability also need to be considered prior to finalizing operational parameters.

5.7.2 Impact of increasing methanol content and buffer ionic strength on resin wash and product elution efficiency

Originally, PGDM elution from the XAD-7 resin was performed using a 60/40 % (v/v) methanol to 5 mM sulphuric acid solution. However, microscale investigation revealed that increasing the methanol content results in increased PGDM elution from resin (Figure 5.4). This is logical as PGDM adsorbs based on a hydrophobic interaction, thus reducing the water content of the elution buffer would promote the increased desorption of the lantibiotic. However, due to the low solubility of PGDM in methanol, 40 mg.L⁻¹, as opposed to > 4 g.L⁻¹ in water (Medaglia, 2009), the elution cannot be performed with pure methanol, as precipitation of the saturated PGDM would block the resin pores. The microscale data also indicates that increasing the methanol fraction of the elution buffer leads to higher overall product purity (Figure 5.4). This is probably caused by the increased efficiency of PGDM elution at higher methanol content in comparison to the total culture broth impurities adsorbed. Indeed it is expected that under uniform broth pH, wash pH, temperature, process time and agitation conditions, the amount of total impurity and product adsorbed by the XAD-7 resin would be constant for a unit mass of resin. Hence logically, increased purity levels would be attributable to higher product recovery.

The finding that efficient PGDM elution from the XAD-7 resin requires high methanol is consistent with prior work by Kellner *et al.* (1988) and Medaglia, (2009). It suggests that low amounts of methanol (up to 10 % (v/v)) could be incorporated in the resin wash buffer to increase the purity of eluted antibiotic.

The methanol washes were shown to remove higher amounts of broth impurities, as well as resulting in the elution of a higher purity product, however the overall antibiotic recovery was higher without the use of methanol in wash buffer (Figure 5.5). This is because, along with the removal of higher amounts of impurity, the methanol content of the wash buffer managed to elute small amounts of PGDM from the resin as well. However, the product losses when using a methanol based wash were limited to 18 % of total when compared with no methanol wash, while increasing purity by 10 %.

The ionic strength of the wash buffer was not as significant in impurity removal as pH. However it was observed that increasing the ionic strength of a wash buffer that contained no methanol reduced the purity and recovery of PGDM. This outcome was unexpected as stability studies had shown no noticeable change in the rate of antibiotic degradation when using higher ionic strength buffers. However one possible explanation for the reduced PGDM recovery is that using a higher concentration of the salts necessary to create the buffer result in a 'salting-out' of a small amount of the PGDM. Indeed one of the methods suggested for the primary capture of antibiotics by certain authors is an ammonium sulphate precipitation (Furmanek *et al.*, 1999; Jack *et al.*, 1995; Holtmark *et al.*, 2006; Georgalaki *et al.*, 2002).

In comparison to the wash buffer, increasing the ionic strength of the elution buffer (Methanol/ acidified water) had no impact on PGDM purity. It did however impact product recovery, with higher ionic strength of the acidified water increasing the amount of PGDM eluted from the resin. This is logical as increasing acid content would reduce the pH of the water, which has been

shown to promote lantibiotic solubility and stability (Rollema *et al.*, 1995), allowing a larger mass of the lantibiotic to dissolve in a given volume of water, while promoting the hydrophilic nature would enable more product to elute.

5.7.3 Potential as a platform for informing process design

The application of the data obtained from the microscale analysis is not just limited to DSP e.g. the GDM stability is shown to be very sensitive to temperature increases, with the antibiotic product degrading rapidly at 37 °C, information which is useful when scheduling fermentation runs and determining how quickly broth refrigeration would be required. The data obtained would suggest that the PGDM not be activated to GDM in the fermentation broth (maintained at 37 °C), in order to prevent unnecessary product losses.

The information enables the optimisation of the hydrophobic adsorption/desorption in this work. The initial DSP described in Section 4.2, included a process with adsorption at neutral pH (required for optimal growth of *S.gallinarum* Δp), washing with a 0.02 M buffer at pH 8; and desorbed with a 60/40 % (v/v) methanol/ 5 mM H₂SO₄ elution buffer. This resulted in an overall PGDM yield of 57 % and purity of 28 % as indicated in Table 4.2.

Based on the results presented in Section 5.3 to 5.6, data from the established microscale methods indicates that adsorption from culture broth would be best at pH 6, followed by a resin wash with a 0.04 M buffer at pH 7 containing 10% methanol (v/v) followed by elution with 75/25% (v/v) methanol/2.5mM H₂SO₄ . This would result in a product recovery of 70% and purity of roughly 80%.

These optimisation studies enabled the redesign of the downstream purification process to eliminate ion exchange chromatography as a secondary purification step and increase overall process yield to 42% from the original 13%, a 3-fold increase (Table 5.2). The original DSP sequence in Table 5.1 is provided for comparison.

It has been recommended that the microscale methods become an integral part of the manufacturing platform for novel antibiotics, owing to the substantial cost and time which can potentially be saved by early acquisition of optimal process parameters (Ongey & Neubauer, 2016). Additionally, they provide the ability to continuously improve a manufacturing process when faced with variations in production processes; such as changes in fermentation media (Jackson *et al.*, 2006), changes in process parameters or the use of novel strains (Smanski *et al.*, 2016; Sandiford, 2014) due to relocating production or producing alternative compounds.

Table 5.1 Purification table summarizing the PGDM step yield and purity for the whole downstream process sequence

| Process | Total Mass of PGDM(g) | Overall Yield (%) | Step Yield (%) | Concentration (g.L ⁻¹) | Purity (%) |
|----------------------|-----------------------|-------------------|----------------|------------------------------------|------------|
| Fermentation | 14 | 100 | 100 | 0.7 | 0.56* |
| Centrifugation | 14 | 100 | 100 | 0.7 | 0.56 |
| HI† | 8 | 57 | 57 | 0.4 | 28 |
| IEX | 4.1 | 29 | 51 | 0.2 | 72 |
| HI | 3.1 | 22 | 76 | 0.15 | 80 |
| Lyophilization | 3.1 | 22 | 100 | 0.15 | 80 |
| Trypsinization | 1.9 | 13.5 | 60 | 0.09 | 70** |
| Total Process | 1.9 | 13.5 | NA | 0.09 | 70 |

*purity as a percentage of all dissolved components in cell culture

**reduction in purity due to presence of cleaved leader sequence which requires removal

†Hydrophobic Interaction

Table 5.2 Purification table summarizing the step yield and purity for the redesigned downstream process sequence

| Process | Total Mass of PGDM(g) | Overall Yield (%) | Step Yield (%) | Concentration (g.L ⁻¹) | Purity (%) |
|----------------------|-----------------------|-------------------|----------------|------------------------------------|------------|
| Fermentation | 14 | 100 | 100 | 0.7 | 0.56* |
| Centrifugation | 14 | 100 | 100 | 0.7 | 0.56 |
| HI† | 9.8 | 70 | 70 | 0.49 | 80 |
| Lyophilization | 9.8 | 70 | 100 | 0.49 | 80 |
| Trypsinization | 5.9 | 42 | 60 | 0.3 | 70** |
| Total Process | 5.9 | 42 | NA | 0.3 | 70 |

*purity as a percentage of all dissolved components in cell culture

**reduction in purity due to presence of cleaved leader sequence which requires removal

†Hydrophobic Interaction

5.8 Summary

The aim of this chapter was to establish microscale methods to determine certain physico-chemical properties for the novel antibiotic pregallidermin, which would enable optimisation of the selected product purification process and enable informed decisions on the future design of DSP sequences for large scale product manufacture.

The initial objective was to establish a series of microscale methods to enable the rapid analysis of product physico-chemical properties; this would aid in the optimisation of downstream processes, as evident by the determination of the optimal parameters for primary capture by Hydrophobic interaction. Parameters were determined where the primary recovery of the PGDM could be increased from 57% of total produced to >70% and purity increased from 28% to > 80%. (Table 5.1 and Table 5.2)

The product data obtained was also useful in redesigning the determined DSP sequence. Based on the optimized primary capture, it became logical to redesign the DSP to remove the ion exchange chromatography. This would reduce the capital investment required and the consumables cost by resizing the column needed to process a feed-stream containing fewer impurities.

The microscale methods were shown to additionally provide product data that could be used to make production plant design and process scheduling decisions, such as the GDM stability data, which suggests that fermentation broth which contains activated GDM may require refrigeration, something that may have to be factored into the purchase of the bioreactors and building of the

liquid storage areas. The sensitivity of PGDM to alkaline conditions suggested that resin washes during the batch adsorption/desorption may need to be performed rapidly, as prolonged exposure to high pH buffers could lead to product losses.

Thus, it is suggested that the microscale methods be included as a tool to inform the design and operation of the lantibiotic manufacturing platform. Microscale methods have previously demonstrated their utility in elucidating process data that can inform process decisions at scale (Voulgaris *et al.*, 2016; Sandiford, 2014). Due to their utility in process design and optimisation, it is strongly recommended that they become an integral part of bioprocess development for novel lantibiotics. This recommendation is supported by evidence from the wider bioprocess industries, where they have gained widespread usage and acceptance (Ongey & Neubauer, 2016; Micheletti & Lye, 2006).

The microscale studies were performed using the 'one factor at a time' (OFAT) method, the most commonly used bioprocess optimization technique (Ducros *et al.*, 2009). However, it is notable that OFAT is time consuming, especially when several factors need to be analysed. Additionally, OFAT ignores possible interactions between factors, which are important when determining the optimal process operating conditions. An alternative approach could be the use of the 'Design of Experiments' (DOE) methodology, a combinatorial optimization method that can look at multiple variables at a time and reduces the number of experiments needed to elucidate optimal conditions (Smanski *et al.*, 2016). The current OFAT based work acts as a useful screening study in preparation for a

full DOE. Indeed, a combination of DOE with high through-put studies based on microscale methods is used widely throughout industry to shorten process development times (Li *et al.*, 2010).

6. Conclusions and future work

6.1 Conclusion and novel findings

This research aimed to develop and analyse processes for the production of a novel modified peptide antibiotic, pregallidermin, at scale. Characterisation of the process parameters would be done to allow the reproduction of results between process runs, in view of outlining a potential generic platform process. This was followed up with the creation of microscale methods that would allow the rapid analysis of the production process, enabling informed decisions to be made about process design and optimisation. As described in Chapters 3-5 this aim has been largely achieved by demonstrating that a viable process for the production of pregallidermin at pilot scale has been developed.

Although some initial work has been reported on attempting to develop production processes for the wild type antibiotic, gallidermin (Section 1.5.1), the auto-toxicity displayed by the molecule to the producing organism resulted in low titres, $< 300\text{mg.L}^{-1}$ that would be impractical for a commercial manufacturing process. Thus the use of a novel genetically modified precursor, pregallidermin, was examined in this work. Preliminary studies carried out at ETH Zurich indicated that this has a considerably lower auto-toxicity, potentially allowing higher product yields (Valsesia *et al.*, 2007). However, this requires an additional trypsination step be included in the downstream process sequence, in order to remove the leader peptide and form mature, biologically active lantibiotic. At present there is no published work on the development and analysis of a

manufacturing process feasible for the large scale production and purification of the precursor lantibiotic, pregallidermin. The current lack of information is what this thesis set out to address.

The main conclusions and novel findings of this work are:

- A procedure for the pilot scale (30L) fed-batch fermentation of *S.gallinarum* Δp was established that enabled production of up to 0.7 g.L⁻¹ of pregallidermin (Figure 3.10). This was based on research at the 7.5 L bioreactor scale (Table 3.1) that attempted to define parameters that are critical to reproducibly achieve high cell density and product yield fermentations. The work also demonstrated the importance of maintaining those parameters at similar levels (aeration, feed rate, and culture agitation rate) in scaling up the process. The main conclusions from this work are that in order to achieve high PGDM titres fed-batch cultures are required in which it is necessary to feed both Maltose and Yeast-extract (Figure 3.8) while maintaining a dynamic process environment by changing key process parameters in response to the cellular growth behaviour. The best fermentation biomass yields were obtained when bioreactor DOT control involved initial increase of the aeration rate before increases in agitation rate (Section 3.7.1). However, yields of pregallidermin were lower than those achieved by Medaglia, (2009) using an exponential substrate feed regime, demonstrating that the process can be optimised further.

This is the first time that the lantibiotic precursor, pregallidermin, has been produced at pilot scale using the modified *S.gallinarum* Δp .

- A DSP sequence capable of processing pilot-scale quantities (30L) of fermentation broth containing the novel antibiotic PGDM was developed (Section 4.2). The process utilises hydrophobic interaction between the pregallidermin and the acrylic Amberlite XAD-7 resin as the primary capture method recovering 57 % of PGDM at a product purity of 28% (Table 4.2). This is followed by an ion exchange chromatography as the high resolution purification step with a 51 % product recovery and increase in purity to 72 % (Section 4.6), the yeast-extract culture broth components proved the most difficult to remove. The sequence is demonstrated to achieve material suitable for activation to gallidermin by trypsinization (Section 4.8). The identity of the product was verified by using HPLC and MALDI-MS (Figure 4.6), with findings consistent with identification studies by Valsesia *et al.* (2007) and Medaglia, (2009). The main conclusions from this work are that the outlined DSP sequence is scalable, with high throughput processes such as centrifugation, resin adsorption/desorption and ion exchange chromatography demonstrably capable of producing PGDM to a purity level sufficient for trypsinization and final processing (Table 4.2). The developed sequence could thus provide a generic template for the DSP sequence in the large scale manufacture of lantibiotics from the same structural grouping and biosynthesis pathway as gallidermin

Based on the extensive review of literature, this work is the first time that pilot scale DSP operations have been attempted for the purification of a lantibiotic precursor.

- The development of microscale methods to determine the physico-chemical properties of pregallidermin and generate process data on pregallidermin interaction in specific process environments such as the impact of pH on stability (Section 5.4.1), which demonstrated results consistent with previous studies on the Type A (1) lantibiotic Nisin (Rollema *et al.*, 1995). It was demonstrated that the data was useful to rapidly analyse the suitability of the production process, which allowed the optimisation of purification processes and also informed the redesign of the DSP sequence (Section 5.7.3). The main conclusions from this work are that microscale methods are extremely useful in the rapid generation of process data through high throughput experimentation and reduced material requirements i.e. < 1g of product (Section 5.4.1), allowing optimisation studies to be conducted concurrently with developmental studies, saving the expense of pilot scale optimisation studies. The generated data allows informed process design choices, as demonstrated by the redesign of the pilot scale DSP sequence for PGDM to improve overall yield (Table 5.2). Thus, the microscale methods are recommended as a generic tool for rapid analysis and optimisation of the lantibiotic manufacturing processes

The present study was the first to attempt the combination of fermentation, DSP and microscale methods into a platform process to

inform process design of lantibiotic precursor manufacture. Additionally, it was also the first study to examine the impact on lantibiotic yield and purity of optimising the resin wash steps during primary product capture.

Overall this thesis resulted in the development of a scalable production process for modified lantibiotic compounds that could potentially serve as a platform process for the manufacture of novel lantibiotics. The process when combined with suitable lantibiotic modification and fermentation development studies, could potentially enhance the existing antibiotic pipeline, increasing the likelihood of a lantibiotic based clinical product being developed. The results also present a case, for the integrated platform (fermentation, DSP sequence and microscale methods), to be used as a tool for performing rapid analysis on other candidate lantibiotics, to find those most commercially feasible by increasing the throughput of pilot scale studies.

6.2 Future Work

The platform process identified has scope for further improvement in order to make the process data generated for a lantibiotic candidate more comprehensive. There is also scope for additional research on variations to the process that will solve some of the difficulties encountered during process development and the microscale methods. Work suggested to improve the production platform and microscale analysis methods is as follows:

- The replacement of yeast-extract in the fermentation media with defined components. A defined medium that optimises lantibiotic production by

enabling the accurate calculation of yield coefficient. Additionally, a defined medium would enhance recovery and purity by reducing the selection of suitable DSP processes, aiding in removing many of the unknown components from yeast extract.

- The testing of a variety of hydrophobic resins to identify the optimal resin for PGDM adsorption. XAD-7 was utilised because of its relatively low cost and easy availability in the lab, however it is possible a different resin would show increased adsorption/desorption efficiency, increasing the cost effectiveness of a manufacturing process.
- Optimization studies on the ion exchange chromatography step for maximum recovery of lantibiotic, including operational parameters and type of resin. The redesign of the DSP has eliminated the need for ion exchange in the purification of PGDM; however ion exchange chromatography would still be required post trypsinization as a polishing step to remove the cleaved leader sequence to obtain the active lantibiotic.
- Automation of the microscale methods on a robotic microscale liquid handling system would improve accuracy by removing human error in liquid handling. It would also reduce the time taken to setup and conduct the experiments, increasing the speed of data gathering.
- The scalability of the platform should be tested by attempting a 100L *S.gallinarum* Δp fermentation and running the same DSP sequence. This

would confirm whether the parameters of feed-rate, agitation and broth aeration are important at all scales, establishing the generic nature of the process and its applicability to all structurally similar lantibiotics.

- Perform the process with different precursor lantibiotics in order to test if precursor manufacture is a generic solution to overcome product auto-toxicity.
- Perform microscale analysis of different modified lantibiotic variants e.g. structural mutants of Nisin. Evaluate if the developed methods allow physico chemical data to be obtained for individual structural modifications and determine if the developed DSP sequence is sufficiently generic to purify novel lantibiotics.
- Perform microscale optimisation using a full DOE. Elucidate optimal process conditions from a multivariable, combinatorial analysis and run the outlined DSP sequence to purify pregallidermin. Compare the results of the DOE optimised process with the existing results.

7. Outlook and Practical Applications†

7.1 Outlook

The increasing number of bacteria developing resistance, to existing antibiotic compounds, has been identified as a problem that will have a major negative impact on global health systems (Walsh, 2014). Antibiotics that were used as the standard treatment for bacterial infections now no longer work. A report by The Economist (2014), points out that in the USA, standard antibiotics used to treat wound infections fail to work half the time. The report outlines a similar situation in China, where a standard antibiotic used to prevent lung infections fails to work 1/3rd of the time.

The drying up of the antibiotic pipeline has multiple reasons, including the failure to discover any new classes of antibiotics since 1987 (World Economic Forum, 2013) and the low monetary returns for pharmaceutical companies that have invested in antibiotic development (The Economist, 2012). This means new antibiotic discoveries are becoming time pressured, with the costs to treat antibiotic resistance set to increase dramatically and medical procedures facing disruption (Gallagher, 2014). In order to mitigate the actualization of these harmful outcomes, it is necessary to enhance the antibiotic product pipeline.

This research attempts to expedite the development of novel antibiotics by providing a powerful tool capable of rapidly acquiring process data, analysis of which can determine the commercial viability of a drug candidate by determining scalability. The increasing cost of novel antibiotic development, in

†This chapter is included as part of the requirements for award of the UCL EngD in Bioprocess Engineering Leadership

some cases greater than \$500 million (Charles and Grayson, 2004) becomes a huge hindrance to the product pipeline, with large pharmaceutical companies opting to devote resources to the pursuit of higher profitability sectors e.g. oncology. If the platform is improved to make the data collection more comprehensive (Chapter 6.2), it could greatly reduce the cost of commercialisation, by indicating non-viable candidates early in the development phase. Furthermore, it is suggested that in combination with a high-throughput antibiotic modification platform and a rapid antibiotic screening process (Sandiford, 2014), the outlined platform could potentially enable the identification of a library of lantibiotics capable of treating existing drug-resistant infections that show the most commercial viability.

7.2 Practical Implementation

The rapid analysis platform developed is outlined in Figure 7.1. It illustrates how the pilot scale antibiotic manufacture generates sufficient material to conduct the rapid microscale analyses, generating a feedback cycle which allows the production process to be optimised during process developmental studies. This would save time and cut the costs of having to perform multiple pilot scale runs for testing a large number of artificially created antibiotics.

It is also noteworthy that the comprehensive bioprocess and product physico-chemical data generated by the tandem microscale analysis could be used to inform large scale manufacturing process design, plus initial antibiotic development and modification. As an example, in Chapter 5 of the thesis it was discovered that the lantibiotic pregallidermin is most stable under acidic conditions; however impurity removal during the purification process is highest

under alkaline conditions. This information could be used to modify the antibiotic further to allow higher stability under alkaline conditions, optimising the product to the chosen DSP sequence. These possibilities are illustrated in figure 7.2.

There are also practical aspects to be considered when implementing microscale rapid analysis at industrial scale, such as instrument maintenance. Working with small quantities of product and liquid volumes means slight variations due to human error or uncalibrated equipment could be magnified in the results. Hence, SOP's would need to be created for equipment maintenance, cleaning procedures, contamination prevention and standard techniques for data analysis.

The technology finds most application in bringing novel antibiotics to market, specifically the lantibiotics (Type A1) which have demonstrated high therapeutic potential against multi-resistant infections, and have similar physical properties and biosynthesis pathways. However, the platform could be applicable to other novel pharmaceutical or industrial compounds (such as enzymes) developed using synthetic biology processes and produced by cell culture. The platform could serve as a generic test-bed for commercial viability testing of engineered biological products from similar types of bacterial cells.

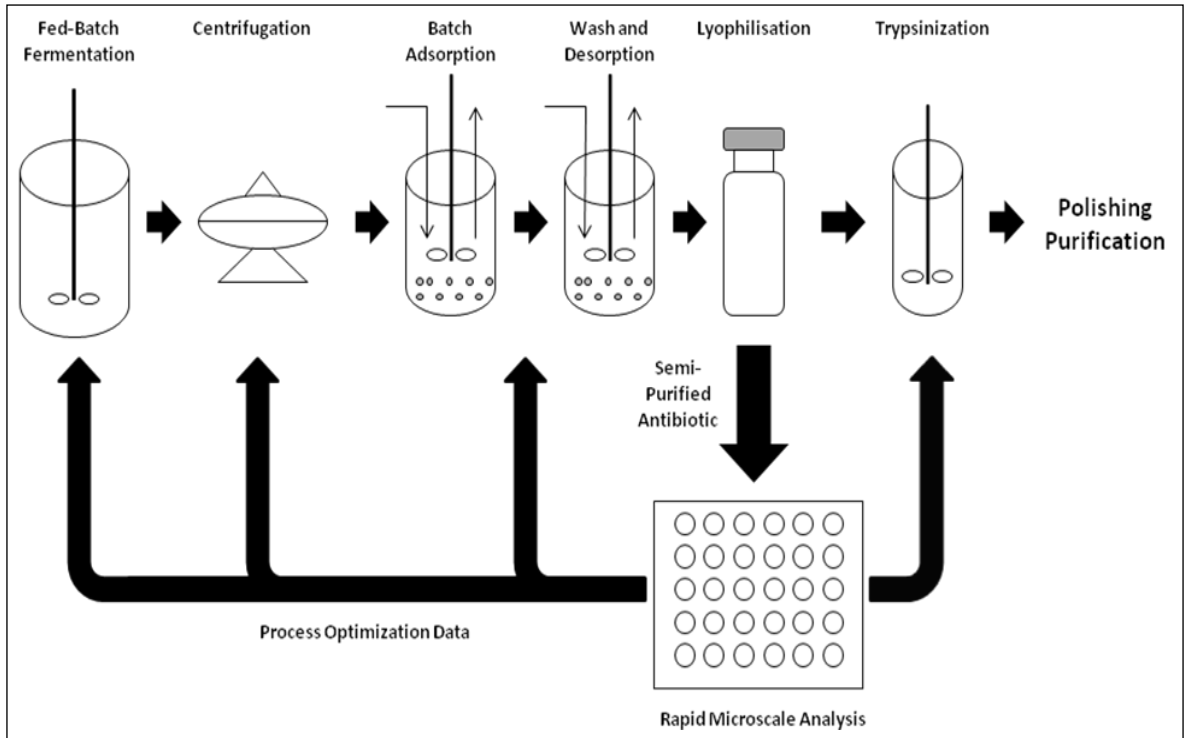


Figure 7.1: Flowsheet representing the platform antibiotic production process with integrated microscale methods for process optimization and rapid product analysis

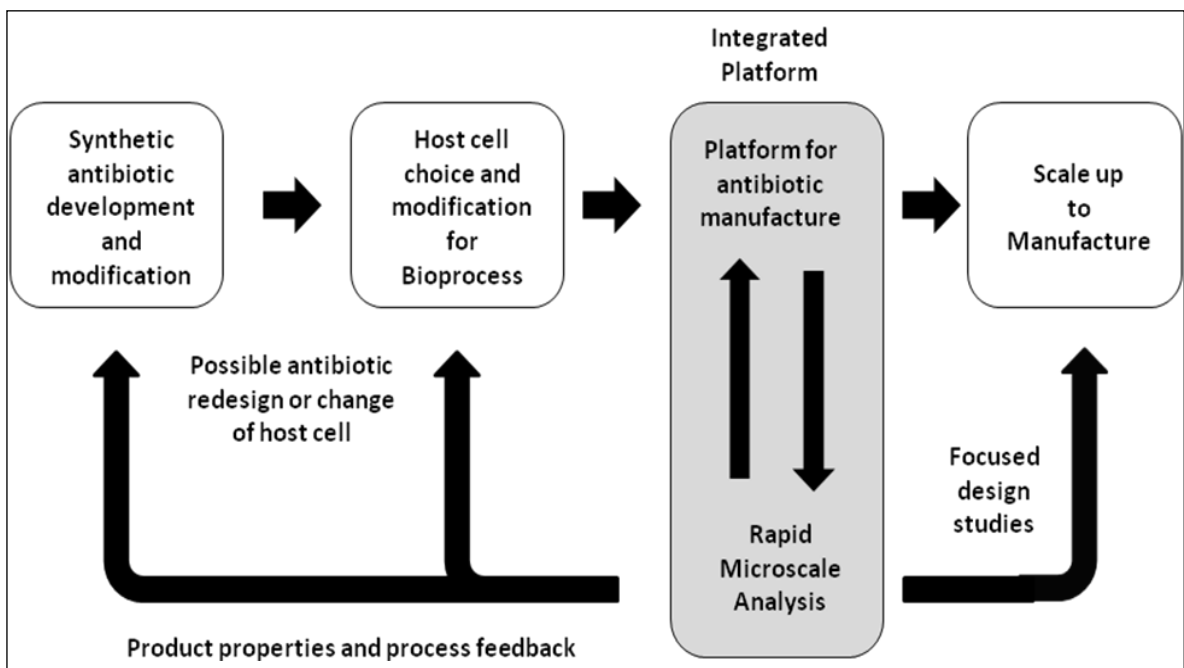


Figure 7.2: How the rapid manufacturing and analysis platform (from figure 7.1) can become part of a complete antibiotic design and manufacturing process, with the microscale methods generating process and product data that can optimize manufacture by providing feedback to both process and antibiotic development.

Appendix

Appendix 1: Full list of Chemicals used

Acetic Acid

Acetonitrile

Amberlite XAD-7 HP

Ammonium Hydroxide

D+ Maltose

Ethanol

Kanamycin Sulphate

Methanol

Milli Q water

Phosphoric Acid

Polypropylene Glycol (PPG)

Sodium Acetate

Sodium Chloride

Sodium Dibasic

Sodium Hydroxide

Sodium Monobasic

SP HP Resin

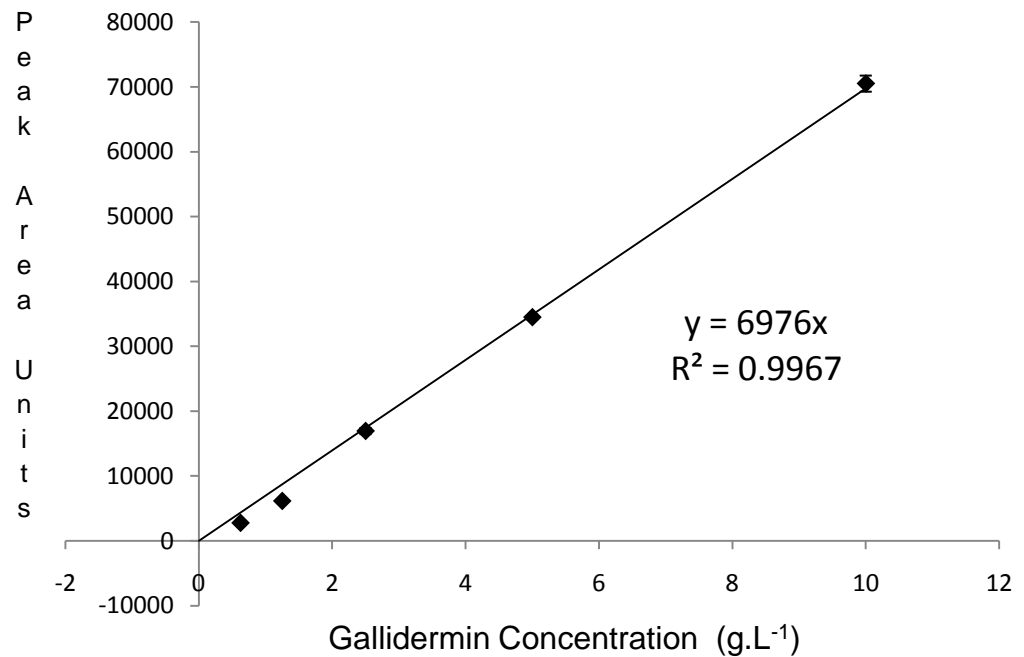
Sulphuric Acid

Tetracycline

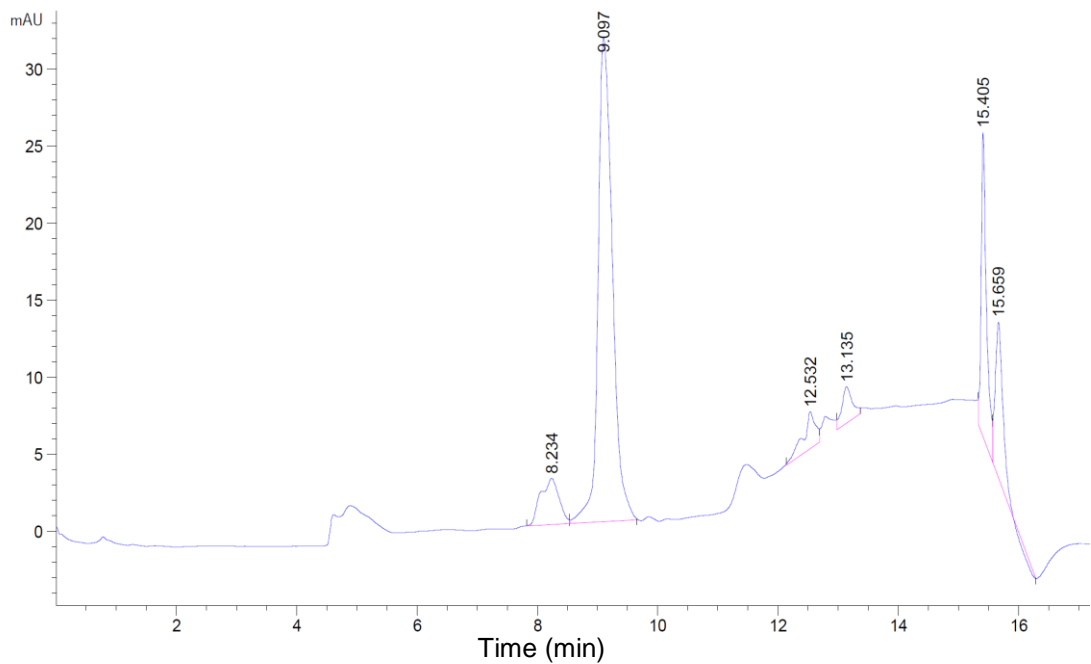
Trypsin (Porcine)

Yeast Extract

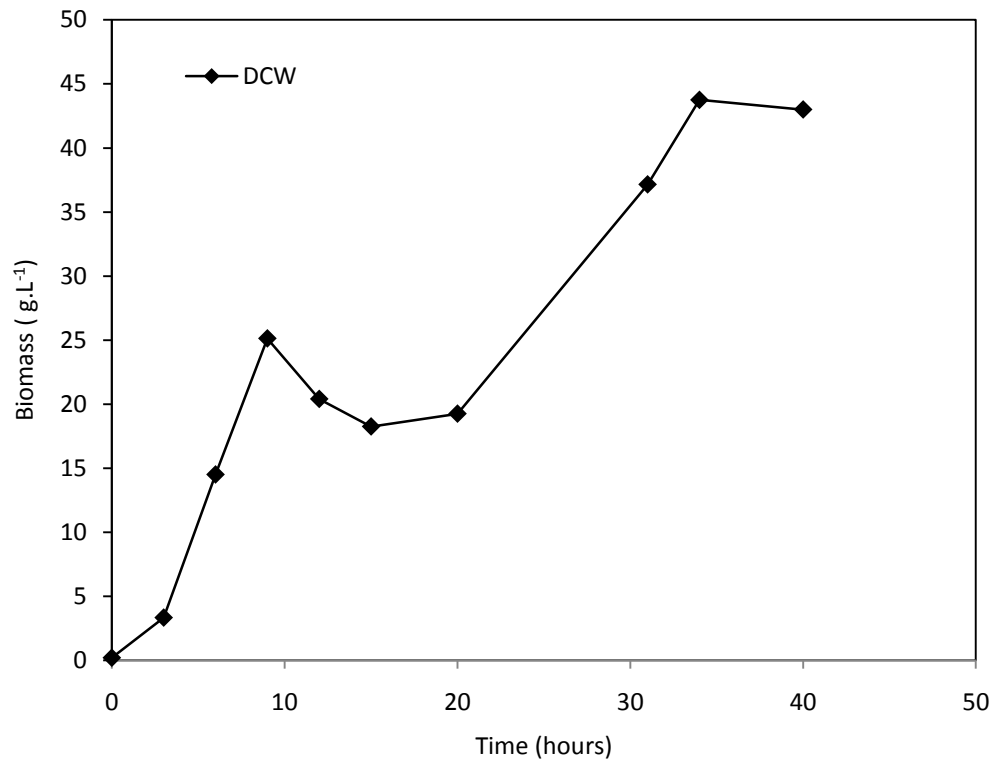
Appendix 2: Calibration Curves



Calibration curve determined by comparing gallidermin concentration against peak area. An example of a Chromatogram to determine peak area is given below where peak at time 9.1 is pure gallidermin.



Appendix 3: 30 L STR fermentation: automated dual feed fed-batch



The above figure illustrates the results of *S.gallinarum* Δp fermentation at 30 L scale when using an exponential feed strategy on the dual 500 g.L⁻¹ and 300 g.L⁻¹ substrate feed (feed data not shown). The exponential feed profile was calculated using a reduced specific growth rate in an attempt to prolong the cellular growth phase by slowing the growth rate.

Appendix 4: Contour Plot Data

| Molarity/MeoH Conc. | 0.02/0 |
|----------------------------|---------------|
| Peak Area | 721.12 |
| | 450.50 |
| | 319.34 |
| | 485.69 |
| | 370.58 |
| | 391.07 |
| | 450.55 |
| | 193.77 |
| | 256.01 |
| | 203.51 |
| PGDM 1 Peak Area | 486.69 |
| PGDM 2 Peak Area | 199.79 |
| Total Area | 4528.64 |
| Total PGDM | 686.49 |
| PGDM Purity | 15.16 |
| PGDM Conc. | 0.11 |
| Average Purity | 15.17 |
| Averag Conc. | 0.11 |
| Molarity/MeoH Conc. | 0.02/0 |
| Peak Area | 723.84 |
| | 454.50 |
| | 316.41 |
| | 484.47 |
| | 381.98 |
| | 383.93 |
| | 464.71 |
| | 185.82 |
| | 267.30 |
| | 203.86 |
| PGDM 1 Peak Area | 482.82 |
| PGDM 2 Peak Area | 209.25 |
| Total Area | 4558.89 |
| Total PGDM | 692.07 |
| PGDM Purity | 15.18 |
| PGDM Conc. | 0.11 |

Table representing data necessary to calculate an individual contour point on contour plots. PGDM purity is calculated using Equation 2.5 and PGDM concentration using a conversion based on the calibration curve (Section 2.5.3).

References

- Ali, L., Goraya, M.U., Arafat, Y., Ajmal, M., Chen, J.L. and Yu, D., 2017. Molecular Mechanism of Quorum-Sensing in *Enterococcus faecalis*: Its Role in Virulence and Therapeutic Approaches. *International Journal of Molecular Sciences*, 18(5), p.960.
- Allgaier, H., Walter, J., Schlüter, M. and Werner, R.G., 1991. Strategy for purification of lantibiotics. *Nisin and Novel Lantibiotics*. *Escom Publishers, Leiden, The Netherlands*, pp.422-433.
- AlKhatib, Z., Lagedroste, M., Fey, I., Kleinschrodt, D., Abts, A. and Smits, S.H., 2014. Lantibiotic immunity: inhibition of nisin mediated pore formation by NisI. *PloS One*, 9(7), p.e102246.
- Al-Mahrous, M.M. and Upton, M., 2011. Discovery and development of lantibiotics; antimicrobial agents that have significant potential for medical application. *Expert Opinion on Drug Discovery*, 6(2), pp.155-170.
- Andrianantoandro, E., Basu, S., Karig, D.K. and Weiss, R., 2006. Synthetic biology: new engineering rules for an emerging discipline. *Molecular Systems Biology*, 2(1).

- Arias, A.A., Ongena, M., Devreese, B., Terrak, M., Joris, B. and Fickers, P., 2013. Characterization of amylolysin, a novel lantibiotic from *Bacillus amyloliquefaciens* GA1. *PLoS One*, 8(12), p.e83037.
- Arifin, Y., Archer, C., Lim, S., Quek, L.E., Sugiarto, H., Marcellin, E., Vickers, C.E., Krömer, J.O. and Nielsen, L.K., 2014. *Escherichia coli* W shows fast, highly oxidative sucrose metabolism and low acetate formation. *Applied microbiology and biotechnology*, 98(21), pp.9033-9044.
- Arnusch, C.J., Bonvin, A.M., Verel, A.M., Jansen, W.T., Liskamp, R.M., de Kruijff, B., Pieters, R.J. and Breukink, E., 2008. The vancomycin–nisin (1– 12) hybrid restores activity against vancomycin resistant Enterococci. *Biochemistry*, 47(48), pp.12661-12663.
- Barbour, A., Philip, K. and Muniandy, S., 2013. Enhanced production, purification, characterization and mechanism of action of salivaricin 9 lantibiotic produced by *Streptococcus salivarius* NU10. *PloS One*, 8(10), p.e77751.
- Bio FAB Group, 2006. Engineering life: building a fab for biology. *Scientific American*, 294(6), pp.44-51.
- Bellancini, M., 2015. *Engineering the synthesis of lantibiotics in e. Coli by combining the cynnamicin and nisin modification systems* (Doctoral dissertation).

Benner, S.A. and Sismour, A.M., 2005. Synthetic biology. *Nature Reviews. Genetics*, 6(7), p.533.

Bonelli, R.R., Schneider, T., Sahl, H.G. and Wiedemann, I., 2006. Insights into in vivo activities of lantibiotics from gallidermin and epidermin mode-of-action studies. *Antimicrobial Agents and Chemotherapy*, 50(4), pp.1449-1457.

Breukink, E. and de Kruijff, B., 2006. Lipid II as a target for antibiotics. *Nature reviews. Drug discovery*, 5(4), p.321.

Brötz, H., Bierbaum, G., Leopold, K., Reynolds, P.E. and Sahl, H.G., 1998. The lantibiotic mersacidin inhibits peptidoglycan synthesis by targeting lipid II. *Antimicrobial Agents and Chemotherapy*, 42(1), pp.154-160.

Brötz, H., Josten, M., Wiedemann, I., Schneider, U., Götz, F., Bierbaum, G. and Sahl, H.G., 1998b. Role of lipid-bound peptidoglycan precursors in the formation of pores by nisin, epidermin and other lantibiotics. *Molecular Microbiology*, 30(2), pp.317-327.

Chan, W.C., Dodd, H.M., Horn, N., Maclean, K., Lian, L.Y., Bycroft, B.W., Gasson, M.J. and Roberts, G.C., 1996. Structure-activity relationships in the peptide antibiotic nisin: role of dehydroalanine 5. *Applied and Environmental Microbiology*, 62(8), pp.2966-2969.

- Charles, P.G. and Grayson, M.L., 2004. The dearth of new antibiotic development: why we should be worried and what we can do about it. *Medical Journal of Australia*, 181, pp.549-553.
- Chatterjee, C., Paul, M., Xie, L. and van der Donk, W.A., 2005. Biosynthesis and mode of action of lantibiotics. *Chemical Reviews*, 105(2), pp.633-684.
- Chubukov, V., Mukhopadhyay, A., Petzold, C.J., Keasling, J.D. and Martín, H.G., 2016. Synthetic and systems biology for microbial production of commodity chemicals. *npj Systems Biology and Applications*, 2, p.16009.
- Cotter, P.D., Hill, C. and Ross, R.P., 2005. Bacterial lantibiotics: strategies to improve therapeutic potential. *Current Protein and Peptide Science*, 6(1), pp.61-75.
- Davies, M.J., Munro, I., Tan, C., Tracey, M.C. and Szita, N., 2014. Electromagnetic Actuated Stirring in Microbioreactor Enabling Easier Multiplexing and Flexible Device Design. *4th Micro and Nano Flows Conference*, London , 2014
- de Freire Bastos, M.D.C., Coelho, M.L.V. and da Silva Santos, O.C., 2015. Resistance to bacteriocins produced by Gram-positive bacteria. *Microbiology*, 161(4), pp.683-700.
- de Vuyst, L., and E. J. Vandamme. (1994). *Bacteriocins of Lactic Acid Bacteria*. Blackie Academic & Professional, ,London, England.

Delves-Broughton, J., Blackburn, P., Evans, R.J. and Hugenholtz, J., 1996. Applications of the bacteriocin, nisin. *Antonie van Leeuwenhoek*, 69(2), pp.193-202.

Devriese, L.A., Poutrel, B., Kilpper-Bälz, R. and Schleifer, K.H., 1983. *Staphylococcus gallinarum* and *Staphylococcus caprae*, two new species from animals. *International Journal of Systematic and Evolutionary Microbiology*, 33(3), pp.480-486.

Dischinger, J., Chipalu, S.B. and Bierbaum, G., 2014. Lantibiotics: promising candidates for future applications in health care. *International Journal of Medical Microbiology*, 304(1), pp.51-62.

Ducros, E., Ferrari, M., Pellegrino, M., Raspanti, C. and Bogni, C., 2009. Effect of aeration and agitation on the protease production by *Staphylococcus aureus* mutant RC128 in a stirred tank bioreactor. *Bioprocess and Biosystems Engineering*, 32(1), pp.143-148.

Elander, R.P., 2003. Industrial production of β -lactam antibiotics. *Applied Microbiology and Biotechnology*, 61(5-6), pp.385-392.

European Science Foundation, <http://www.esf.org/activities/eurocores/running-programmes/eurosynbio.html>. Accessed 10-12-2010

Ferber, D., 2004. Microbes made to order. *Science*, 303(5655), p.158.

- Fiedler, H.P., Hörner, T. and Decker, H., 1988. Purification of the hydrophilic antibiotics epidermin, gallidermin and nikkomycin Z by preparative reversed-phase HPLC. *Chromatographia*, 26(1), pp.215-220.
- Field, D., Cotter, P.D., Hill, C. and Ross, R.P., 2015. Bioengineering lantibiotics for therapeutic success. *Frontiers in microbiology*, 6.
- Flickinger, M.C. and Perlman, D., 1979. Application of oxygen-enriched aeration in the production of bacitracin by *Bacillus licheniformis*. *Antimicrobial Agents and Chemotherapy*, 15(2), pp.282-293.
- Furmanek, B., Kaczorowski, T., Bugalski, R., Bielawski, K. and Bogdanowicz, J., 1999. Identification, characterization and purification of the lantibiotic staphylococcin T, a natural gallidermin variant. *Journal of Applied Microbiology*, 87(6), pp.856-866.
- Gallagher, J (2014) Antibiotic resistance rise continues. *BBC News Website*.
<http://www.bbc.com/news/health-29553435>
- Gallup, J.L. and Sachs, J.D., 2001. The economic burden of malaria. *The American Journal of Tropical Medicine and Hygiene*, 64(1, 2 suppl), pp.85-96.
- Garcia, H.G., Brewster, R.C. and Phillips, R., 2016. Using synthetic biology to make cells tomorrow's test tubes. *Integrative Biology*, 8(4), pp.431-450.

Garcia-Ochoa, F., Gomez, E., Santos, V.E. and Merchuk, J.C., 2010. Oxygen uptake rate in microbial processes: an overview. *Biochemical Engineering Journal*, 49(3), pp.289-307.

Garcia-Ojalvo, J., Khalil, A.S. and McCarthy, J., 2016. Biological insights from synthetic biology. *Integrative Biology*, 8(4), pp.380-382.

Georgalaki, M.D., Van den Berghe, E., Kritikos, D., Devreese, B., Van Beeumen, J., Kalantzopoulos, G., De Vuyst, L. and Tsakalidou, E., 2002. Macedocin, a food-grade lantibiotic produced by *Streptococcus macedonicus* ACA-DC 198. *Applied and Environmental Microbiology*, 68(12), pp.5891-5903.

Gill, N.K., Appleton, M., Baganz, F. and Lye, G.J., 2008. Quantification of power consumption and oxygen transfer characteristics of a stirred miniature bioreactor for predictive fermentation scale-up. *Biotechnology and Bioengineering*, 100(6), pp.1144-1155.

Gomes, K.M., Duarte, R.S. and de Freire Bastos, M.D.C., 2017. Lantibiotics produced by Actinobacteria and their potential applications (a review). *Microbiology*, 163(2), pp.109-121.

Götz, F., Perconti, S., Popella, P., Werner, R. and Schlag, M., 2014. Epidermin and gallidermin: staphylococcal lantibiotics. *International Journal of Medical Microbiology*, 304(1), pp.63-71.

- Guder, A., Wiedemann, I. and Sahl, H.G., 2000. Posttranslationally modified bacteriocins—the lantibiotics. *Peptide Science*, 55(1), pp.62-73.
- Hancock, R.E. and Sahl, H.G., 2006. Antimicrobial and host-defense peptides as new anti-infective therapeutic strategies. *Nature Biotechnology*, 24(12), p.1551.
- Héchar, Y. and Sahl, H.G., 2002. Mode of action of modified and unmodified bacteriocins from Gram-positive bacteria. *Biochimie*, 84(5), pp.545-557.
- Heinemann, M. and Panke, S., 2006. Synthetic biology—putting engineering into biology. *Bioinformatics*, 22(22), pp.2790-2799.
- Hillman, J.D., 2002. Genetically modified *Streptococcus mutans* for the prevention of dental caries. In *Lactic Acid Bacteria: Genetics, Metabolism and Applications* (pp. 361-366). Springer Netherlands.
- Hjertén, S., 1973. Some general aspects of hydrophobic interaction chromatography. *Journal of Chromatography A*, 87(2), pp.325-331.
- Holtsmark, I., Mantzilas, D., Eijsink, V.G.H. and Brurberg, M.B., 2006. Purification, characterization, and gene sequence of michiganin A, an actagardine-like lantibiotic produced by the tomato pathogen *Clavibacter michiganensis* subsp. *michiganensis*. *Applied and Environmental Microbiology*, 72(9), pp.5814-5821.

- Hurst, A., 1981. Nisin. *Advances in Applied Microbiology*, 27, pp.85-123.
- Hutchison, C.A., Chuang, R.Y., Noskov, V.N., Assad-Garcia, N., Deerinck, T.J., Ellisman, M.H., Gill, J., Kannan, K., Karas, B.J., Ma, L. and Pelletier, J.F., 2016. Design and synthesis of a minimal bacterial genome. *Science*, 351(6280), p.aad6253.
- Hutchinson, N., Bingham, N., Murrell, N., Farid, S. and Hoare, M., 2006. Shear stress analysis of mammalian cell suspensions for prediction of industrial centrifugation and its verification. *Biotechnology and Bioengineering*, 95(3), pp.483-491.
- Islam, M.R., Nagao, J., Zendo, T. and Sonomoto, K., 2012. Antimicrobial mechanism of lantibiotics. *Biochemical Society Transactions*, 40(6), pp.1528-1533.
- Islam, R.S., Tisi, D., Levy, M.S. and Lye, G.J., 2008. Scale-up of *Escherichia coli* growth and recombinant protein expression conditions from microwell to laboratory and pilot scale based on matched kLa. *Biotechnology and bioengineering*, 99(5), pp.1128-1139.
- Jack, R.W., Tagg, J.R. and Ray, B., 1995. Bacteriocins of gram-positive bacteria. *Microbiological Reviews*, 59(2), pp.171-200.

- Jackson, N.B., Liddell, J.M. and Lye, G.J., 2006. An automated microscale technique for the quantitative and parallel analysis of microfiltration operations. *Journal of Membrane Science*, 276(1), pp.31-41.
- Jerris, R. C. (1995). Helicobacter. *Manual of Clinical Microbiology*, 6, 492-498.
- Joo, H.S. and Otto, M., 2015. Mechanisms of resistance to antimicrobial peptides in staphylococci. *Biochimica et Biophysica Acta (BBA)- Biomembranes*, 1848(11), pp.3055-3061.
- Juhas, M., 2016. On the road to synthetic life: the minimal cell and genome-scale engineering. *Critical Reviews in Biotechnology*, 36(3), pp.416-423.
- Jung, G. and Sahl, H.G. eds., 1991. *Nisin and Novel Lantibiotics*. Springer Science & Business Media.
- Junker, B.H., 2004. Scale-up methodologies for Escherichia coli and yeast fermentation processes. *Journal of bioscience and bioengineering*, 97(6), pp.347-364.
- Keasling, J.D. and Chou, H., 2008. Metabolic engineering delivers next-generation biofuels. *Nature Biotechnology*, 26(3), pp.298-299.
- Kelley, B., 2007. Very large scale monoclonal antibody purification: the case for conventional unit operations. *Biotechnology Progress*, 23(5), pp.995-1008.

- Kellner, R., Jung, G., Hörner, T., Zähner, H., Schnell, N., Entian, K.D. and Götz, F., 1988. Gallidermin: A new lanthionine-containing polypeptide antibiotic. *European Journal of Biochemistry. The FEBS Journal*, 177(1), pp.53-59.
- Kempf, M., Theobald, U. and Fiedler, H.P., 1997. Influence of dissolved O on the fermentative production of gallidermin by *Staphylococcus gallinarum*. *Biotechnology Letters*, 19(11), pp.1063-1065.
- Kempf, M., Theobald, U. and Fiedler, H.P., 1999. Economic improvement of the fermentative production of gallidermin by *Staphylococcus gallinarum*. *Biotechnology Letters*, 21(8), pp.663-667.
- Kempf, M., Theobald, U. and Fiedler, H.P., 1999B. Correlation between the consumption of amino acids and the production of the antibiotic gallidermin by *Staphylococcus gallinarum*. *Biotechnology Letters*, 21(11), pp.959-963.
- Kempf, M., Theobald, U. and Fiedler, H.P., 2000. Production of the antibiotic gallidermin by *Staphylococcus gallinarum*—development of a scale-up procedure. *Biotechnology Letters*, 22(2), pp.123-128.
- Kerr, K.G., Copley, R.M. and Wilcox, M.H., 1997. Activity of nisin against *Clostridium difficile*. *The Lancet*, 349(9057), pp.1026-1027.

Khosla, C. and Keasling, J.D., 2003. Metabolic engineering for drug discovery and development. *Nature Reviews. Drug Discovery*, 2(12), p.1019.

Kleerebezem, M., 2004. Quorum sensing control of lantibiotic production; nisin and subtilin autoregulate their own biosynthesis. *Peptides*, 25(9), pp.1405-1414.

Klößner, W., Gacem, R., Anderlei, T., Raven, N., Schillberg, S., Lattermann, C. and Büchs, J., 2013. Correlation between mass transfer coefficient $k_L a$ and relevant operating parameters in cylindrical disposable shaken bioreactors on a bench-to-pilot scale. *Journal of Biological Engineering*, 7(1), p.28.

Kruszewska, D., Sahl, H.G., Bierbaum, G., Pag, U., Hynes, S.O. and Ljungh, Å., 2004. Mersacidin eradicates methicillin-resistant *Staphylococcus aureus* (MRSA) in a mouse rhinitis model. *Journal of Antimicrobial Chemotherapy*, 54(3), pp.648-653.

Kuipers, O.P., Beerthuyzen, M.M., de Ruyter, P.G., Luesink, E.J. and de Vos, W.M., 1995. Autoregulation of nisin biosynthesis in *Lactococcus lactis* by signal transduction. *Journal of Biological Chemistry*, 270(45), pp.27299-27304.

Kuipers, O.P., Bierbaum, G., Ottenwälder, B., Dodd, H.M., Horn, N., Metzger, J., Kupke, T., Gnau, V., Bongers, R., van den Bogaard, P. and Kusters,

- H., 1996. Protein engineering of lantibiotics. *Antonie Van Leeuwenhoek*, 69(2), pp.161-170.
- Kupke, T., Kempter, C., Jung, G. and Gotz, F., 1995. Oxidative decarboxylation of peptides catalyzed by flavoprotein EpiD. Determination of substrate specificity using peptide libraries and neutral loss mass spectrometry. *Journal of Biological Chemistry*, 270(19), pp.11282-11289.
- Kuthning, A., Durkin, P., Oehm, S., Hoesl, M.G., Budisa, N. and Süßmuth, R.D., 2016. Towards biocontained cell factories: an evolutionarily adapted *Escherichia coli* strain produces a new-to-nature bioactive lantibiotic containing thienopyrrole-alanine. *Scientific Reports*, 6.
- Ling, L.L., Schneider, T., Peoples, A.J., Spoering, A.L., Engels, I., Conlon, B.P., Mueller, A., Schäberle, T.F., Hughes, D.E., Epstein, S. and Jones, M., 2015. A new antibiotic kills pathogens without detectable resistance. *Nature*, 517(7535), pp.455-459.
- Liu, H.F., Ma, J., Winter, C. and Bayer, R., 2010, September. Recovery and purification process development for monoclonal antibody production. *MAbs* (Vol. 2, No. 5, pp. 480-499). Taylor & Francis.
- Lye, G.J., Dalby, P.A. and Woodley, J.M., 2002. Better biocatalytic processes faster: new tools for the implementation of biocatalysis in organic synthesis. *Organic Process Research & Development*, 6(4), pp.434-440.

- Lye, G.J., Ayazi-Shamlou, P., Baganz, F., Dalby, P.A. and Woodley, J.M., 2003. Accelerated design of bioconversion processes using automated microscale processing techniques. *Trends in Biotechnology*, 21(1), pp.29-37.
- Lye, G.J., Asenjo, J.A. and Pyle, D.L., 1994. Protein extraction using reverse micelles: kinetics of protein partitioning. *Chemical Engineering Science*, 49(19), pp.3195-3204.
- Lye, G.J. and Woodley, J.M., 1999. Application of in situ product-removal techniques to biocatalytic processes. *Trends in Biotechnology*, 17(10), pp.395-402.
- Marr, A.K., Gooderham, W.J. and Hancock, R.E., 2006. Antibacterial peptides for therapeutic use: obstacles and realistic outlook. *Current Opinion in Pharmacology*, 6(5), pp.468-472.
- Mu, D., Montalbán-López, M., Deng, J. and Kuipers, O.P., 2015. Substrate selectivity of the lantibiotic reductase LtnJ assessed by a collection of nisin derivatives as substrate. *Applied and Environmental Microbiology*, pp.AEM-00475.
- Medaglia, G., 2009. *Development of a novel two-stage process for the production of the lantibiotic gallidermin* (Doctoral dissertation).

- Mehta, A., Tse, M.L., Fogle, J., Len, A., Shrestha, R., Fontes, N., Lebreton, B., Wolk, B. and Reis, R.V., 2008. Purifying therapeutic monoclonal antibodies. *Chemical Engineering Progress*, 104(5), p.S14.
- Micheletti, M. and Lye, G.J., 2006. Microscale bioprocess optimisation. *Current Opinion in Biotechnology*, 17(6), pp.611-618.
- Micheletti, M., Barrett, T., Doig, S.D., Baganz, F., Levy, M.S., Woodley, J.M. and Lye, G.J., 2006. Fluid mixing in shaken bioreactors: Implications for scale-up predictions from microlitre-scale microbial and mammalian cell cultures. *Chemical Engineering Science*, 61(9), pp.2939-2949.
- Nagao, J.I., Asaduzzaman, S.M., Aso, Y., Okuda, K.I., Nakayama, J. and Sonomoto, K., 2006. Lantibiotics: insight and foresight for new paradigm. *Journal of Bioscience and Bioengineering*, 102(3), pp.139-149.
- Nealon, A.J., O'Kennedy, R.D., Titchener-Hooker, N.J. and Lye, G.J., 2006. Quantification and prediction of jet macro-mixing times in static microwell plates. *Chemical Engineering Science*, 61(15), pp.4860-4870.
- Okeke, I.N., Lamikanra, A. and Edelman, R., 1999. Socioeconomic and behavioral factors leading to acquired bacterial resistance to antibiotics in developing countries. *Emerging Infectious Diseases*, 5(1), p.18.

- Ongey, E.L. and Neubauer, P., 2016. Lanthipeptides: chemical synthesis versus in vivo biosynthesis as tools for pharmaceutical production. *Microbial Cell Factories*, 15(1), p.97.
- O'Neill, J., 2014. *Review on Antimicrobial Resistance: Tackling a Crisis for the Health and Wealth of nations*. HM Government, Wellcome Trust: London, 2014
- Ottenwalder, B.I.R.G.I.T., Kupke, T., Brecht, S., Gnau, V., Metzger, J., Jung, G. and Gotz, F., 1995. Isolation and characterization of genetically engineered gallidermin and epidermin analogs. *Applied and Environmental Microbiology*, 61(11), pp.3894-3903.
- Parente, E. and Ricciardi, A., 1999. Production, recovery and purification of bacteriocins from lactic acid bacteria. *Applied Microbiology and Biotechnology*, 52(5), pp.628-638.
- Patel, V.K., Sahoo, N.K., Patel, A.K., Rout, P.K., Naik, S.N. and Kalra, A., 2017. Exploring microalgae consortia for biomass production: a synthetic ecological engineering approach towards sustainable production of biofuel feedstock. In *Algal Biofuels* (pp. 109-126). Springer International Publishing.
- Piva, A. and Headon, D.R., 1994. Pediocin A, a bacteriocin produced by *Pediococcus pentosaceus* FBB61. *Microbiology*, 140(4), pp.697-702.

- Rayat, A.C., Chatel, A., Hoare, M. and Lye, G.J., 2016. Ultra scale-down approaches to enhance the creation of bioprocesses at scale: impacts of process shear stress and early recovery stages. *Current Opinion in Chemical Engineering*, 14, pp.150-157.
- Reardon, S., 2014. Antibiotic resistance sweeping developing world: bacteria are increasingly dodging extermination as drug availability outpaces regulation. *Nature*, 509(7499), pp.141-143.
- Rollema, H.S., Kuipers, O.P., Both, P., De Vos, W.M. and Siezen, R.J., 1995. Improvement of solubility and stability of the antimicrobial peptide nisin by protein engineering. *Applied and Environmental Microbiology*, 61(8), pp.2873-2878.
- Ross, A.C., Liu, H., Pattabiraman, V.R. and Vederas, J.C., 2009. Synthesis of the lantibiotic lactocin S using peptide cyclizations on solid phase. *Journal of the American Chemical Society*, 132(2), pp.462-463.
- Sahl, H.G. and Bierbaum, G., 1998. Lantibiotics: biosynthesis and biological activities of uniquely modified peptides from gram-positive bacteria. *Annual Reviews in Microbiology*, 52(1), pp.41-79.
- Sahl, H.G., Jack, R.W. and Bierbaum, G., 1995. Biosynthesis and biological activities of lantibiotics with unique post-translational modifications. *The FEBS Journal*, 230(3), pp.827-853.

- Sandiford, S.K., 2014. Advances in the arsenal of tools available enabling the discovery of novel lantibiotics with therapeutic potential. *Expert opinion on drug discovery*, 9(3), pp.283-297.
- Saising, J., Dube, L., Ziebandt, A.K., Voravuthikunchai, S.P., Nega, M. and Götz, F., 2012. Activity of gallidermin on *Staphylococcus aureus* and *Staphylococcus epidermidis* biofilms. *Antimicrobial Agents and Chemotherapy*, 56(11), pp.5804-5810.
- Severina, E., Severin, A. and Tomasz, A., 1998. Antibacterial efficacy of nisin against multidrug-resistant Gram-positive pathogens. *The Journal of Antimicrobial Chemotherapy*, 41(3), pp.341-347.
- Slavov, N., Budnik, B.A., Schwab, D., Airoidi, E.M. and van Oudenaarden, A., 2014. Constant growth rate can be supported by decreasing energy flux and increasing aerobic glycolysis. *Cell Reports*, 7(3), pp.705-714.
- Smanski, M.J., Zhou, H., Claesen, J., Shen, B., Fischbach, M.A. and Voigt, C.A., 2016. Synthetic biology to access and expand nature's chemical diversity. *Nature Reviews Microbiology*, 14(3), pp.135-149.
- Smith, L. and Hillman, J.D., 2008. Therapeutic potential of type A (I) lantibiotics, a group of cationic peptide antibiotics. *Current Opinion in Microbiology*, 11(5), pp.401-408.

Souza, E.C., Azevedo, P.O.D.S.D., Domínguez, J.M., Converti, A. and Oliveira, R.P.D.S., 2017. Influence of temperature and pH on the production of biosurfactant, bacteriocin and lactic acid by *Lactococcus lactis* CECT-4434. *CyTA-Journal of Food*, pp.1-6.

Suarez, A.M., Azcona, J.I., Rodríguez, J.M., Sanz, B. and Hernandez, P.E., 1997. One-step purification of nisin A by immunoaffinity chromatography. *Applied and Environmental Microbiology*, 63(12), pp.4990-4992.

Suárez, J.M., Edwards, A.N. and McBride, S.M., 2013. The *Clostridium difficile* cpr locus is regulated by a noncontiguous two-component system in response to type A and B lantibiotics. *Journal of Bacteriology*, 195(11), pp.2621-2631.

Tabor, A.B., 2011. The challenge of the lantibiotics: synthetic approaches to thioether-bridged peptides. *Organic & Biomolecular Chemistry*, 9(22), pp.7606-7628.

The Economist, 2014. Antibiotic Resistance: The drugs don't work . *The Economist, Print Edition*, May 3, 2012

The Economist, 2012. The path of least resistance. *The Economist, Print Edition*, May 12, 2012

- Titchener-Hooker, N.J., Dunnill, P. and Hoare, M., 2008. Micro biochemical engineering to accelerate the design of industrial-scale downstream processes for biopharmaceutical proteins. *Biotechnology and Bioengineering*, 100(3), pp.473-487.
- Valsesia, G., Medaglia, G., Held, M., Minas, W. and Panke, S., 2007. Circumventing the effect of product toxicity: development of a novel two-stage production process for the lantibiotic gallidermin. *Applied and Environmental Microbiology*, 73(5), pp.1635-1645.
- Valsesia, G., 2008. *Genetic engineering of Staphylococcus gallinarum for overproduction of the lantibiotic gallidermin* (Doctoral dissertation).
- Van der Meer, J.R., Polman, J., Beerthuyzen, M.M., Siezen, R.J., Kuipers, O.P. and De Vos, W.M., 1993. Characterization of the Lactococcus lactis nisin A operon genes nisP, encoding a subtilisin-like serine protease involved in precursor processing, and nisR, encoding a regulatory protein involved in nisin biosynthesis. *Journal of Bacteriology*, 175(9), pp.2578-2588.
- van Heel, A.J., Mu, D., Montalbán-López, M., Hendriks, D. and Kuipers, O.P., 2013. Designing and producing modified, new-to-nature peptides with antimicrobial activity by use of a combination of various lantibiotic modification enzymes. *ACS Synthetic Biology*, 2(7), pp.397-404.

- van Heel, A.J., Montalban-Lopez, M. and Kuipers, O.P., 2011. Evaluating the feasibility of lantibiotics as an alternative therapy against bacterial infections in humans. *Expert Opinion on Drug Metabolism & Toxicology*, 7(6), pp.675-680.
- van Kraaij, C., de Vos, W.M., Siezen, R.J. and Kuipers, O.P., 1999. Lantibiotics: biosynthesis, mode of action and applications. *Natural Product Reports*, 16(5), pp.575-587.
- Van Staden, A.D.P., 2015. *In vitro and in vivo characterization of amyloliqueducidin, a novel two-component lantibiotic produced by Bacillus amyloliquefaciens* (Doctoral dissertation, Stellenbosch: Stellenbosch University).
- Voulgaris, I., Chatel, A., Hoare, M., Finka, G. and Uden, M., 2016. Evaluation of options for harvest of a recombinant E. Coli fermentation producing a domain antibody using ultra scale-down techniques and pilot-scale verification. *Biotechnology Progress*, 32(2), pp.382-392.
- Walser, M., Pellaux, R., Meyer, A., Bechtold, M., Vanderschuren, H., Reinhardt, R., Magyar, J., Panke, S. and Held, M., 2009. Novel method for high-throughput colony PCR screening in nanoliter-reactors. *Nucleic Acids Research*, 37(8), pp.e57-e57.
- Walsh, F (2014) Antibiotic resistance: Cameron warns of medical 'dark ages'. *BBC News Website*. <http://www.bbc.com/news/health-28098838>

Weil, H.P., Beck-Sickinger, A.G., Metzger, J., Stevanovic, S., Jung, G., Josten, M. and Sahl, H.G., 1990. Biosynthesis of the lantibiotic Pep5. *European Journal of Biochemistry, The FEBS Journal*, 194(1), pp.217-223.

Wenzel, M., Kohl, B., Münch, D., Raatschen, N., Albada, H.B., Hamoen, L., Metzler-Nolte, N., Sahl, H.G. and Bandow, J.E., 2012. Proteomic response of *Bacillus subtilis* to lantibiotics reflects differences in interaction with the cytoplasmic membrane. *Antimicrobial Agents and Chemotherapy*, 56(11), pp.5749-5757.

Wescombe, P.A. and Tagg, J.R., 2003. Purification and characterization of streptin, a type A1 lantibiotic produced by *Streptococcus pyogenes*. *Applied and Environmental Microbiology*, 69(5), pp.2737-2747.

Wiedemann, I., Benz, R. and Sahl, H.G., 2004. Lipid II-mediated pore formation by the peptide antibiotic nisin: a black lipid membrane study. *Journal of Bacteriology*, 186(10), pp.3259-3261.

Willey, J.M. and Van Der Donk, W.A., 2007. Lantibiotics: peptides of diverse structure and function. *Annual Review of Microbiology*, 61, pp.477-501.

Winkler, M.A. ed., 1990. *Chemical engineering problems in biotechnology* (Vol. 29). pp. 180-181, Springer Science & Business Media.

- World Economic Forum (2013). The Dangers of Hubris on Human Health. *Global Risks 2013, Eighth Edition*, p.28
- Yang, R., Johnson, M.C. and Ray, B.I.B.E.K., 1992. Novel method to extract large amounts of bacteriocins from lactic acid bacteria. *Applied and Environmental Microbiology*, 58(10), pp.3355-3359.
- Yoneyama, H. and Katsumata, R., 2006. Antibiotic resistance in bacteria and its future for novel antibiotic development. *Bioscience, Biotechnology, and Biochemistry*, 70(5), pp.1060-1075.
- Zhang, M.M., Wang, Y., Ang, E.L. and Zhao, H., 2016. Engineering microbial hosts for production of bacterial natural products. *Natural Product Reports*, 33(8), pp.963-987.
- Zhou, L., Shao, J., Li, Q., van Heel, A.J., de Vries, M.P., Broos, J. and Kuipers, O.P., 2016. Incorporation of tryptophan analogues into the lantibiotic nisin. *Amino Acids*, 48(5), pp.1309-1318.
- Zhou, L., van Heel, A.J. and Kuipers, O.P., 2015. The length of a lantibiotic hinge region has profound influence on antimicrobial activity and host specificity. *Frontiers in Microbiology*, 6. pp.1-8
- Zimmermann, N. and Jung, G., 1997. The Three-Dimensional Solution Structure of the Lantibiotic Murein-Biosynthesis-Inhibitor Actagardine

Determined by NMR. *European Journal of Biochemistry, The FEBS Journal*, 246(3), pp.809-819.